Tracking Inorganic Solids in Biological Enhanced Phosphorus Removal Wastewater Treatment Systems

Prepared by:

Oodally Adam (BSc in Civil Engineering)

Supervised by:

Ikumi S. David (Doctor of Philosophy)

Proposal submitted in fulfilment of the requirements for the degree of

Master of Science in Water Quality Engineering

Department of Civil Engineering

University of Cape Town, Private Bag Rondebosch, 7700

University of Cape Town

The copyright of this thesis vests in the author. No quotation from it or information derived from it is to be published without full acknowledgement of the source. The thesis is to be used for private study or non-commercial research purposes only.

Published by the University of Cape Town (UCT) in terms of the non-exclusive license granted to UCT by the author.

University of Cape Town

Declaration

I know the meaning of plagiarism and declare that all the work in the document, save for that which is properly acknowledged, is my own. This thesis/dissertation has been submitted to the Turnitin module (or equivalent similarity and originality checking software) and I confirm that my supervisor has seen my report and any concerns revealed by such have been resolved with my supervisor.

Signed: Signed by candidate Date: 01.01.2022

Acknowledgements

God Almighty – First and foremost, praises and thanks to God the Almighty for his blessings and guidance through this journey.

Professor David S. Ikumi – Thank you for your support, guidance and assistance throughout my undergraduate and postgraduate degree. I am always humbled by your understanding of the wastewater treatment field and the passion you have for it. I feel blessed to have you as my supervisor and to be able to learn from the best.

Professor George Ekama– Thank you for the guidance during the brief conversations we had. I would also like to thank you for being my inspiration to further study wastewater treatment. I hope one day to become as well versed as you in this field.

Njabulo Thela and Hector Mufungwa – A huge thanks to you Njabulo for your assistance in the Water Quality laboratory.

Professor Dyllon Randall – Thank you for support you have provided in the Water Quality laboratory. I am very grateful to have known and worked with such an accomplished researcher.

Nasseela Hytoolakhan Lal Mahomed – Thank you Nasseela for being there for me during this journey. I cannot emphasize enough how your help and support were fundamental towards the completion of this project. I am eternally grateful to have you by my side.

My Parents and family – Thank you for the unconditional support through this journey. Your support means the world to me.

My Friends – To Alex, Shanil, Matthieu, Ismayeel, Zuleikha, Aleeshah, Irshaad, Hyderally, Tanweer and all the others, thank you for all the support. You have provided the perfect balance between work and fun time.

National Research Foundation (NRF) and the Water Research Commission (WRC) – Thank you for providing financial support.

Executive summary

The modelling and tracking of solids in wastewater treatment plants (WWTPs) has historically been focussed on the different types of organic solids. Conversely, there is currently limited information on the composition of inorganic solids, and how they behave across different WWTP unit operations. For the biological removal of organics or nitrogen, this limited information on inorganic solids has no implications as the inorganic solids (sediments) do not interact with the biochemical processes of the WWTP units. For enhanced biological phosphorus removal (EBPR) systems, biochemical processes result in the generation of additional forms of inorganic solids. This includes the formation of polyphosphate by phosphorus accumulating microorganisms (PAOs) and precipitation of inorganic minerals (e.g., struvite). Up until now, the only test that provides information on inorganic settleable or suspended solids (ISS) is the total solids test which yields the total lumped ISS mass of sewage or sludge samples. Furthermore, although there are several models that can provide useful information on the forms and concentrations of ISS in WWTP units (Musvoto *et al.*, 2000; Ekama *et al.*, 2006; Kazadi *et al.*, 2015), no experimental tests exist that can verify the assumptions or predictions of these models.

The ISS in EBPR systems can potentially be made up of the following: sediments (clay, silt and sand), polyphosphate (polyP) and mineral precipitates. Based on the ionic concentrations, as well as the conditions in WWTP units, the main forms of mineral precipitates present in EBPR systems are struvite and amorphous calcium phosphate (ACP). For sludge treatment processes downstream of EBPR activated sludge (AS) systems, several assumptions are made on the forms of inorganic solids present in the sludge. For instance, prior to the anaerobic and aerobic sludge digesters, mineral precipitation is currently not simulated, and the polyP molecules are assumed to remain unchanged from the AS system to the anaerobic digesters (AD). Post anaerobic digestion, it is assumed that all polyP has been hydrolysed and the released ions participate in mineral precipitation.

The objective of this research is to develop and evaluate an ISS characterisation procedure. The output of the ISS characterisation procedure is a fully characterised ISS i.e., the individual ISS components and their respective concentrations. This ISS characterisation procedure was made up of two major components: an experimental test (named as an ISS characterisation test (ICT)) and a data modelling procedure (DMP). The former is a laboratory test that can be applied to a sample to provide input data for the DMP. The approach taken towards the development of the ICT was to identify base methods from previous literature, and thereafter modifying them to provide analytical measurements to the DMP. Several potential base methods for the ICT were identified in the literature and assessed using a multicriteria decision analysis. The base method was then modified to an ICT. The DMP was developed based on the expected effect of the ICT on the sludge samples, as well as stoichiometric ratios of the different inorganic compounds. To evaluate the performance of the ICT and DMP, the sample set was made up using solution with (i) known amount of mineral precipitate, (ii) EBPR sludge, (iii) a mixture of EBPR sludge and mineral precipitate. The EBPR sludge was obtained from a parallel study that aimed at growing an enhanced culture of PAOs in a University of Cape Town (UCT) configured AS system.

Through the multicriteria analysis it was deduced that the cold perchloric acid (PCA) fractionation procedure by De Haas *et al.* (2000) was the most suitable base method for the ICT. Short extraction times of EBPR sludge with cold PCA acid was proven to be efficient in dissolving mineral precipitates without hydrolysis of polyP molecules (De Haas *et al.*, 2000). The cold PCA fractionation procedure was modified (to the ICT) to include more analytical measurements such as magnesium (Mg), potassium (K), calcium (Ca), free and saline ammonia (FSA) and orthophosphate (OP), such that these measurements can be used in the DMP to characterise ISS. The DMP I (denoted as DMP I for being the first attempt) was developed based on the expected effect of the cold PCA fractionation procedure on the EBPR sludge sample with mineral precipitates.

The analysis of the results from the application of the ICT on the EBPR sludge samples showed significant findings. It was demonstrated that the ICT was successful in dissolving the maximum expected concentration of mineral precipitates in its PCA extracts. The application of the ICT on the EBPR sludge sample showed that the hydrolysis of polyP did occur in the PCA extract. PolyP phosphate and counter-ions (Mg, K and Ca) were released into the PCA extract. Results from the application of the ICT on a mixture of EBPR sludge and mineral precipitates showed that the PCA extract contained both mineral precipitates ions and polyP ions. The FSA measurements on the PCA extract showed that the FSA was from the dissolution of struvite only, and there was negligible N from the hydrolysis of biomass. The release of polyP phosphate was consistent for all tests carried on sludge samples. On the other hand, the release of polyP counter-ions Mg and Ca were varied amongst the test cases with sludge samples.

The results of the ICT were used as input to the DMP. The output of the DMP I was significantly inaccurate. The concentration of struvite and ACP were overpredicted by 66% and 129%, respectively. The concentration of polyP (as mgP/L) was underpredicted by 28%. It was deduced that the release of polyP counter-ions into the PCA extract led to the overprediction of the mineral precipitate and the release of polyP phosphates into the PCA extract led to the underprediction of polyP phosphate concentration. Following this analysis, a second DMP was developed (DMP II) and evaluated. Using the DMP II, the error in struvite and ACP prediction improved to 15% and 25%, respectively. The error in prediction in polyP concentration increased slightly to 31%.

The ICT was not successful in separating the polyP and mineral precipitates due to the hydrolysis of polyP molecules. Hence the percentage error in the prediction of the ISS constituents concentrations were high using both DMPs. The DMP II showed an improvement in the prediction of mineral precipitate concentration. However, there are several caveats to the application of DMP II. First, it depends largely on a few parameters (such as the soluble ammonium) and thus inaccurate measurements of these parameters can result in significant mispredictions form the model. Second, it depends on parameters (namely the Mg:P ratio in polyP and extent of polyP hydrolysis) that need to be calibrated for each experimental investigation. Further research is required to determine what affects these ratios and how it can be parametrised into the DMP II.

Although, this research has successfully identified, developed and evaluated a potential ISS characterization procedure for EBPR systems, there is still further research that still needs to be performed on this topic to achieve a fully calibrated and validated procedure.

Table of Contents

List of Figures

List of Tables

Acronyms and abbreviations

AAD	Aerobic Anoxic digestion
ACP	Amorphous calcium phosphate
AD	Anaerobic digestion
AerD	Aerobic digestion
ANO	Autotrophic nitrifying organisms
AS	Activated sludge
ATP	Adenosine triphosphate
BNR	Biological nutrient removal
BOD	Biological oxygen demand
BSM	Benchmark simulation model
COD	Chemical oxygen demand
CSLM	Confocal laser scanning microscopy
DAF	Dissolved air floatation
DCPD	Dicalcium phosphate dihydrate
DMP	Data modelling procedure
EBPR	Enhanced biological phosphorus removal
FA	Fully aerobic
FISH	Fluorescence in site hybridization
FSA	Free and saline ammonia
HAP	Hydroxyapatite
HVPD	High voltage pulsed discharge
ICT	ISS characterisation test
IDS	Inorganic dissolved solids
ISS	Inorganic settleable and/or suspended solids
MBR	Membrane bioreactor
MLSS	Mixed liquor suspended solids
MLE	Modified Ludzack-ettinger
ND	Nitrification denitrification
NDEBPR	Nitrification denitrification enhanced biological phosphorus removal
NMR	Nuclear magnetic resonance
OCP	Octacalcium phosphate
OHO	Heterotrophic microorganisms
OP	Orthophosphate
PAO	Phosphate accumulating organisms
PCA	Perchloric acid
PHA	Poly-hydroxy-alkanoates
PHB	Poly-3-hydroxy butyrate
PLS	Partial least square
PolyP	Polyphosphate
PS	Primary sludge
PST	Primary settling tank

QIA	Qualitative image assessment
SEM	Scanning electron microscope
SMT	Standard, measurements and techniques
SRT	Sludge retention time
TOC	Total organic carbon
TOD	Total oxygen demand
TCP	Tricalcium phosphate
TKN	Total Kjeldahl nitrogen
TP	Total phosphate
TSS	Total settleable and/or suspended solids
UCT	University of Cape Town
UPO	Unbiodegradable particulate organics
USO	Unbiodegradable soluble organics
VFA	Volatile fatty acid
VSS	Volatile settleable and/or suspended solids
WAS	Waste activated sludge
WW	Wastewater
WWRF	Wastewater resource recovery facilities
WWTP	Wastewater treatment plant

Symbols

b_{GT}	Endogenous respiration rate for PAOs
b_{HT}	Endogenous respiration rate for OHOs
f_{avOHO}	Fraction of the VSS concentration which is OHOs
f_{avPAO}	Fraction of the VSS concentration which is PAOs
f_{EG}	Endogenous residue fraction of the PAOs
f_{EH}	Endogenous residue fraction of the OHOs
f_{iOHO}	Inorganic content of OHO cell mass
f_{iPAO}	Inorganic content of PAO cell mass
f_{iPAOBM}	Inorganic solids content of the PAO active biomass
$f_{Sbıs}$	Influent readily biodegradable COD with respect to biodegradable COD
$f_{\mathrm{S}ı\mathrm{up}}$	Influent unbiodegradable particulate COD
$f_{Sıus}$	Influent unbiodegradable soluble COD
f_{XBGP}	Total P content of PAOs
f_{XBGPBM}	Total P content of PAOs
MS_{ti}	COD mass load on reactor
MX_{Io}	Mass of ISS in reactor
MX_t	Mass of TSS in reactor
MX_v	Mass of VSS in reactor
P_{polyP}	PolyP P concentration in PAO VSS
P_{ti}	Total P concentration in influent
P_{te}	Total P concentration in effluent
P_s	Total P concentration in sludge
R_{hn}	Hydraulic retention time
R_s	Sludge retention time
X_{Io}	ISS concentration in biological reactor
X_{Ioi}	Influent ISS concentration
X_v	VSS concentration in biological reactor
Y_G	Yield coefficient of PAOs
Y_H	Yield coefficient of OHOs

1 Introduction

1.1 Background

With the decline of natural resources, there is a need for effective resource management as societal problems such as food scarcity become of increasing concern. Phosphorus (P), which forms part of the building blocks of living matter, is an essential dietary requirement and thus its management is directly linked to food security. Phosphorus is mainly extracted from the non-renewable phosphorite ore (Cordell, 2010). Above 80% of phosphorus produced is used for fertilizer production with the remaining for industrial application such as the manufacture of detergents (Cordell, 2010). With increasing world population and associated food demand, the supply of phosphorus for the required crop yield may not eventually match the demand. Hence, a more sustainable approach is required for the management of phosphorus. The different measures that have been considered include: (i) management of fertilizer production, (ii) replacement of phosphorus in detergents and, (iii) phosphorus recovery in wastewater treatment plants (WWTPs) (Cordell, 2010).

Currently, the removal of phosphorus in WWTPs can be done chemically or biologically. The former consists of addition of chemicals such as aluminium or ferrous elements ($AlSO_4$ or $FeSO_4$) to form precipitates with the dissolved phosphorus in the wastewater (De Haas, 1998). The precipitates are then removed as part of the waste activated sludge (WAS). However, sludge containing phosphorus and ferrous elements are harder to degrade in the natural environment (Shu *et al.*, 2006) and thus they cannot be commercialized as fertilizers. Moreover, because of the relatively higher cost of chemical P removal, the focus quickly shifted towards biological P removal with respect to the recovery of phosphorus in WWTP (Quevauvilliers & Ikumi, 2021). Enhanced biological phosphorus removal (EBPR) activated sludge (AS) system is a type of biological nutrient removal (BNR) unit operation of the WWTP. These systems make use of a special group of bacteria known as phosphorus accumulating organisms (PAOs) to attain low phosphorus level in the effluent. The PAOs accomplish this removal by accumulating high concentrations of phosphorus as polyphosphate (polyP) chains under aerobic conditions of the EBPR reactors. This way the phosphorus becomes part of the PAOs that exit the reactor as part of the sludge. The waste sludge can be stabilised using anaerobic digestion (AD) or aerobic-anoxic digestion (AAD). The PAO biomass is degraded and the polyP is released into the aqueous phase as phosphates, which form part of the bulk liquid in the AD effluent. Ideally, this phosphorus can be recovered as a mineral precipitate called struvite [$MgNH_4PO_4.6H_2O$] through application of crystallisation units to treat the AD dewatering liquor (the nutrient rich effluent that is generated with thickening of the AD effluent sludge) (Pastor *et al.*, 2010). As compared to aluminium phosphate or iron phosphate, struvite makes a better fertilizer as it releases phosphorus at a lower rate and thus is a more economically viable method to recover phosphorus (Shu *et al.*, 2006).

For the above-mentioned unit processes (EBPR, AD or AAD, struvite crystallization), mathematical models are critical decision-making tools in the implementation of operational strategies that will ensure minimum costs and optimum yield of useful products. These mathematical models contain set of equations coded into computer simulation programmes to

virtually replicate real systems. Current research interests are towards the development of system wide water and resource recovery facility (WRRF) models i.e., extending the plant-wide models (combination of different WWTP unit models) to include the fate of products generated by WWTPs. The system wide WRRF models could be used to generate expert advice on operational strategies and design procedures that can result in resource recovery and sustainable infrastructure for management of WWTP (Ikumi, 2015).

The calibration of WRRF models is an important step towards ensuring that the model replicates system performance accurately. This way, there can be a high level of confidence in predicted model outputs, including the products generated towards resource recovery. The mass balanced University of Cape Town (UCT)/ University of KwaZulu Natal (UKZN) three phase plant wide model (PWM_SA; Ikumi, 2015)) constitutes of the following unit models, namely:

a) BNR AS systems which includes EBPR and nitrification denitrification EBPR system (NDEBPR)

b) Anaerobic digestion (AD) of primary sludge

c) AD or AAD of waste activated sludge (WAS)

d) Interlinking non-reactive thickening physical units.

To yield accurate and consistent predictions based on input values, these models need to be calibrated with experimental observations for different types of feed. To date, the AS and AAD model (PWM_SA_AS) has been calibrated for different type of organics (Ikumi *et al.*, 2015; Ikumi and Harding, 2020) whilst the AD model (PWM_SA_AD) has been calibrated for primary sludge and WAS from fully aerobic (FA) or nitrification denitrification (ND) systems (Ikumi *et al.*, 2014; Ikumi, 2020; Maake and Ikumi, 2021).

1.2 Research problem

When modelling WWTP unit operations, there has been generally a greater emphasis on the organic fraction of sewage or sludge as compared to the inorganic fraction. Consequently, the development of laboratory tests has been focused on the organic portion of the sewage or sludge. Numerous laboratory tests such as chemical oxygen demand (COD), total oxygen demand (TOD), biological oxygen demand (BOD) or total organic carbon (TOC) provide information on the organic content of sewage or sludge. Comparatively, there is significantly less tests developed regarding the inorganic fraction of sewage or sludge. Up to now, only the total solids test (APHA, 1985; Ekama and Wentzel, 2004) yields the concentration of the total inorganic solids.

When modelling organic or nitrogen removal systems, the lack of information on inorganic solids does not have an impact on the accuracy of the outputs from the model. This is primarily because the inorganic mass originates mainly from sediments which are inert. On the other hand, in EBPR system (such as the UCT AS system) followed by AD or AAD, additional forms of inorganic solids such as mineral precipitates or polyP exist. As opposed to sediments, both compounds can affect the processes occurring in the WWTP units. Currently, there are several assumptions taken on the forms and concentrations different inorganic solids in EBPR system due to this lack of information. Therefore, in EBPR systems it becomes critical to gather more information on the

inorganics solids in the sewage or sludge to evaluate these assumptions and accurately calibrate the models.

With regards to modelling and tracking of inorganic solids, two parameters are relevant: individual composition (i.e., the empirical formulae of the inorganic compounds where relevant) and concentrations of the different inorganic solid components. At this stage there is currently no experimental test or procedure that allows for the individual identification of the inorganic solids in terms of composition and concentration.

1.3 Research questions

The above research problem gives rise to the following research questions:

a) What are the different components of inorganic solids in sewage or sludge?

b) Is it feasible to characterise these inorganic solids? If so, is there an existing laboratory test that can be retrofitted towards the characterisation of the identified inorganic solids?

c) Can the results from the laboratory tests be integrated in a data-driven modelling procedure to characterise the inorganic solids?

1.4 Objectives

The aim of this research is to develop and evaluate an inorganic solids characterisation procedure for sewage or sludge from wastewater treatment plants.

The objectives of this research are:

a) Development of a laboratory test protocol to collect analytical measurements for a data-modelling procedure.

b) Development of a data modelling procedure (DMP) to fully characterise inorganic solids into its individual component's composition and concentration. The output of the DMP relies on results from the laboratory test protocol developed in (a).

c) Evaluate the feasibility of the developed procedure (i.e., the laboratory test protocol and the data-modelling procedure) in characterising inorganic solids.

1.5 Scope and limitations

In the past, there has been little efforts in developing a characterisation procedure for inorganic solids. This investigation pioneers the research in the topic of wastewater inorganic solids characterisation. Henceforth, a major and critical component of this research is a thorough literature review evaluating the various possible methods that can be used towards achieving the abovementioned objectives. Due to time constraints (the 120 National Qualification Framework credits, requires about 1200 hours of work for the research project), laboratory space and capital (to purchase new equipment), not all the methods identified from the literature review are assessed experimentally. Instead, a decision tool was used to determine the most suitable method to yield the required output of this research.

As mentioned later on in the methodology chapter, it was necessary to obtain an enhanced culture of PAOs at steady state. To achieve this goal, a continuous NDEBPR membrane bioreactor (MBR), configured as a UCT process (from now on referred to as UCT AS system), was operated as a parallel but separate research project. The operation of this reactor as well as the analysis of the results are not part of the scope of this study. Furthermore, the national lockdown during the year 2020 prompted the closure of the Water Quality Laboratory at UCT and consequently the inability for this UCT AS system to be operated during this period. This has consequently impacted this research scope due to a limited time of two months to perform the experiments involving NDEBPR WAS sludge. The limitation of the methods, procedures or tests are outlined explicitly in the methodology chapter.

2 Literature review

The first sections in this chapter provide an explicit definition of inorganic suspended and/or settleable solids (ISS) and an identification of the different constituents of ISS. Without sufficient knowledge on the exact forms and concentrations of inorganic solids across WWTP units, several assumptions have been made in models that replicate WWTP unit processes. These assumptions were identified in this literature. It was also highlighted how an ISS characterisation procedure can help towards the calibration of these models. The last section explores various experimental base methods that could be employed to generate input for the proposed DMP.

2.1 Description of ISS

In wastewater characterisation, the definition of inorganic solids is based on the total solids test (see Section 3.5.1 for detailed description of the test). The purpose of the total solids test is to determine the volatile (organic), inorganic and total solids of a sludge or sewage sample. In this test the solids, sewage or sludge samples are subjected to a temperature of 600 ^{0}C for 20 minutes. The mass of solids that vaporise is defined as volatile settleable and/or suspended solids (VSS) whilst any solid that remains unchanged is defined as ISS. The sum of the ISS and VSS is the total settleable and/or suspended solids (TSS). Depending on the method employed to obtain the solids (e.g., 0.45 µM filtration, sedimentation or centrifuging), the solids can be classified as settleable, non-settleable (also called suspended) or both (settleable and non-settleable). In a reactor, non-settleable inorganic solids enmeshes and settles with biomass. Hence, for AS reactor sludge all ISS are usually deemed settleable.

2.2 ISS composition

This section describes the various constituents of ISS in the different units of WWTPs as identified in literature. In the raw wastewater, the ISS are generally assumed to be made up of only clay, silt and sand. Although these materials do not affect the chemical reactions occurring inside the reactor, they do affect the design of WWTP units as they accumulate with solids retention time, taking up part of the reactor volume. Raw wastewater is typically composed of influent ISS concentration in the range 90-110 mgISS/L, whilst for settled wastewater it can range from 15-30 mg/L (Henze *et al.*, 2008). Inside the biological reactor, besides the sediments from the influent, other forms of ISS exist. In FA or Modified Ludzack-ettinger (MLE) AS systems, biomass contains intracellular ions that reflect as ISS during the total solids test. In EBPR systems, other than the inorganic fraction of biomass, polyP also form part of the ISS since they are inorganic (Ekama & Wentzel, 2004).

2.2.1 The inorganic fraction of biomass

Of the total mass (TSS) of PAOs, the measured VSS consist of the poly-b-hydroxy-butyrate (PHB), organic part of biomass and glycogen whilst the ISS consist of the inorganic fraction of the biomass and polyP. The inorganic fraction of biomass corresponds to the uptake of dissolved ions by the organisms which precipitate as mineral solids when incinerated during the total solids test. The ISS contribution of the inorganic fraction of the biomass for both OHOs and PAOs is 0.15 mgISS/VSS (Ekama & Wentzel, 2004).

2.2.2 Polyphosphate (polyP)

The polyP inside PAOs is made up of linear structured polymers of ortho-phosphate with varying chain lengths (Harold, 1966). Figure 1 shows the configuration of a linear structured polyP. The links between each phosphate monomers are energy-rich phosphoanhydride bonds, like those found in adenosine triphosphate (ATP) molecules (Harold, 1966). Since polyP is an inorganic molecule, its energy content cannot be measured during a COD test. For the same reason, during a total solids test, polyP inside PAOs is detected as ISS. PolyP is stored as volutin granules as illustrated by the dark irregular spots in Figure 2, which are found in the cell cytoplasm. Depending on the sampling point and the influent composition, the proportions of polyP in the PAO vary and can reach a maximum of 0.38 mgP/mgPAOVSS (Wentzel *et al.*, 1990). The polyP content of PAOs is not measured analytically as there is currently no accurate and simple procedure to directly measure polyP. Instead, the polyP content is determined using the P removal, as discussed later in Section 4.1 (Henze *et al.*, 1995).

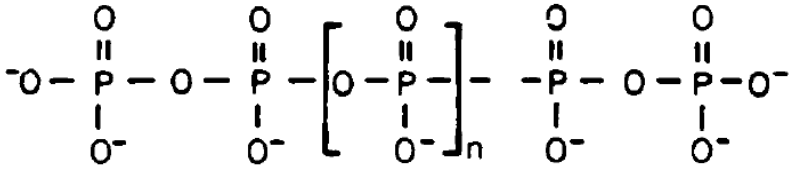

Figure 1. Linear polyP chain (Harold, 1966)

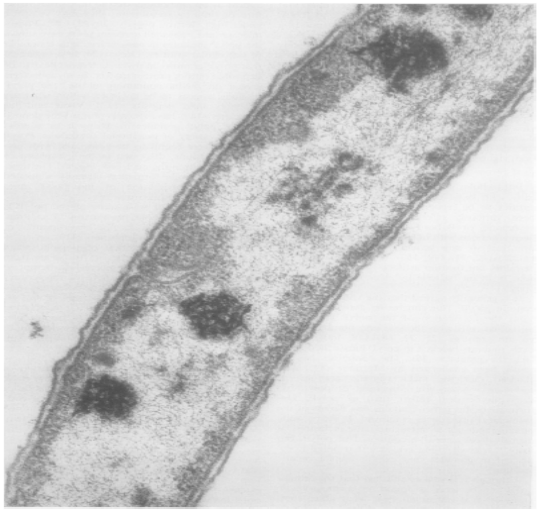

Figure 2. Volutin granules inside the cell wall of PAO (Harold, 1966)

Each monomer has a net negative charge. To neutralise the charge inside the PAOs, metal ions attach to the polyP (Harding & Ekama, 2009). The molar ratio of the metal ions is not fixed and has been shown to vary across different studies as demonstrated in Table 1**.** However, the charges of the metal ions attached to a phosphate ion should always add up to +1 such that the net charge of the polyP is zero.

Table 1. Ratio of counter-ions (K, Mg, Ca) to P in polyP molecules (Comeau *et al.*, 1986)

	P release	P release	P release or uptake	P release	P release	PolyP content	PolyP content
K^+/P	0.27	0.23	0.34	0.2	0.23	0.34	0.31
Mg^{2+}/P	0.26	0.32	0.24	0.28	0.27	0.30	0.30
Ca^{2+}/P	0.00	0.05	0.06	0.09	0.12	0.03	0.053
Charge balance	0.79	0.97	0.94	0.94	1.01	1.00	1.00
Study	Miyamoto-Mills *et al.* (1983)	Arvin and Holm Kristensen (1985)	Comeau *et al.* (1986)			Harding and Ekama (2009)	Ikumi (2015)

The concentration of Ca^{2+} (with respect to phosphorus) is relatively small as compared to the concentrations of Mg^{2+} and K^+, which both lie in the range 0.20-0.35. Miyamoto-Mills *et al.* (1983) did not measure any calcium. Except from the study done by Miyamoto-Mills *et al.* (1983), a neutral charge balance was always obtained over the polyP molecule. There is no clear trend in the cation content of polyP. The Mg:P, K:P or Ca:P ratios are not constant across the different studies. The factors influencing the ratio of the cation concentration to phosphorus in polyP is currently not well-established. The ISS contribution of the polyP is approximately 3.19 mgISS/mgP (Ekama & Wentzel, 2004), but can vary depending on its elemental composition.

2.2.3 Mineral precipitates

The formation of mineral precipitates depends strongly on ion concentrations. At high ionic concentrations, the ionic product exceeds the solubility product and mineral solids precipitate out of solution. In WWTP, high ionic concentrations generally occur in AD or AAD units. This is specially the case when the sludge contains high concentrations of N and P, such as in EBPR waste activated sludge. In conventional AS systems, the formation of mineral precipitates has rarely been observed due to high retention times and low ionic concentrations. Conversely, mineral precipitates are present in membrane EBPR AS systems due to high ionic concentrations and availability of nucleation sites. On the lab-scale membrane bioreactor (MBR) UCT AS system, mineral precipitates were detected on the membranes during operation.

Musvoto *et al.* (2000) outlined the different types of mineral precipitates that can be present in wastewater based on previous literature (Abbona *et al.*, 1982). In the physico-chemical model developed by Musvoto *et al.* (2000), these identified mineral precipitates were modelled as potential solid phases. This model has been used extensively for the simulation of the liquid-solid interphase transfer processes in AAD and AD units, and has shown close correlation with

experimental measurements (Van Rensburg *et al.*, 2003; Ekama *et al.*, 2006). The following sub sections describe the possible mineral precipitates as identified by Musvoto *et al.* (2000) and reviews the simulation results from subsequent studies using this model.

2.2.3.1 Magnesium phosphates

In the presence of magnesium, orthophosphate (OP) and ammonium species in solution, four precipitates can form: struvite [$MgNH_4PO_4.6H_2O$], newberyite [$MgHPO_4.3H_2O$], trimagnesium phosphate dihydrate [$Mg_{3(}PO_4)_2.2H_2O$] and bobierrite [$Mg_3(PO_4)_2.8H_2O$]. Struvite precipitates at a neutral and higher pH provided that the Mg/Ca molar ratio >0.6; newberyite precipitates significantly only at a lower pH (<6.0) and at high concentrations of Mg and P; trimagnesium phosphate dihydrate, having a low precipitation rate (Mamais *et al.*, 2019), does not form in the pH range in digestors (6.0-9.0) (Musvoto *et al.*, 2000).

The physico-chemical model developed by Musvoto *et al.* (2000) has been widely integrated with other models to simulate the liquid-solid interphase transfer processes in wastewater treatment unit operations. To calibrate this model, Musvoto *et al.* (2000) carried out experiments on the aeration of two types of anaerobic digestates and compared the results to simulated data. The first simulation modelled the aeration of sewage sludge digestate supernatant, which correlated well with experimental measurements. Two types of magnesium phosphates formed part of the possible solid phases namely, struvite and newberyite. The former was the major precipitate (85%) whilst the latter occurred in small amounts (0.2%). The second simulation involved the aeration of spent wine digestate supernatant, which yielded very similar results except for the proportion of struvite which decreased slightly (82.3%) due to the formation of magnesite.

Most studies on aeration of anaerobic digester supernatant or mixed liquor have demonstrated that struvite is the major form of precipitate whilst newberyite occurred in negligible quantity (Ekama *et al.*, 2006; Kazadi *et al.*, 2015). However, a study by Vogts (2015) on aerobic digestion of NDEBPR WAS did not show any struvite precipitation even though it was considered as a possible solid phase in the chemical equilibria model. The main forms of precipitates from the model were newberyite and bobierite. This is because nitrification is allowed to occur prior to any precipitation in the model. Consequently, the ammonia concentration in the modelled aqueous phase is too low to support struvite precipitation. Yet, it is more likely that precipitation is occurring simultaneously with nitrification. As opposed to Musvoto *et al.* (2000), Vogts (2015) did not use a kinetic approach but a chemical equilibrium approach to model precipitation, which is more difficult to integrate with biological processes modelled kinetically (Henze *et al.*, 2008).

2.2.3.2 Calcium phosphates

In the presence of calcium and phosphate ions, five calcium phosphate crystals can precipitate from solution. These are classified in order of decreasing solubility as follows: hydroxyapatite [HAP, $Ca_5(PO_4)_3OH$], tricalcium phosphate [TCP, $Ca_3(PO_4)_2$], octacalcium phosphate [OCP, $Ca_8(HPO_4)_2(PO_4)_4.5H_2O$], monenite [DCP, $CaHPO_4$] and dicalcium phosphate dihydrate [DCPD, $CaHPO_4.2H_2O$] (Musvoto *et al.*, 2000). As HAP is the thermodynamically most stable phase, it is most likely to precipitate. However, other calcium phosphate species such as

amorphous calcium phosphate (ACP; with approximate formulation $Ca_3(PO_4)_2.xH_2O$), OCP and DCPD act as precursors. From experimental investigations, it was found that in highly supersaturated solutions containing Ca, Mg and P, DCPD and ACP are the phases that precipitate first, with DCPD precipitating at low pH (<7.0) and ACP at higher pH (Musvoto *et al.*, 2000). The conversion of ACP to HAP depends on several factors. ACP is stabilized by high Mg/Ca ratio, high ionic strength, lack of HAP seed material, high HCO_3^-/PO_4^{3-}molar ratio, presence of pyrophosphate as well as certain proteins. Moreover, the conditions in wastewaters slow the conversion of ACP to HAP such that for the retention time of AAD or AD <60 days, this conversion does not take place (Musvoto *et al.*, 2000).

In the light of the abovementioned reasons, ACP was set as the only possible calcium phosphate mineral precipitate to form when Musvoto *et al.* (2000) simulated the aeration of anaerobic digester supernatant. Hence, ACP was the next major mineral precipitate (11.1% and 13.3% for sewage sludge and spent wine digestate, respectively) after struvite. Other studies have also found ACP as the second major precipitate during AAD simulations (Ekama *et al.*, 2006; Kazadi *et al.*, 2015). Kazadi *et al.* (2015) allowed for the formation of ACP, OCP and DCPD when simulating aeration of piggery (spiked with PO_4) and sewage sludge digestate and synthetic wastewater. ACP precipitated in small quantities in the sludge digestate whilst OCP and DCPD were sparsely detected in the synthetic wastewater. The results agree with the above paragraph as the pH of the synthetic wastewater at a value of 2.5 was much lower than that of the sludge digestate (7.3-7.4). During the simulation of anaerobic digestion of NDEBPR WAS, the ACP concentration was much lower (2.6%) (Van Rensburg *et al.*, 2003). This could be due to the high level of ammonia (as nitrification is inhibited in anaerobic conditions) which favours the precipitation of struvite over ACP.

The state of hydration of ACP used in physico-chemical models is not explicit from the previous studies. Some authors have not specified the state of hydration (Musvoto *et al.*, 2000; Ekama *et al.*, 2006) in the models whilst others assumed no hydration at all (Van Rensburg *et al.*, 2003; Kazadi *et al.*, 2015). Studies on crystallization of calcium phosphates have shown that the state of hydration of ACP is 15-20% by weight which corresponds to x=3-4.5 in the molecular formula: $Ca_3(PO_4)_2.xH_2O$ (Wang & Nancollas, 2008).

2.2.3.3 Other mineral precipitates

Given that Ca is present in solution, three crystalline structure of $CaCO_3$ can precipitate, namely: calcite, aragonite and vaterite. The factors determining which form precipitates include temperature, degree of supersaturation, presence of foreign ions, nucleation, and crystal growth rate (Musvoto *et al.*, 2000). Calcite is the most thermodynamically stable structure at ambient temperature and atmospheric pressure. Hence, calcite is expected to precipitate in WWTP units. Magnesium carbonates and calcium magnesium carbonates can also precipitate from the mixture of ions found in wastewater. Two forms of magnesium carbonate are possible, namely: magnesite [$MgCO_3$] and nesquehonite [$MgCO_3.3H_2O$]. The former is stable below a pH of 11 whilst the latter is not. Thus, in WWTP units where pH is normally considerably less than 11, it is expected that magnesium carbonates exist as $MgCO_3$. Calcium magnesium carbonates exist as two forms, namely: dolomite [$CaMg(CO_3)_2$] and huntite [$CaMg(CO_3)_4$]. However, attempts to precipitate

both dolomite and huntite under atmospheric conditions have failed and thus it is not likely that these precipitates can form in WWTP units (Musvoto *et al.*, 2000).

Calcite is included in the physico-chemical model of Musvoto *et al.* (2000). When modelling the aeration of sludge digestate, a small concentration of calcite was predicted (3.7% by mass of all precipitates) in sewage sludge digestate whereas no calcite formation was predicted in spent wine digestate. The precipitation rate of calcite is sensitive to the concentration of magnesium, dissolved organic compounds, iron, organic and inorganic phosphates. Fe^{2+} is the strongest inhibitor and can considerably reduce the precipitation rate of calcite at even low iron level (Dromgoole & Walter, 1990). Mg^{2+} is the weakest inhibitor and the extent of inhibition depends on the Mg:Ca and Mg:P ratios, with precipitation rate decreasing with increasing Mg:Ca ratio and enhanced with Mg:P ratio between 1.5 and 2 (Danen-Louwerse *et al.,* 1995). The Mg:Ca ratio in the two sludge digestates was slightly higher for the spent wine digestate supernatant. Thus, the absence of calcite precipitation in the simulation of the aeration of spent wine digestate could be due to Mg/Ca ratio. Musvoto *et al.* (2000) also suggested that the slightly higher organic content in the spent wine digestate inhibited calcite precipitation. As Fe^{2+} concentration was not measured, its effect on calcite precipitation was not discussed. Negligible concentrations of calcite were predicted in the aeration of swine wastewater and anaerobic digestion liquor (Van Rensburg *et al.*, 2003; Ekama *et al.*, 2006). Low concentrations of calcite were reported in synthetic wastewater, and during the aeration of piggery and sewage sludge digestate (Kazadi *et al.*, 2015).

Like calcite, the formation of magnesite has generally been negligible when modelling WWTP unit processes. Ekama *et al.* (2006) and Musvoto *et al.* (2000) reported negligible concentrations of magnesite during the simulation of swine wastewater and sewage sludge aeration, respectively. Trivial amounts of magnesite were also reported in the simulation of anaerobic digestion liquor (Van Rensburg *et al.*, 2003). Kazadi *et al.* (2015) did not report any formation of magnesite in synthetic wastewater, and the aeration of piggery and sludge digestate. However, low concentrations of magnesite (40 mg/L, 4.3% by mass of all precipitate) were predicted in the aeration of spent wine digestate (Musvoto *et al.*, 2000). The pH was particularly high (> 9), and the solution was oversaturated with respect to magnesite as most of the carbonate species exist as CO_3^{2-}. Vogts *et al.* (2015) also predicted the formation of magnesite during the aerobic treatment of NDEBPR WAS. In their simulation, there was no formation of struvite. Hence, the competition for Mg uptake was significantly reduced and the Mg concentration was not a limiting factor to the formation of magnesite.

2.2.4 Closure

The main forms of ISS as discussed above are described as follows: the raw wastewater influent ISS, ISS fraction of biomass, polyPs and mineral precipitates. Various forms of precipitates can exist from the available ions present in the WWTP units. Nonetheless, through simulation and experimental observations, it was deduced that the major forms of precipitates that can possibly exist at any point in a WWTP plant are struvite and ACP. Considering the other precipitates present in much smaller quantities (such as CaCO3, MgCO3 or $Mg_3(PO_4)_2$) adds complexity to the ISS characterisation procedure without considerably improving the end-result. Hence, from

this point forward, the only mineral precipitates present in NDEBPR sludge are considered to be struvite and ACP.

2.3 Plant-wide tracking of ISS components

With changes in the conditions, such as temperature, pressure, DO, pH or ion concentrations, in the different WWTP units, inorganic solids can also form or change state. Subsequently these changes have the potential to further alter the bio-chemical processes occurring in the units. It is thus important to track the components of inorganic solids in the different units. Currently, inorganic solids are only measured as a lumped sum of their mass in the total solids test. However, it is more important to obtain the individual concentrations of the inorganic solids as each react differently to different conditions. To facilitate this discussion, a typical NDEBPR system, followed by sludge treatment is illustrated in Figure 3.

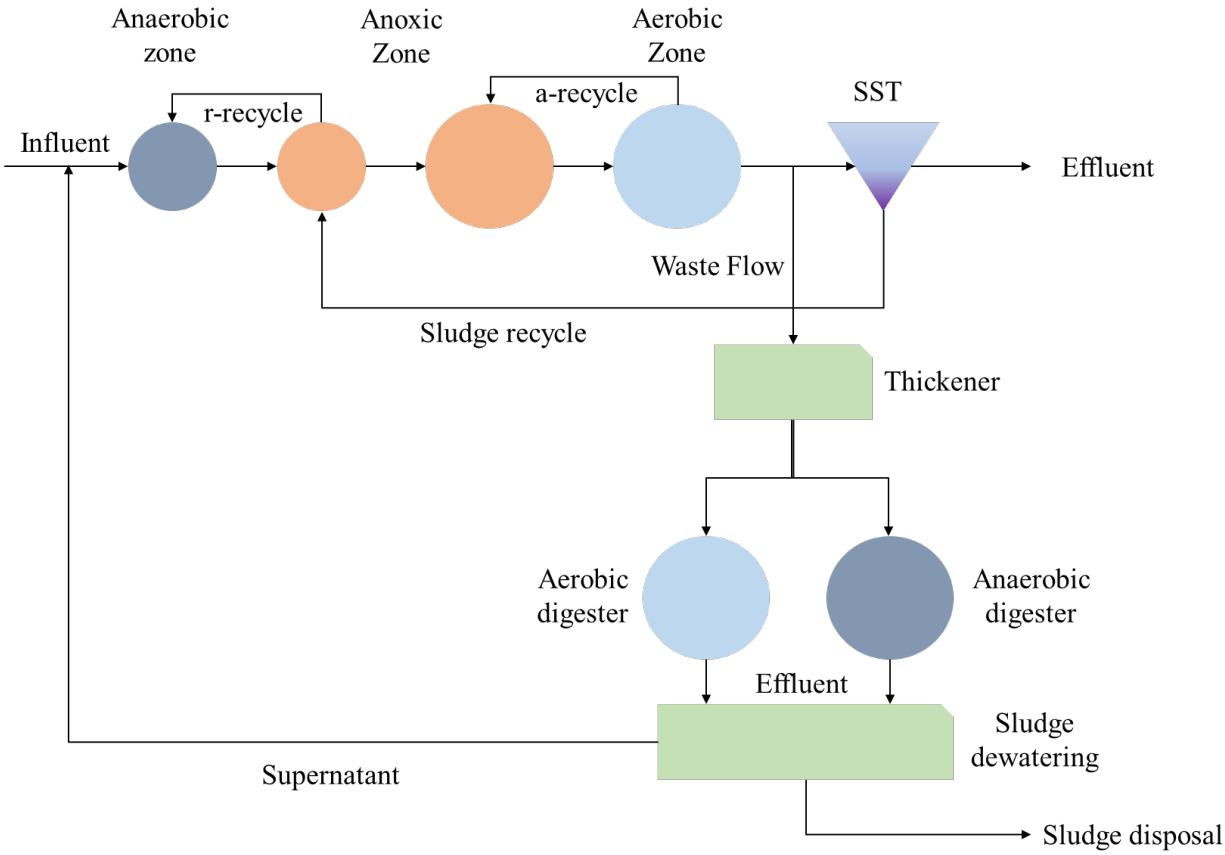

Figure 3. NDEBPR system with sludge treatment processes. Adapted from Henze *et al.* (2008)

2.3.1 Influent wastewater

The influent inorganic solids have been described as a group of inert solids that accumulates in the biological reactor (Wentzel et al., 2002; Ekama & Wentzel, 2004). Up to now, no research has explicitly identified the different components of the influent inorganic solids and investigated how each component behaves in the unit reactors. Sediments such as clay, silt or sand form part of the influent ISS (Ikumi, 2015) and accumulate in the reactor as they are stable compounds. The presence of mineral precipitates in the influent wastewater is also possible but has not been

investigated in the past due to the complexity of modelling influent wastewater and the lack of a characterisation procedure for ISS. Furthermore, due to low ionic products, lack of nucleation sites, turbulent conditions and inadequate mixing conditions, the formation of mineral precipitates is not favoured. It is thus assumed that influent wastewater contains negligible amount of mineral precipitate unless pre-precipitation is implemented. Pre-precipitation is not a common treatment method in EBPR activated sludge systems as the phosphorus attains very low concentrations such that EBPR is ineffective.

In the case where a primary settling tank is present, a fraction of the ISS settles and leaves as primary sludge. Measurements at the Mitchell's Plain WWTP on raw and settled wastewater showed that 5-15% of the raw ISS was settleable (Ekama & Wentzel, 2004). Heavy sediments such as sand makes up most of the settleable ISS. The settleability of mineral precipitates depend on the size of the crystals, affinity with other sludge particles and retention time of the PST. However, since the proportion of mineral precipitates in influent wastewater is deemed negligible, its contribution to the primary sludge is also insignificant.

2.3.2 Biological reactor

There are several assumptions made regarding the modelling of inorganic solids in a biological reactor. First, it is assumed that the influent ISS accumulates in the reactor based on the sludge age and does not participate in any biological or chemical reaction (Ekama *et al.*, 2006). As mentioned in the previous section, the influent wastewater contains mostly sediments in the form of sand, silt, or clay. These particles are very stable and unlikely taking part in any biological or chemical process, and would indeed simply accumulate in the bioreactor with solids retention time.

It is also assumed that there is no mineral precipitation or dissolution occurring in the biological reactor. In conventional biological reactors, mineral precipitation has rarely been observed due to the low retention time and ionic concentrations. However, in membrane reactors mineral precipitation on the membrane has been observed, especially when ions concentrations are high (Iorhemen *et al*., 2016). Membrane bioreactors (MBRs) are emerging as an alternative to the conventional activated sludge systems. Although MBRs have shown several advantages such as smaller WWTP footprint or independency from sludge settleability, they are prone to membrane fouling. The membrane foulants occur mostly in the form of bacterial deposition (bio-foulant) or organic particles (organic foulant). Nonetheless, if ionic concentrations become too high, mineral precipitates can potentially foul the membrane. This was observed in the lab-scale MBR system at the Water Quality lab at the UCT. The membrane had to be cleaned frequently when calcium and phosphorus concentrations were high as ACP was fouling the membrane. The early detection of mineral precipitates in the sludge can help lower the frequency of membrane cleaning.

The conditions inside the biological reactors allow for the growth of several microorganisms which contributes to the reactor ISS in two forms: biomass ISS and polyP. Microorganisms uptake inorganic dissolved solids as an essential requirement for their growth. These ions are present in the liquid phase inside the biomass in the reactor. However, when the total solids test is performed, these ions precipitate out of the solution when the sludge samples are dried. Thus,

they reflect as part of the ISS fraction (Ekama & Wentzel, 2004). The ISS contribution of the active biomass is 0.15 mgISS/mgPAOVSS (or OHOVSS) (Ekama & Wentzel, 2004).

Polyphosphate forms a major part of ISS in EBPR systems. EBPR systems consist of an anaerobic and aerobic zones as shown in Figure 3. In the anaerobic zone, PAOs use up their polyP reserve to uptake volatile fatty acid (VFA) and form high energy poly-hydroxy-alkanoates (PHA; high energy storage organics, of which PHB is a common form). OP and attached metal cations (see Section 2.2.2) are consequently released in the bulk solution. In the aerobic region, the PAOs use up their PHA reserve for growth and replenish their polyP reserves (using oxygen as the terminal electron acceptor). A higher uptake of phosphorus occurs in the aerobic zone as new growth happens. Thus, the polyP concentration is normally the lowest in the anaerobic zone and highest in the aerobic zone. Figure 4 shows the observations made on an anaerobic-aerobic sequence batch reactor.

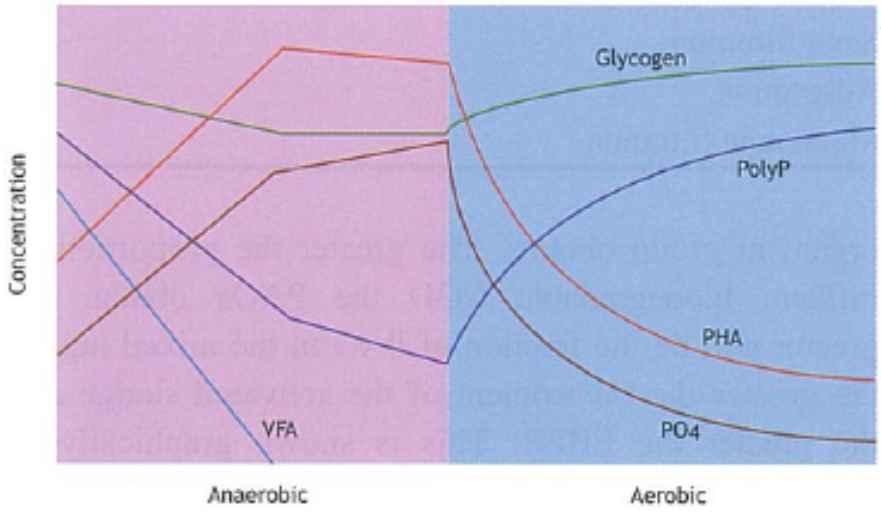

Figure 4. Schematic diagram showing the changes in concentration of VFA, phosphate, PHA, glycogen and polyP with respect to time in anaerobic and aerobic zones (Henze *et al.*, 2008)

There is a decrease in polyP and VFA concentrations and an increase in the PHA concentration in the anaerobic zone with time. In the aerobic zone, the level of polyP increases whilst PHA and OP concentrations decrease with respect to time. Glycogen is used as source of electron for cell maintenance (Henze *et al.*, 2008) or as a source of electrons and protons for the formation of reducing agents (Ikumi *et al.*, 2019). As polyP is an inorganic solid with an ISS:P ratio of approximately 3.19 mgISS/mgP (see Section 2.2.2), it contributes significantly to the PAO mass. Given a fully aerobic P uptake, the ISS contribution of PAO is 1.30 mgISS/mgPAOVSS with only 0.15 mgISS/mgPAOVSS reserved for the biomass inorganic fraction (Ekama & Wentzel, 2004). Hence, as polyP level increases between the anaerobic and aerobic zone, the ISS level rises significantly

Using experimental data from the operation of a MBR NDEBPR by Harding and Ekama (2009), the relative concentrations of ISS and ISS constituents in the biological reactors are reported in Figure 5. Four sludge samples were selected for this purpose. The AS systems, fed with municipal water were operating at steady state and the Wentzel *et al.* (1990) steady state model was used to simulate biological processes. Close correspondence with experimental data was

generally observed. The VSS, TSS and ISS masses shown in Figure 5 were measured using the total solids test as described in Section 3.5.1.

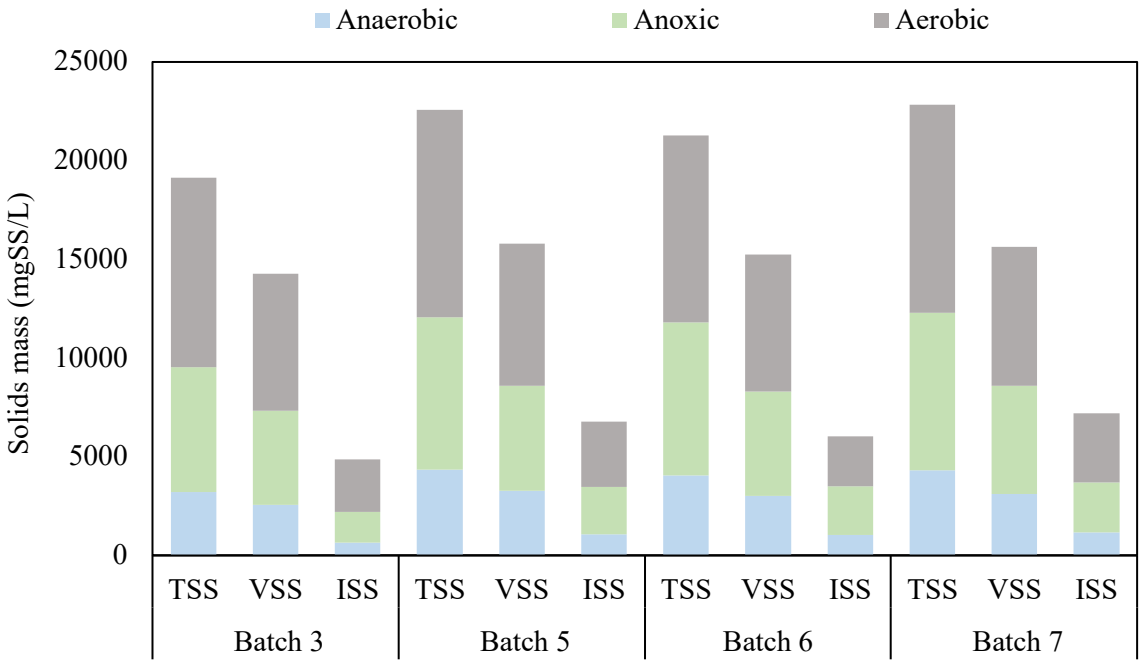

Figure 5. TSS, VSS and ISS concentration in the anaerobic, anoxic and aerobic reactor of a NDEBPR system (Harding & Ekama, 2009)

On average, the VSS and ISS concentration in the aerobic reactor were 1.4 and 2.4 times the concentration in the anaerobic reactor, except for batch 6. The ISS concentration was sensitive to the PAO VSS concentration, which contains high concentration of the inorganic polyP. For batch 6, it was speculated that considerable anoxic P uptake by PAOs occurred, which decreased the efficiency of P uptake and polyP formation in the aerobic reactor.

Ekama and Wentzel (2004) applied the ISS model to predict the composition of ISS in a nitrification-denitrification (ND) and NDEBPR systems treating raw wastewater with an ISS/COD ratio of 0.031 mgISS/mgCOD. In this model, 0.15 mgISS/mgOHOVSS was used for OHO biomass ISS. For the determination of the total PAO ISS concentration (which includes polyP and biomass ISS), the mass fraction 1.30 mgISS/mgPAOVSS. This fraction was based on the assumption of a maximum phosphorus content of 0.38 mgP/mgPAOVSS (Wentzel *et al.*, 1990). The ISS content of each component was calculated for different sludge ages based on the principles and formulae provided in Section 2.4.1. Figure 6 and Figure 7 show the results for the ND and NDEBPR systems, respectively. It can be observed that as the sludge age increases the influent ISS contributes more to the reactor ISS. As compared to the ND/FA system, the influent ISS contributes significantly less to the total ISS in the NDEBPR system. This agrees with observations made by Harding and Ekama (2009). For sludge age less than 5 days in the ND/FA systems and at all sludge ages in the NDEBPR system, the influent ISS contribution has a small effect on the reactor ISS. For these systems, the reactor ISS is strongly affected by the active biomass. For the NDEBPR system, the polyP content of the PAOs considerably affects the reactor ISS concentration whilst OHO and PAO biomass ISS constitute of a small percentage (approximately 10% for sludge ages greater than 10 days) of the total reactor ISS.

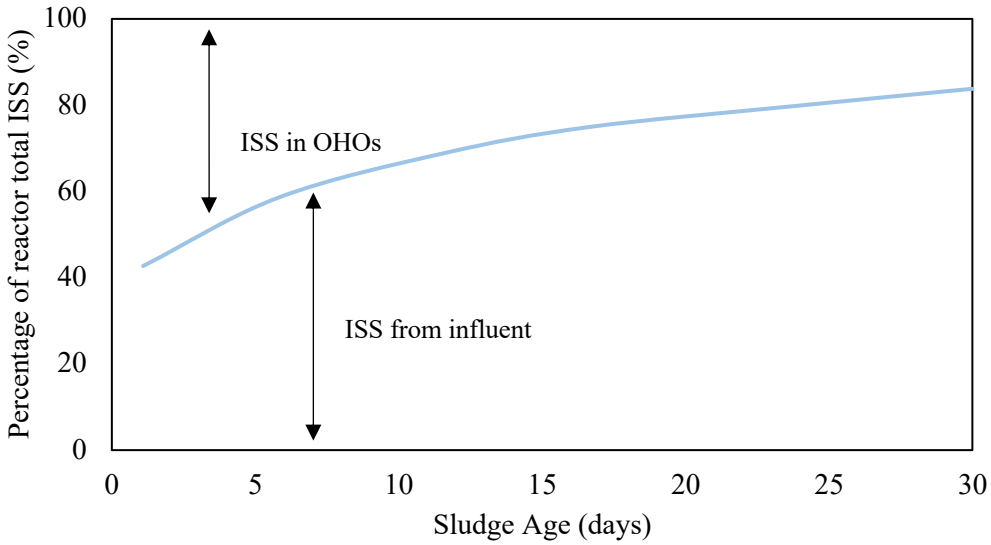

Figure 6. Model predicted percentage of reactor ISS for ND system (Ekama & Wentzel, 2004)

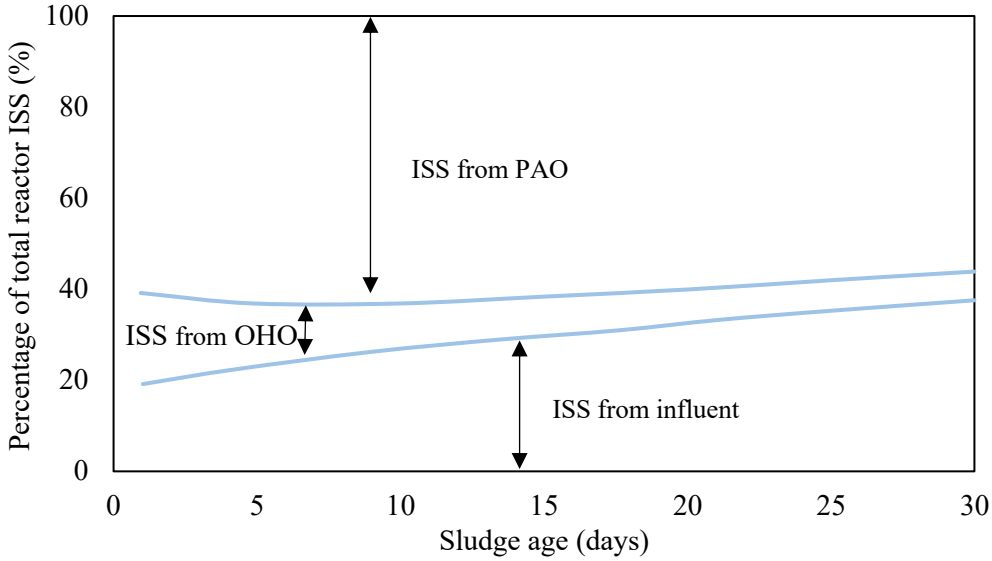

Figure 7. Model predicted percentage of reactor ISS for NDEBPR system (Ekama & Wentzel, 2004)

There is currently no standard laboratory test to determine the concentration of polyP in a sludge sample. The polyP concentration is determined by assuming a maximum polyP P (phosphate in polyP) uptake per PAO mass (0.38 mgP/mgPAOVSS). The PAO biomass concentration is determined assuming all the readily biodegradable organics are taken by the PAOs. Alternatively, the polyP concentration can be determined using the measured P removal (accounting for the P in biomass). Both methods have their limitations. The maximum polyP content is only achievable under certain circumstances. These include low anoxic P uptake, high influent P concentration and availability of cations (Mg, K and Ca). Thus, using the maximum polyP content potentially overpredicts the amount of polyP accumulated by the PAOs which also results in the overestimation of the ISS. When the polyP content is calculated from the P removal ($P_{polyP}=P_{ti} - P_{te} - P_s$), it can also overpredict the concentration of polyP if other forms of P removal is occurring simultaneously. This is particularly the case for membrane EBPR reactors where mineral precipitation can take place. Henceforth, acquiring a method to directly determine the

concentration of polyP in a sludge sample is highly beneficial towards the calibration of EBPR models.

2.3.3 Thickener

Two types of thickeners are typically used in WWTPs, namely: gravity and dissolved air floatation (DAF) thickeners. The former is not used to thicken EBPR WAS as anaerobic conditions inside the thickener cause the release and hydrolysis of polyP. The latter is used to thicken EBPR WAS as it ensures an aerobic environment that prevents the premature release of phosphorus from polyP. Provided an EBPR state is achieved, EBPR WAS contains low levels of soluble phosphorus, ammonia, and metal cations. Thus, precipitation is not likely to occur in DAFs.

In practice, high concentrations of OP, FSA and metal cations have been observed in the thickener supernatant (Barat *et al.*, 2009). This occurred due to the presence of anaerobic pockets in the DAF units. However, due to the low pH inside the thickener, precipitation did not occur.

Clarification or thickening are modelled as purely physical processes with no chemical or biological processes occurring (Takács *et al.*, 1991). When Kazadi *et al.* (2016) simulated the thickening of WAS from a NDEBPR system, the pH was significantly overpredicted. Although the author suggested that pH overprediction was attributed to the transformation of soluble organic compounds into VFA, it is also possible that the pH difference is due to the occurrence of mineral precipitation. As there is currently no existing procedure to differentiate between polyP and mineral precipitates, the quantification of mineral precipitates in the thickener cannot be performed.

2.3.4 Anaerobic digester

When modelling the AD of NDEBPR WAS, most authors have assumed that the feed ISS is made up of polyP, biomass and the influent wastewater ISS (Harding & Ekama, 2009; Ikumi, 2015) but contains no mineral precipitate. Upon entrance in the AD, OP and metal ions are released into the bulk solution due to polyP hydrolysis (Barat *et al.*, 2009). Precipitates start forming as ion concentration increases. The accumulated influent ISS is carried over to the AD. Thus, the sludge in the AD is assumed to be made up of mineral precipitates and the accumulated influent ISS. Figure 8 summarises the constituents of ISS in the feed and effluent, as well as the ISS-related processes occurring in the AD.

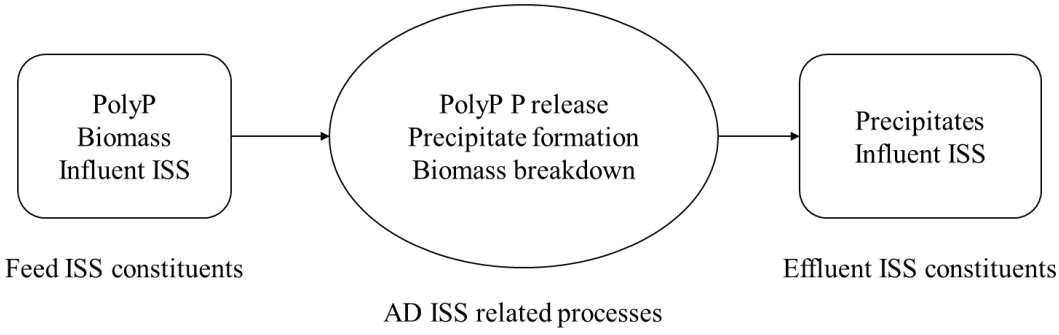

Figure 8. The ISS constituents in the NDEBPR WAS feed and the effluent

Under anaerobic conditions, PAOs use their high energy polyP bonds to form PHAs. In the subsequent aerobic conditions, the PHA molecules are used for growth. In the case of the AD, the PAOs are not aware of the absence of a subsequent aerobic zone and starts using up their polyP reserve (Ikumi *et al.*, 2019). Harding and Ekama (2009) showed that all polyP were released under anaerobic conditions after five days. This was deduced from the variation of TP and OP with time, with the OP concentration closest to TP concentration after five days. Nonetheless, the maximum OP concentration observed was not equal to the predicted OP concentration, which was calculated as 97% of the TP (based on a biomass P fraction 0.03 mgP/mgVSS). When comparing the Mg, NH_4 and K concentrations, it was clear that mineral precipitation of struvite ($MgNH_4PO_4.6H_2O$) occurred as the K concentration was much higher than the Mg and NH_4 concentrations. It was concluded that all polyP was indeed released within five days, but the OP was captured in struvite. This correlated closely with Jardin *et al.* (1994), who obtained a complete polyP release after seven days. Hence, for AD normal operating sludges (>5 days), the effluent is expected to contain no polyP. These findings and assumptions can be experimentally confirmed with the development of a characterisation procedure for ISS which can potentially differentiate between polyP and mineral precipitates.

The formation of precipitates has been reported widely during the AD of NDEBPR WAS (Van Rensburg *et al.*, 2003; Harding & Ekama, 2009; Ikumi, 2015). Mineral precipitation is a concentration-driven process. During the AD of NDEBPR WAS, the increase in the concentration of soluble ions (and the higher pH) favours precipitation. The OP concentration increases as polyP is used up by PAOs or as PAOs are hydrolysed by the AD biomass. Soluble ammonium concentration also rises as biomass and complex proteins are hydrolysed by the AD biomass. Magnesium and calcium ions are released in the bulk solution as polyP is used up. Consequently, the ionic products of the different possible solid phases exceed their solubility products and precipitation is favourable. The different mineral precipitates are not quantified experimentally since there is currently no developed inorganic characterisation procedure. Instead, the concentrations of the mineral precipitates are calculated by fitting the specific rate constant to the measured soluble ion concentrations (Musvoto *et al.*, 2000; Batstone *et al.*, 2015). Using this modelling approach with the AD of NDEBPR WAS, Ikumi (2015), Van Rensburg *et al.*(2003) and Kazadi *et al.* (2015) observed that struvite was the major precipitate with minor quantities of ACP. This agrees with observations made at WWTP where struvite precipitation has been extensively observed to form on the walls and pipes of anaerobic digestors treating NDEBPR WAS (Maqueda *et al.*, 1994). Calcite and magnesite have not been reported during the AD of NDEBPR WAS.

2.3.5 Closure

It can be concluded there is uncertainty in the form of inorganic solids is in the NDEBPR sludge, the thickening units, as well as any downstream sludge treatment units. The reason for this uncertainty is mostly due to the lack of an ISS characterisation process that can determine the concentration of each inorganic solids.

2.4 Modelling of ISS in WWTP units

Up until now, the modelling of ISS has not received the same attention as the modelling of VSS in WWTP units. In the steady-state AS models, the TSS, which is the sum of ISS and VSS, was calculated empirically based on an assumed VSS/TSS (f_i) ratio (WRC, 1984). This ratio was estimated from historical data and depended on the type of wastewater or type of activated sludge systems. For EBPR systems, the reactor TSS concentration was calculated from a constant VSS/TSS ratio of 0.46 for PAOs and their endogenous residue to account for polyP. When developing activated sludge models, for each component of the sludge i.e. PAO and OHO biomass, endogenous residue and UPO, a fraction of their mass was attributed an ISS mass (Wentzel *et al.*, 2002). However, using this approach a significant difference between the measured and modelled influent ISS was observed. Another approach was then employed by Ekama and Wentzel (2004) which was validated against 48 experimental investigations. The Ekama and Wentzel ISS model (2004), which can be applied to AS and sludge treatment units, has shown close correlation with experimental observations and is described in Section 2.4.1.

Several models have been developed for sludge treatment units with mineral precipitation. Musvoto *et al.* (2000) established a kinetic-based model for multiple mineral precipitation, which is described in Section 2.4.2. This has since been integrated with the PWM_SA model of Ikumi *et al.* (2015) to simulate mineral precipitation in sludge treatment processes. Kazadi *et al.* (2015) also developed a similar model which has been integrated with benchmark simulation model No.2 (BSM2) plant wide model. This is described in section 2.4.3.

2.4.1 Ekama and Wentzel (2004) model

The reactor ISS concentration model (with no chemical precipitant addition) of Ekama and Wentzel (2004) is based on the following:

a) The inorganic solids in the influent (X_{Ioi}) accumulate in the reactor. The ISS contribution due to the influent ISS is given by Equation 2.1.

$$X_{Io} = X_{Ioi}\frac{R_s}{R_{hn}} \tag{2.1}$$

$Where,$

$X_{Io} = Accumulated\ influent\ ISS, in\ mgISS/L$

$X_{Ioi} = Influent\ ISS, in\ mgISS/L$

$R_s = Sludge\ age, days$

$R_{hn} = Hydraulc\ retention\ time, days$

b) Precipitation or dissolution of minerals in the AS systems is negligible.

c) Only the active biomass is considered to contain an inorganic fraction. The OHOs and PAOs take up dissolved solids intracellularly as part of their cell contents. During the drying step of the total solids test procedure, the cell contents precipitate as inorganic solids (Ekama & Wentzel, 2004). The contribution of autotrophic nitrifying organisms (ANOs) to ISS is considered negligible (<2%).

d) PAOs take up inorganic dissolved solids (IDS) to form polyPs.

Hence, following the above statements, the reactor ISS concentration is given by Equation 2.2.

$$X_{Io} = X_{Ioi}\frac{R_s}{R_{hn}} + X_v(f_{\text{iOHO}}f_{avOHO} + f_{\text{iPAO}}f_{avPAO}) \quad (2.2)$$

$$\begin{aligned} &Where, \\ f_{iOHO} &= Inorganic\ mass\ fraction\ of\ OHOs \\ f_{avOHO} &= Active\ mass\ fraction\ of\ OHOs \\ f_{iPAO} &= Inorganic\ mass\ fraction\ of\ PAOs \\ f_{avPAO} &= Active\ mass\ fraction\ of\ PAOs \\ X_v &= Volatile\ solids\ concentration \end{aligned}$$

The fraction of active OHO and PAO biomass can be determined from the existing activated sludge models. The inorganic fractions of the active biomass were determined experimentally by Ekama and Wentzel (2004). By feeding synthetic wastewater containing no influent inorganic solids, it was determined that the inorganic mass fraction of OHOs biomass (f_{iOHO}) was equal to 0.15 mgISS/mgVSS. The inorganic fraction of the PAOs (f_{iPAO}) was observed to be proportional to the PAOs polyphosphate content and is given by Equation 2.3. The portion of this inorganic mass fraction that is attributed to the biomass of PAOs (f_{iPAOBM}) was determined to be equal to the inorganic mass fraction of OHO biomass (the remainder being due to polyP). Moreover, in order to use the reactor ISS model, the influent inorganic solid concentration (X_{Ioi}, in mg ISS/L) must be measured experimentally.

$$f_{iPAO} = f_{iPAOBM} + 3.286(f_{XBGP} - f_{XBGPBM}) \quad (2.3)$$

$$\begin{aligned} &Where, \\ f_{iPAO} &= Inorganic\ mass\ fraction\ of\ PAOs \\ f_{iPAOBM} &= Inorganic\ mass\ fraction\ of\ PAOs\ biomass \\ f_{XBGP} &= Total\ P/VSS\ fraction\ of\ PAOs \\ f_{XBGPBM} &= Biomass\ P/VSS\ fraction\ of\ PAOs \end{aligned}$$

When integrating Equation 2.2 with Wentzel *et al.* (1990) NDEBPR AS model, the following equations were obtained for VSS, ISS and TSS masses (Ekama & Wentzel, 2004).

$$\begin{aligned} \frac{MX_v}{MS_{ti}} = (1 - f_{S\prime us} - f_{S\prime up})[(1 - \frac{\%}{100}f_{Sb\prime s})\frac{Y_H R_s}{1 + b_{HT}R_s} \times (1 + f_{EH}b_{HT}R_s) \\ + \frac{\%}{100}f_{Sb\prime s}\frac{Y_G R_s}{1 + b_{GT}R_s}(1 + f_{EG}b_{GT}R_s] + \frac{f_{S\prime up}}{f_{cv}}R_s \end{aligned} \quad (2.4)$$

$$\begin{aligned} \frac{MX_{Io}}{MS_{ti}} = (1 - f_{S\prime us} - f_{S\prime up})[(1 - \frac{\%}{100}f_{Sb\prime s})\frac{Y_H R_s}{1 + b_{HT}R_s}f_{iOHO} \\ + \frac{\%}{100}f_{Sb\prime s}\frac{Y_G R_s}{1 + b_{GT}R_s}f_{iPAO}] + \frac{X_{Ioi}}{S_{ti}}R_s \end{aligned} \quad (2.5)$$

$$\frac{MX_t}{MS_{ti}} = (1 - f_{S\prime us} - f_{S\prime up})[(1 - \frac{\%}{100} f_{Sb\prime s}) \frac{Y_H R_s}{1 + b_{HT} R_s} \times (1 + f_{EH} b_{HT} R_s + f_{iOHO}) + \frac{\%}{100} f_{Sb\prime s} \frac{Y_G R_s}{1 + b_{GT} R_s} (1 + f_{EG} b_{GT} R_s + f_{iPAO}] + (\frac{f_{S\prime up}}{f_{cv}} + \frac{X_{Ioi}}{S_{ti}}) R_s \quad (2.6)$$

$Where,$

$MX_v = Mass\ of\ volatile\ solids, in\ mgVSS$

$MX_t = Mass\ of\ total\ solids, in\ mgTSS$

$MX_{io} = Mass\ of\ inorganic\ solids, in\ mgISS$

$MS_{ti} = Total\ influent\ COD\ mass, in\ mgCOD$

$f_{S\prime us} = Fraction\ of\ total\ COD\ that\ is\ unbiodegradable\ soluble$

$f_{S\prime up} = Fraction\ of\ total\ COD\ that\ is\ unbiodegradable\ particulate$

$f_{Sb\prime s} = Fraction\ of\ biodegradable\ COD\ that\ is\ soluble$

$f_{EH} = Unbiodegradable\ fraction\ of\ fraction\ of\ OHOs = 0.20$

$Y_H = Yield\ of\ OHOs = 0.45\ mgVSS/mgCOD$

$b_{HT} = Death\ rate\ of\ OHOs, in\ d^{-1}$

$Y_G = Yield\ of\ PAOs = 0.45\ mgVSS/mgCOD$

$b_{GT} = Death\ rate\ of\ PAOs, in\ d^{-1}$

2.4.2 Musvoto *et al.* (2000) Physico-chemical model

2.4.2.1 Mixed weak acid/base system

Musvoto *et al.* (2000) developed a three-phase kinetic based physico-chemical model. For the mixed weak acid/base system, a kinetic approach is used rather than the widely accepted equilibrium approach (Loewenthal *et al.*, 1989) as difficulties (such as choosing a reference species) were encountered when integrating the physico-chemical model. The mixed weak acid/base system is described in terms of rate equations. Equation 2.7 and 2.8 show an example of the rate equations for the ammonia system.

$$r_f = K_f(NH_4^+) = K_r f_m[NH_4^+] = K_f'[NH_4^+] \quad (2.7)$$

$$r_r = K_r(NH_3) = K_r f_m[NH_3] = K_r'[NH_3] \quad (2.8)$$

$Where,$

r_f = rate of forward reaction

r_r = rate of reverse reaction

$f_m = Monoprotic\ activity\ coefficient$

$K_f = Specific\ rate\ constant\ for\ forward\ reaction$

$K_r = Specific\ rate\ constant\ for\ reverse\ reaction$

$K_f' = Apparent\ Specific\ rate\ constant\ for\ forward\ reaction$

$$K_r' = Apparent\ Specific\ rate\ constant\ for\ forward\ reaction$$

The values for the apparent specific rate constants are chosen such that the equilibrium is reached instantaneously. This approach of modelling mixed weak acid/base systems allows for a seamless integration with biological kinetic models and facilitates any further addition of other mixed weak acid/base systems.

2.4.2.2 Ion pairing

The effect of ion pairing was considered in the model for ionic strengths higher than 0.025. Lower ionic strengths were considered to have negligible effect on the concentration of free ions (Musvoto *et al.*, 2000). Similar to the mixed weak acid/base system, a kinetic approach was also considered for the ionic pairs with a forward and reverse kinetic equations.

2.4.2.3 Mineral precipitation

The rate of mineral precipitation in the model developed by Musvoto *et al.* (2000) is based on the theory of Koutsoukos *et al.* (1980). For surface-controlled processes, the latter stated that the rate of mineral precipitation of a sparingly soluble salt is given by Equation 2.9:

$$\frac{d}{dt}(M_{v+}A_{v-}) = -k's[([M^{m+}]^{v+}[A^{a-}]^{v-})^{1/v} - {K_{sp}}^{1/v}]n \quad (2.9)$$

$$Where,$$

$$\frac{d}{dt}(M_{v+}A_{v-}) = Rate\ of\ mineral\ precipitation$$

$$k' = Apparent\ precipitation\ constant$$

$$s = Factor\ for\ avaibility\ of\ growth\ site$$

$$[M^{m+}] = concentration\ of\ crystal\ lattice\ cation$$

$$[A^{a-}] = concentration\ of\ crystal\ lattice\ anion$$

$$v^+ = Total\ number\ of\ anionic\ species$$

$$v^- = Total\ number\ of\ cationic\ species$$

$$v = v^- + v^+$$

$$n = 2, for\ divalent\ sparing\ soluble\ salts$$

Similar to most mineral precipitation models, the rate of mineral precipitation is driven by the difference between the solubility product and the ionic product. In Equation 2.9, n is a constant determined experimentally and is equal to 2 for a number of divalent sparingly soluble salts. Musvoto *et al.* (2000) assumed that no seed material was initially present and simplified the k's term into k'$_r$. Although the dissociation of mineral precipitates affects the aqueous phase chemistry, it is not considered in this model.

2.4.3 Kazadi *et al.* (2015) multiple mineral precipitation model

The model developed by Kazadi *et al.* (2015) is also a kinetic-based approach. This precipitation model is based on a semi-empirical kinetic law (Nielsen & Toft, 1984). Equation 2.10 shows the rate equation, using calcite as example.

$$r_{CaCO_3} = k_{cryst}\, X_{CaCO_3}\, \sigma^n \quad (2.10)$$

$$\sigma = \left(\frac{(Ca^{2+}) \times (CO_3^{2-})}{K_{sp,calcite}}\right)^{0.5} - 1 \quad (2.11)$$

$Where,$

$r_{CaCO_3} = Rate\ of\ calcite\ precipitation$

$k_{cryst} = Empirical\ kinetic\ rate\ coefficient$

$X_{CaCO_3} = Concentation\ of\ calcite$

$\sigma = Supersaturation\ coefficient$

$(Ca^{2+}) = Activity\ of\ calcium\ ion$

$(CO_3^{2-}) = Activity\ of\ carbonate\ ion$

$K_{sp,calcite} = Solubility\ product\ of\ calcite$

As opposed to Musvoto *et al.* (2000), the presence of seed material was allowed in this model as a seed concentration of precipitate could be defined initially (i.e., at time zero). To obtain the initial mineral precipitate concentration, the ISS to the AAD or AD must first be characterised.

2.5 Wastewater characterisation

The aim of this section is to outline the current characterisation procedures and their limitations with respect to inorganic solids. In the following chapters, two characterisation procedures are discussed: influent wastewater and sludge characterisation. The latter has been discussed in detail as it was used to fractionate the NDEBPR WAS in this research.

2.5.1 Influent wastewater characterisation

Influent wastewater is generally classified based on the behaviours of the various compounds in the units of the WWTP. The organic and inorganic fractions of the wastewater are first divided based on their physical characteristics, into three groups: settleable, non-settleable and dissolved. For the organic fractions, each group is further divided into biodegradable and unbiodegradable. This is depicted by Table 2 below. The physical characterisation procedure involves the use of a solid-liquid separation process (such as sedimentation or filtration) followed by analytical measurements such as COD, FSA, TKN, total solids test, TP or OP. However, these tests cannot distinguish between biodegradable and unbiodegradable organics (Ikumi *et al.*, 2015).

The biodegradability of organics is determined by performing BOD test or taking measurements on the effluent and biological reactor mixed liquor at steady state. The COD of unbiodegradable soluble organic (USO) fraction is given by the effluent COD as USOs remains unchanged in the reactor. The difference between the COD of the total soluble and USO yields the COD of biodegradable soluble organic (BSO). The unbiodegradable particulate organic (UPO) is obtained by solving for $f_{S'up}$ in Equation 2.6 with the M_{XT} value obtained experimentally at steady state. The COD of the BPO is the difference between the COD of the total particulate and UPO. The $f_{S'up}$ ratio can also be obtained by using the experimentally measured OUR in the activated sludge (Henze *et al.*, 2008).

As observed from Table 2, the current characterisation process only divides the inorganic particulate fraction into settleable and suspended. All inorganic particulate matter is modelled to enmesh with the sludge mass without incurring any reaction such as dissolution (Ekama & Wentzel, 2004). The current activated sludge models do not account for precipitation unless chemical precipitants have been added. Precipitates, if formed, would be part of the inorganic settleable solids as they would enmesh with sludge mass and settle.

Table 2. Wastewater characterisation. Abstracted from Henze *et al.* (2008)

<table>
<tr><th colspan="4">Wastewater Constituents</th><th colspan="2">Reaction</th><th colspan="2">Sludge constituent</th></tr>
<tr><td rowspan="7">Organic</td><td rowspan="2">Soluble</td><td>Dissolved</td><td>Unbiodegradable</td><td colspan="2">Escapes with effluent</td><td colspan="2"></td></tr>
<tr><td>Dissolved</td><td>Biodegradable</td><td colspan="2">Transforms to active organisms</td><td rowspan="6">Total settleable solids</td><td rowspan="4">Volatile settleable solids</td></tr>
<tr><td rowspan="4">Particulate</td><td rowspan="2">Suspended</td><td>Unbiodegradable</td><td colspan="2">Enmeshed with sludge mass</td></tr>
<tr><td>Biodegradable</td><td colspan="2">Transforms to active organisms</td></tr>
<tr><td rowspan="2">Settleable</td><td>Unbiodegradable</td><td colspan="2">Enmeshed with sludge mass</td></tr>
<tr><td>Biodegradable</td><td colspan="2">Transforms to active organisms</td></tr>
<tr><td rowspan="6">Inorganic</td><td colspan="2" rowspan="2">Particulate</td><td>Settleable</td><td colspan="2">Enmeshed with sludge mass</td><td rowspan="5">Inorganic settleable solids</td></tr>
<tr><td>Suspended</td><td colspan="2">Enmeshed with sludge mass</td></tr>
<tr><td colspan="2" rowspan="4">Soluble</td><td>Precipitable</td><td colspan="2">Transforms to settleable solids</td></tr>
<tr><td rowspan="2">Biologically utilizable</td><td rowspan="2">Transferred to</td><td>Solids</td></tr>
<tr><td>Gas</td><td colspan="2">Escapes as gas</td></tr>
<tr><td>Non precipitable or bio-utilisable</td><td colspan="3">Escapes with effluent</td></tr>
</table>

2.5.2 EBPR waste activated sludge characterisation

The model developed by Sotemann *et al.* (2005) was originally used to simulate anaerobic digestion of primary sludge. Attempts to model the digestion of EBPR WAS with this model resulted in inaccurate predictions for methane and AD effluent characteristics (Quevauvilliers & Ikumi, 2021) since the characterisation procedure did not separate inorganic P from organic P. Thus, a new characterisation method was developed by Harding and Ekama (2009). Figure 9 illustrates the different fractions of the characterisation procedure.

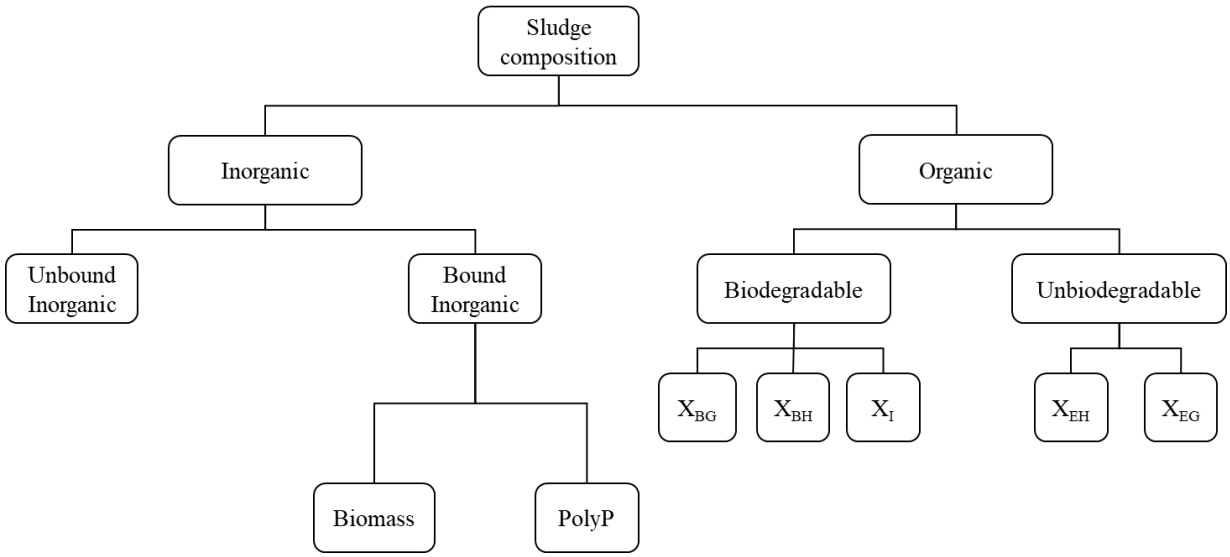

Figure 9. Fractions of Harding and Ekama (2009) characterisation procedure

As seen from Figure 9, three forms of ISS are modelled to form part of the WAS, which are subsequently modelled to be the influent ISS to sludge treatment processes. The three forms of ISS exist: the ISS accumulated in the reactor from the influent wastewater, the polyphosphates in PAOs and the ISS fraction of PAOs and OHOs biomass. The latter is not physically present in the sludge but only reflects during the total solids test. It is assumed that the EBPR WAS contains no precipitates. It is currently assumed that the constituent of the influent to the sludge treatment process remains the same as the WAS. Nonetheless, up to now there is no evidence that polyP remains intact and mineral precipitation does not occur between the AS and AD or AAD.

The formation of mineral precipitates (which are typically found in WWTP units) is favoured at high pH values but this process decreases the pH. If the mineral precipitates were present in the feed to the AD, they would dissolve if the pH dropped and would provide a pool of alkalinity. As the 5-point titration test is done on filtered samples only, this alkalinity is not detected. On top of the components mentioned in Figure 9, mineral precipitates also form part of the ISS mass during a total solids test (Asensi *et al.*, 2019). Thus, developing a test that quantifies each ISS component can help model the alkalinity generation in the AD which can ultimately lead to better pH predictions.

2.6 Potential methods for the characterisation of ISS

The ISS characterisation procedure is a two-phase process. The first phase is to develop a laboratory test that can dissolve mineral precipitates and leave polyphosphates in the solid phase

(Ikumi *et al*., 2019) or vice versa (dissolving polyphosphates and leaving mineral precipitates in the solid phase). The second phase is to develop a data-modelling procedure that uses the results of the laboratory test to fully characterise the ISS. In the this section, possible tests or conditions and their corresponding effects on mineral precipitates or polyP are reviewed to help in developing a laboratory test.

2.6.1 The use of dilution to dissolve mineral precipitates

Dilution of sludge can potentially dissolve the mineral precipitates and leave the polyP in the solid phase. After sufficient dilution, the ionic product of the several mineral precipitates falls below their solubility products. Thereafter, all mineral precipitates are dissolved in the diluted solution. When considering anaerobic digesters in EBPR systems, struvite and ACP have generally been modelled as the major form of precipitate with its concentration ranging from 500-1300 mg/L and 0-200 mg/L, respectively, depending on the influent composition and operating parameters. Assuming a K_{sp} value of 13.6 for struvite, a solution containing 1000 mg/L of struvite would require approximately 200 times dilution to reach Mg, P and N concentrations of less than 1 mg/L to prevent precipitation. Though this is a practically simple laboratory procedure, there is significant loss in accuracy, high variance and low reproducibility in measured data when dealing with very high dilutions. In this respect, suitable analytical methods should be employed to accurately measure such low concentrations.

For metal ions, inductively coupled plasma (ICP) can be used as it has very low detection limits (<100 µg/L) (APHA, 1985). For total phosphate, the ascorbic acid method is suitable for P concentrations less than 1 mgP/L (De Haas, 1998). There are several ways to measure low concentrations of ammonia, namely: ammonia selective electrode method, manual phenate method and automated phenate method (APHA, 1985). Except for the total phosphate ascorbic method, the other mentioned tests were not readily available at the Water Quality Laboratory (WQL) whereby experiments were conducted for this research. Another limitation of using the dilution method is the low rate of dissolution of the mineral precipitates. Due to the very low solubility of struvite and ACP, it is expected that both mineral precipitates take long to dissolve. During this time, the release of OP from polyP is possible as the sample turns anaerobic. Thus, it becomes complex to determine the origin of the OP in the bulk solution.

2.6.2 Applying elevated temperatures to release orthophosphates from PAOs

A second feasible condition that can be used to separate mineral precipitates and polyP is the application of heat to a NDEBPR WAS sample. Enhanced phosphorus recovery by thermal pre-treatment of NDEBPR WAS has been investigated extensively in the past. In this regard, Kuroda *et al.* (2002) and Tao and Xia (2007) have applied a temperature range of 50-90 ºC and 40-70 ºC to NDEBPR sludge, respectively. Kuroda *et al.* (2002) observed that 90% of the polyP initially present in the sludge was released in the bulk solution after 60 min at 70 ºC. The authors speculated that polyP was released due to the relatively high temperature disrupting the cell membrane, thereby allowing polyP to escape from inside the cell. However, this was not confirmed with SEM images of the sludge. It was deduced that with increasing temperature, both the rates of polyP hydrolysis and P release increase. Similar observations were made by Tao and

Xia (2007) even though the rate of polyP release was lower and the polyP was instantaneously hydrolysed to OP.

The effect of temperature on solubility of chemical precipitates is determined by the quantity of heat released or absorbed, as the precipitate dissolves (Bhuiyan *et al.*, 2007). If more energy is required to break the crystal structure of the solid as compared to the energy generated by interaction of the solids with the solvent, then the dissolution reaction is endothermic. According to Le Chatelier's principle, by increasing the temperature the dissolution reaction is favoured in order to counteract this effect. Conversely, if the formation of solids is endothermic, then precipitation is favoured. The effect of temperature on struvite precipitation is well established. Bhuiyan *et al.* (2007) experimentally determined the solubility product of struvite in the temperature range 10-70 ºC. From 10-30 ºC, the solubility of struvite was found to increase. Similar trends have been observed in other studies as illustrated in Figure 10.

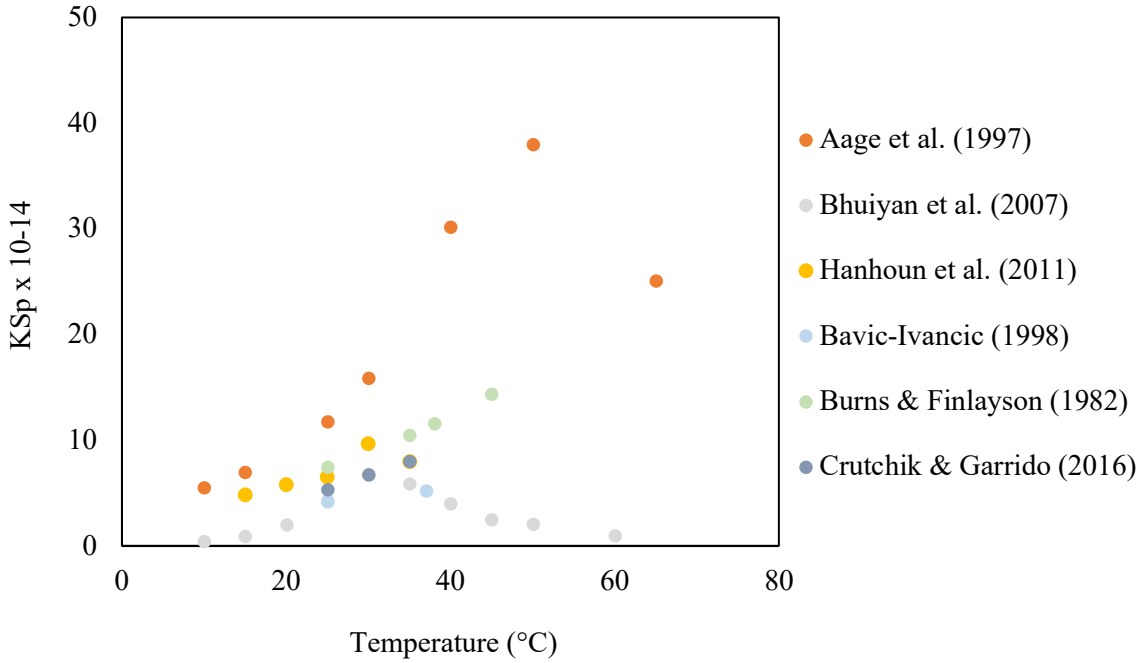

Figure 10. Effect of temperature on struvite precipitation

As seen from Figure 10, in the study by Bhuiyan *et al.* (2007), the maximum solubility is reached at 30 ºC. Thereafter, the solubility decreases with increasing temperature. Therefore, it seems that struvite dissolution is endothermic below 30 ºC whilst the precipitation is endothermic above 30 ºC. A similar trend is observed by Aage *et al.* (1997) but the peak solubility occurs at a temperature of 50 ºC. However, both studies speculate that at high temperatures the solubility decreases as struvite ($MgNH_4PO_4.6H_2O$) changes phase to magnesium ammonium monohydrate ($MgNH_4PO_4.H_2O$). The presence of higher water of crystallization in the hexahydrate makes struvite more soluble than the monohydrate (Aage *et al.*, 1997; Bhuiyan *et al.*, 2007). Nonetheless, these studies have investigated struvite exclusively in their experiments and the presence of other ions or organic compounds as found in wastewater or sludge were not considered. Further investigations are therefore required to determine the effect of high temperatures on struvite in a wastewater medium.

The solubility of calcium phosphate in aqueous solution is more complex because of incongruent dissolution phenomenon and dynamic intermediate equilibria between the different types of calcium phosphate precipitates (Kezia *et al.*, 2017). As a result, the effect of temperature on the precipitation or dissolution of calcium phosphate is not very well understood. A few studies have reported a decrease in solubility of calcium phosphate with increasing temperature in the range 10-50 ºC (Mcdowell *et al*., 1971; Rice *et al.*, 2009). However, Green & Perry (2007) observed a slight increase in monobasic calcium phosphate solubility from 25-37 ºC. Kezia *et al.* (2017) also observed an increase in calcium phosphate solubility after 168 hours and speculated that the different observations on solubility across different studies could be due to the duration of the reaction before analysis. During shorter time intervals (1-2 hours), it is thus expected that the solubility decreases whilst at time infinity (or final equilibrium), it increases. The crystalline structure of calcium phosphate was also observed to be dependent on temperature. With rising temperatures, the calcium content in the precipitate also increases (Kezia *et al.*, 2017). The calculation of K_{sp} or solubility (in mg/L) values over a significant range of temperature is henceforth very complex.

As heating up sludge to 70 ºC releases polyP into the bulk liquid and has shown to decrease the solubility of the mineral precipitates, it is a potential method to characterise ISS. Nonetheless, as the polyP is released into the bulk solution, more mineral precipitates are immediately expected to form as ion concentrations (Mg, K, Ca and OP) increase. Thus, a dilution step before heating is recommended to prevent the ions from going back to the solid phase. As struvite has a very low solubility, a high dilution might be required, which can significantly affect the precision of the test.

2.6.3 Application of electromagnetic field to release orthophosphates from PAOs

To facilitate the recovery of phosphorus from WAS, several authors have explored the effect of treating WAS with an electric or electromagnetic field before feeding it into the AD. Hu *et al*. (2018) and Choi *et al.* (2006) investigated the use of high voltage pulsed discharge (HVPD) to enhance phosphorus release during AD. By treating a WAS sample with HVPD, they observed a considerable increase in OP concentrations. By analysing SEM images before (Figure **11**a) and after treatment (Figure **11**b), Choi *et al.* (2006) have observed that this increase was due to the pulse discharge destroying the cell membrane and cell wall of bacteria. A similar conclusion was reached by Hu *et al*. (2018). The HVPD directly attacks the basic building blocks of the cell membrane (phospholipids) and walls (peptidoglycan). These polar molecules have ligand groups that give a net negative charge on the surface of the cell. This makes the PAO cells susceptible to strong electric field (Salerno *et al.*, 2012).

However, in these studies, as well as other HVPD studies, the extent of polyP release from the biomass could not be determined. The standard, measurements and techniques (SMT) protocol was used to determine the source of P release from the WAS. Since the SMT protocol classifies phosphorus into only four broad categories (non-apatite inorganic phosphorus, apatite phosphorus, organic phosphorus and inorganic phosphorus), the concentration of polyP released cannot be determined from this classification. Furthermore, as counter-metal ion concentrations

(such as K^+) were not measured during the experiment, the extent of polyP released could not be determined.

Up until now, few studies on the effect of electric fields on chemical precipitation have been conducted. Electromagnetic fields have been commonly applied to hard waters to decrease scaling in water treatment systems such as reverse osmosis reactors. Some studies have shown that electromagnetic field increases the growth rate of calcite nuclei whilst others have shown that it either reduces the combination of Ca^{2+} and HCO_3^- ions, or has no considerable effect on precipitation (Rouina *et al.*, 2016; Piyadasa *et al.*, 2017; Han *et al.*, 2018). Thus, although the effect of electric/electromagnetic field on sludge or chemical precipitate is not clear, it constitutes a possible method to separate chemical precipitates and polyP.

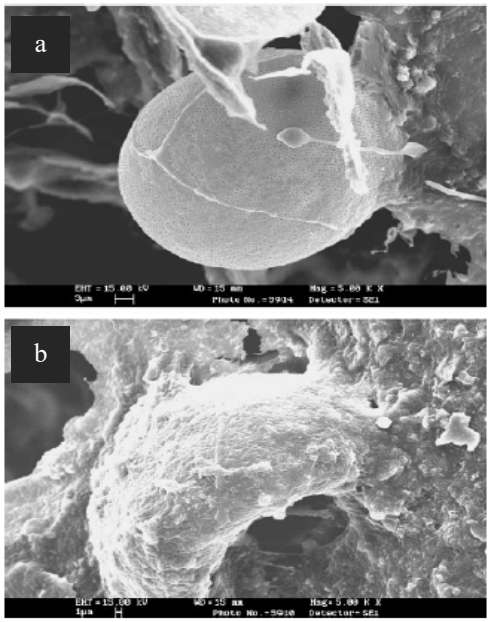

Figure 11**. SEM image of WAS: a) before and (b) after HVPD treatment (Choi *et al*., 2006)**

2.6.4 Cold perchloric acid fractionation procedure

As EBPR systems became more popular, investigations on the effect of chemical precipitation on biological P removal became prominent. During simultaneous chemical P (by addition of chemical precipitants) and biological P removal, both processes compete for phosphorus. It is possible that the efficiency of the individual processes is decerased by the other and the net removal is reduced. To study the dynamics between the two P removal methods, it is clear that a method that could differentiate between polyP and chemical P was necessary. In this respect, there was a general focus on fractionation methods. The fractionation method consists of successive additions of reagents that dissolve specific components of the sludge. By running analytical tests on the extracts (reagents with dissolved components), the concentrations of the different components can be quantified.

The fractionation methods are broadly categorised into two groups by De Haas *et al.* (2000): acidic extraction with or without the use of cold perchloric acid (PCA). De Haas (1989) showed that PCA is effective in dissolving phosphate precipitates. In the case of polyP, many studies have shown that there is negligible polyP hydrolysis to OP if cold PCA with short extraction

times is used (Harold, 1962; Kerdachi & Healey, 1987; De Haas, 1989; De Haas & Greben, 1991; Blonda *et al.*, 1994). This is explained by the low rate of polyP hydrolysis at low temperatures (0-3 ºC). However, Müssig-Zufika *et al.* (1994) demonstrated that cold PCA extractions resulted in 25 % polyP hydrolysis to OP. There is a general agreement that the use of cold PCA at short extraction times is a suitable method to quantify polyP P and chemical P in activated sludge samples.

There are several types of fractionation procedures based on cold PCA (Kerdachi & Healey, 1987; De Haas & Greben, 1991; Blonda *et al.*, 1994; De Haas *et al.*, 2000). Originally, the cold PCA extraction method consisted of separated acid and alkaline extraction steps. The latter involved the use of dilute and concentrated NaOH to extract any remaining complex P (biomass P and complex P) from the residue after the PCA extract. In an effort to simplify the cold PCA procedure, De Haas *et al.* (2000) modified the full PCA procedure by excluding the alkaline steps.

The modified cold PCA fractionation procedure is outlined in Table 17A. The sludge sample is initially centrifuged to extract and test the supernatant. The TP and OP of the supernatant represent the total soluble (inorganic and organic P) and inorganic P content of the sample, respectively. It must be noted that the concentration of soluble organic P is negligible in municipal wastewater. Thereafter, three extractions of five minutes with cold PCA are performed. The OP of the extractant represent the dissolved chemical P precipitates. The acid disrupts the cell membrane of the PAOs and thus its cell contents are released in the bulk liquid. However, as the extraction is carried out with cold acid for a short period of time, the hydrolysis of polyP to OP was seen to be insignificant. The OP test on the extractant does not include the polyP. However, a TP test does include the polyP P, as well as the chemical P and biomass P. The difference between the TP and OP of the PCA extractant yields the polyP and biomass P, named collectively as complex P. Table 3 below summarises the composition of different sludges tested by De Haas *et al.* (2000).

Table 3. Summary of results from the cold fractionation procedure of De Haas *et al.* (2000). MB: Mass balance

Scenario	OrthoP		Chemical P		PolyP		Bio P		MB
	mgP/gVSS	%	mgP/gVSS	%	mgP/gVSS	%	mgP/gVSS	%	%
Completely aerobic system	6.53	20	4.32	16	0.00	0	18.40	63	97
UCT AS system	5.45	9	5.52	9	18.40	6	10.00	17	98
EBPR fed 50 mgCOD/L Acetate	5.80	7	5.43	7	32.63	71	10.00	14	98
EBPR fed 250 mgCOD/L Acetate	13.23	9	6.02	4	98.12	80	10.00	7	98

Scenario	OrthoP		Chemical P		PolyP		Bio P		MB
	mgP/gVSS	%	mgP/gVSS	%	mgP/gVSS	%	mgP/gVSS	%	%
EBPR fed 250 mgCOD/L Acetate and $FeCl_3$	0.20	0	15.62	11	120.76	82	10.00	7	96
EBPR fed 250 mgCOD/L Acetate $FeCl_3$ and OP	6.19	4	31.18	18	123.41	72	10.00	6	97
EBPR sludge before AD	6.46	7	7.26	7	74.78	76	10.00	10	90
EBPR sludge after 4 hrs AD with excess Acetate	65.99	63	7.93	8	21.72	21	10.00	10	96

With the aim to validate the modified cold PCA fractionation procedure, De Haas *et al.* (2000) applied it to different types of sludges. For all the sludges, the sum of TP in the extracts was closely equal to the TP of the mixed liquor. This mass balance demonstrates the ability of the fractionation procedure to recover all the phosphorus in the sludge. It therefore provides a high confidence in the results and the test itself. The results obtained in the study are in agreement with the experimental observations on PAO mechanisms (Henze *et al.*, 1995). For instance, with increasing acetate concentration in the feed there was an increase in the polyP fraction (see Table 3). Moreover, it was also observed that under anaerobic conditions with acetate as substrate, the polyP content of PAOs decreases.

The accuracy of the fractionation procedure was validated by comparing the polyP content with predictions from the UCTPHO model. The UCTPHO model assumes a maximum P content of 0.38 mgP/mgPAOVSS. A good correlation was obtained between this model and the measured polyP concentrations. Hence, this demonstrates the ability of the cold fractionation procedure to accurately quantify polyP and implicitly shows that there is negligible hydrolysis of polyP to OP during PCA extraction. The solubility of the chemical P precipitates in cold PCA is well established (Kerdachi & Healey, 1987; De Haas, 1991). Nonetheless, the use of serial short extraction steps to dissolve chemical P was unprecedented. As observed from Table 3, there was an increase in the OP concentration of the PCA extract when the precipitant $FeCl_3$ is added to the EBPR reactor. The increase in OP concentration corresponds to the dissolved chemical P precipitates. Although these results suggest that the PCA extract is sensible to chemical precipitates, they do not quantify the amount of precipitates that dissolved. As measurements such as the dissolved and total iron concentration were not taken, it is difficult to confirm the observed chemical P precipitates.

In the case where not all precipitates have dissolved in the cold PCA, the chemical P would form part of the residual P. This would ultimately overestimate the polyP content and underestimate the chemical P content. Furthermore, in the experiments the only precipitates present were attributed to the addition of chemical precipitant ($FeCl_3$). The effect of cold PCA on struvite or ACP within a short time interval (<5 min) is not known. In a previous study, De Haas (1989) showed that 99% of struvite and 82% of ACP are soluble in cold PCA after 30 minutes. Further investigations are necessary to determine the behaviour of EBPR WAS precipitates, such as struvite or ACP, with the modified cold PCA fractionation procedure i.e., for short extraction times with PCA.

Although the modified cold PCA fractionation procedure has shown great capability in differentiating between polyP and chemical P, further considerations are required to use it for a full ISS characterisation. Firstly, additional measurements on the extractant are required. In the case where $FeCl_3$ is added as a chemical precipitant, it can be assumed (with negligible error margin) that the chemical P extracted in PCA is mostly attributed to $FePO_4$. However, when co-precipitation is not used, there exists two forms of precipitates in EBPR WAS, namely: struvite and ACP. Therefore, additional measurements such as Mg_T, Mg^{2+}, Ca_T, Ca^{2+}, FSA and TKN become important to differentiate between the different types of P precipitates. When polyP is released in the bulk solution, it is well established that there is negligible hydrolysis to OP. However, no studies have yet determined the fate of the polyP metals (Mg, Ca and K) in the PCA extract. If the metals are released to the bulk solution as cations, they will interfere with the dissolved metal ions from the chemical precipitates. On the contrary, if they remain attached to the released polyP, they will not contribute to the dissolved cations but add to the soluble metal concentration. To determine the fate of the metal cations in polyP, the modified cold PCA fractionation procedure must be performed on polyP solely and metal cation measurements should be taken on the extracts.

2.6.5 Microscopy

This section discusses the feasibility of using microscopy in determining the concentration of polyP in activated sludge samples. As compared to the previously mentioned methods, this approach is rather peculiar as the sample size is relatively small. Nonetheless, the use of microscopy in the wastewater treatment field is not new. Microscopy has been used to characterise activated sludge in terms of the bacteria, such as filamentous or floc-forming (which affects the settleability of the sludge). Furthermore, with the aim to understand the metabolism of certain microorganisms, microscopy has been used in research to study the internal composition of these microorganisms. Since the very first use of conventional methods such as bright-field or phase contrast microscopy, various new approaches and technologies have been developed to yield better results. The methods that can be used to determine the polyP content of an activated sludge sample are outlined below.

2.6.5.1 Staining methods

The use of microscopes such as bright-field or phase-contrast solely is not sufficient to identify polyP inside microorganisms. For this reason, staining with a dye is required for the microscopic identification of polyP. There exist three types of staining methods for polyP identification,

namely: Neisser, Loeffer's and DAPI (4' ,6-diamidino-2-phenylindole dihydrochloride) staining (Serafim *et al.*, 2002).

Until recently, the most common method for polyP detection was Neisser staining. It has notably been used in the wastewater field to qualitatively study the metabolism of PAOs (van Groenestijn *et al.*, 1988; Blackall *et al.*, 2002; Günther *et al.*, 2009; Mesquita *et al.*, 2013). In this method, methylene blue is used to stain a smear (generally a droplet of the sample spread on a glass side) of activated sludge sample. The methylene blue is dissolved in an acidic solution. After rinsing the glass slide, a counter stain solution (Bismarck brown or chrysoidin Y) is then passed through the sample. The smear is then analysed under a bright-field microscope with the help of oil immersion (APHA, 1985). Loeffer's staining method skips the counter stain and the smear is analysed directly after application of methylene blue. Figure 12a and Figure 12b show an EBPR sludge sample analysed via Neisser and Leoffer's staining methods, respectively.

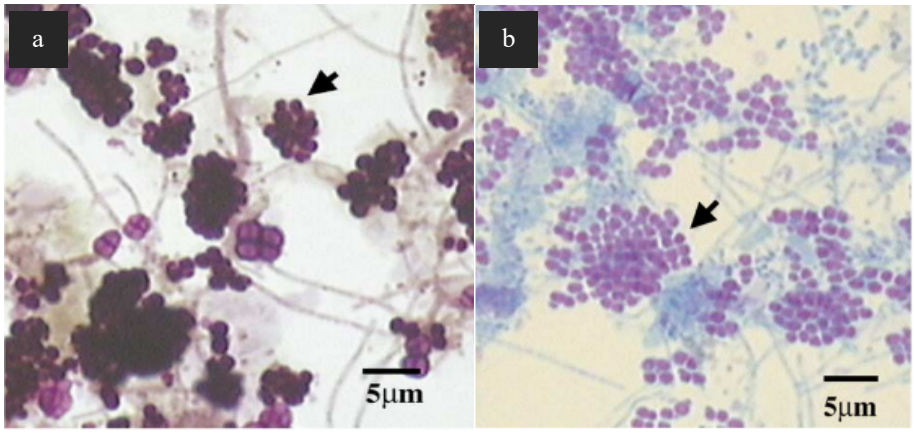

Figure 12. a): EBPR sludge Neisser staining (1000x) b): EBPR sludge Loeffler's (1000x). Obtained from Serafim *et al.* (2002)

Methylene blue is the active component in both the Neisser and Loeffler's methods. It is a metachromatic cation dye with a very high affinity for the volutin granules. When bound to polyP volutin granules, its light absorption changes and it produces a colour that contrasts with the other cell contents. With Neisser staining, dark purple dyed volutins (shown by arrow marked on Figure 12a) against pale brown cells is obtained. With Loeffer's staining, volutin granules are dyed pale pink with a blue cell background. Neisser staining method is more suitable than Loeffer's for the identification of variable amounts of polyP due to the high contrast between volutin granules and the cell. When high concentrations of polyP are expected, as in the aerobic sludge of EBPR, both Neisser's and Leoffer's staining methods are considered suitable. The use of these two staining methods offers the possibility to quantify the amount of polyP in EBPR sludge. However, the raw data obtained from microscopic analysis is qualitative in nature. This raw data must be further processed to convert into quantitative concentrations (this is further discussed in Section 2.6.5.2).

DAPI is a fluorescent dye that is usually used for DNA detection. It is also becoming more popular in EBPR studies and for in-situ microbiological characterisation of activated sludge. At high dye concentrations (50 μg/L), DAPI can stain polyP granules and lipid inclusions (Tijssen *et al.*, 1982; Streichan *et al*., 1990). PolyP granules stains are bright yellow) while lipid inclusions

display a weak yellow colour (see top left corner of Figure 13b) which fades after a few seconds (Streichan *et al.*, 1990; Serafim *et al.*, 2002). The DNA of PAOs stains blue and thus there is a clear contrast of polyP against the cell. Furthermore, DAPI staining offers the advantage of being easily combined with fluorescence in-situ hybridization (FISH) analysis. For these reasons, DAPI has been used to study the microbiology of PAO cultures in EBPR sludge. To name a few, it has been used to: (i) determine the relative abundance of different genus of PAOs (Crocetti *et al.*, 2000; Kawaharasaki *et al.*, 2002) and their respective polyP uptake (Kawaharasaki *et al.*, 1999); (ii) determine the polyP and PHA accumulation traits (Liu *et al.*, 2001) and (iii) study the dynamics of PAOs (Günther *et al.*, 2009).

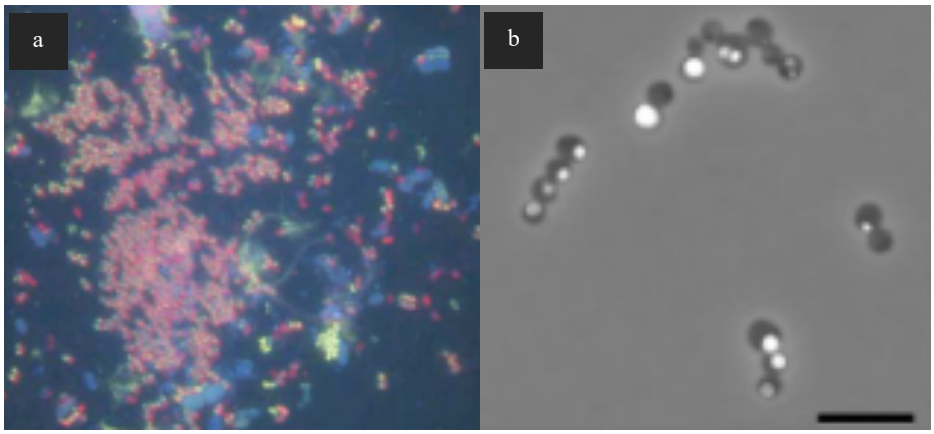

Figure 13. a): DAPI and FISH probe staining of mixed culture (Günther *et al.*, 2009). b): Stained cells of *m.phosphovorus* with DAPI and DNA probe (Seviour *et al.*, 2003)

Despite DAPI fluorescent staining presenting several advantages when qualitatively assessing EBPR sludge, a quantitative assessment is not as straight-forward. The intensity of the volutin granules is proportional to the concentration of polyP. Subsequently, at low concentrations of polyP inside the cell, the intensity of the fluorescence is low. Kawaharasaki *et al.* (1999) mentioned that below 400 µmol polyP/g dry cells, it becomes hard to differentiate between lipid molecules and polyP granules. Hence, the result of a quantitative image analysis (QIA) on a DAPI sample containing low polyP concentrations (such as the AD effluent) is likely to be largely overestimated. In case of EBPR WAS, which is wasted from the aerobic region, the polyP content is expected to be very high and thus this error is likely to be marginal.

2.6.5.2 Quantitative image analysis

As opposed to qualitative image analysis, QIA is a task that requires complex computation of data obtained from microscopy images. This technique can be broadly divided into three parts: image acquisition, processing and analysis. With higher processing capacities as well as better image acquisition technologies, studies using QIA is becoming increasingly common in the wastewater field. Table 4 summarises some of these studies.

Table 4. Studies using microscopy with qualitative image analysis in the wastewater treatment fields (Mesquita & Amaral, 2013)

Plant	Microscopy	Objectives	References
Lab-scale	Bright-field and epifluorescence	Identification of different types of bulking in an AS system	(Mesquita, Amaral & Ferreira, 2011)
Full-scale	Epifluorescence and Confocal laser scanning microscopy (CSLM)	Antibiotic could change the activated sludge bacteria composition, according to their Gram type and bacterial death was followed by bacterial disintegration	(Louvet *et al.*, 2010)
Lab-scale	Phase contrast	Filamentous bulking related to the increase of total filament length and with change in floc shape	(Jenné *et al.*, 2004)
Pilot-scale	Bright field	Filamentous bulking detected using synthetic or municipal water	(Da Motta *et al.*, 2003)
Lab-scale SBR	Phase-contrast	Image analysis information as an indication for the amount of suspended solids in the effluent	(Jenne *et al.*, 2005)
Lab-scale EBPR	Epifluorescence	Determination of glycogen concentration inside PAOs	(Mesquita *et al.*, 2013)
Full-scale	FISH and CLSM	Demonstration of a quantified method for enumerating bacteria in samples in which cells are homogenously distributed	(Daims *et al.*, 2001)

As deduced from Table 4, most studies that have used QIA aimed at understanding sludge settleability. Some studies have also used QIA to obtain absolute or relative abundance of different bacteria in AS. Conversely, the use of QIA to determine the concentration of intracellular compounds is very rare. In this regard, the study by Mesquita *et al.* (2013) was performed to predict the concentrations of PHA (PHB and PHV) and glycogen in EBPR sludge samples using microscopy images. A model was developed by linearly regressing the stain intensity of intracellular compounds against measured concentrations on offline methods. The EBPR sludge samples were stained with nile blue and aniline blue dyes to determine the intracellular concentrations of PHA and glycogen, respectively. Sludge samples (each of 1 ml) were taken at the end of the aerobic and anaerobic stages of an EBPR system. Nile blue or aniline blue was added to the pellets (solid residues) of the centrifuged sludge sample. After removing excess stains with acetic acid, the stained cells were re-suspended in NaCl solution. A pipette with a sectioned tip (to allow large sludge particles through) was used to deposit 10 µL on three microscopy slides for each sample. Images were acquired using epifluorescence microscopy in the bottom, middle and top of the slides resulting in 150 images per slide. The sludge samples were also analysed offline using gas chromatography and high-performance liquid chromatography for PHA and glycogen, respectively.

Using partial least square regression, a model was developed relating the intensity and area of fluorescence to the concentration of the intracellular compounds. The images were first processed to allow for the identification and quantification of glycogen and PHA inclusions area. This involved format conversion of the original image, background corrections and segmentation of the image. From the processed images, parameters such as total and average intensity of background corrected images, total area of glycogen or PHA molecules were obtained and used in the partial least square regression.

Good correlation was obtained for the intracellular concentration of glycogen (R^2=0.85) whilst poor correlation was obtained for PHB, PHV and PHA (R^2 of 0.62, 0.53 and 0.61, respectively). A few factors were identified in the study to justify the poor correlation. Firstly, it is believed that due to low biomass fragmentation, some PHA were concealed in the processed images. It was also speculated that interference from other stained materials such as lipid molecules could have contributed to the poor correlation. Additionally, Mesquita *et al.* (2013) pointed out that a major challenge in QIA is the inability to accurately differentiate between the features within an image. A major source of error can also originate from the sampling size when performing microscopy. Such a small sample size (10 µL) is not likely to represent the distribution of the sludge across the bulk liquid. Nonetheless, the good correlation obtained for glycogen shows that the combination of microscopy and QIA is a potential approach to quantify intracellular compounds.

2.6.6 Nuclear magnetic resonance (NMR) analysis

In vitro NMR technology allows the non-invasive investigation of intracellular physiology. The use of NMR in the wastewater treatment field is not very common. In the past, this analytical technology has been used mostly in research to study the metabolism and intracellular processes of microorganisms. In this regard, in vitro ^{31}P NMR has been used to detect polyP molecules (Roberts & Jardetzky, 1981; Balaban, 1984; Fernandez & Clark, 1987). The linear polyP molecules show a strong resonance at -21 ppm and thus are easily recognisable in an NMR spectrum. Although the detection of polyP molecule is widely reported, its quantification using NMR techniques has not been investigated up until now. Quantification of molecules using NMR analysis is done via comparison between the peak areas of a sample with those of a standard solution. There are two major challenges to this task. Firstly, there is limited literature to support the use of NMR to quantify polyP in sludge. Secondly, it is very likely that noise generated from other compounds in the sludge affects the quantification of polyP.

2.6.7 Anaerobic digestion

Anaerobically digesting an NDEBPR WAS sample can be used to characterise its inorganic solids. In this method, the polyP is released into the bulk solution as its hydrolysis is occurring. Harding and Ekama (2009) show that the complete hydrolysis of polyP P occurs within 5 days. Measurements taken at the start and the end of the anaerobic digestion (after 5 days) can thus yield the polyP concentrations of the sludge. However, there are two major limitations to this method. Firstly, the anaerobic digestion takes place over five days and thus the characterisation of the ISS will be equally long. Secondly, if mineral precipitates are present in the mixed liquor suspended solids (MLSS), it is likely that the solution is already oversaturated with respect to

these mineral precipitates. As the release of P and counter-ions occur, the ions will precipitate out of the solution and the polyP concentration will be underestimated. The mineral precipitate concentration will be overestimated.

2.6.8 Differential settling using a settleometer

Using the differential settling velocity of the ISS components is also a potential method to characterise inorganic solids. The settleometer is a device made up of five vertical transparent PVC columns of equal height and increasing internal diameters (Poinapen *et al.*, 2009). From the smallest diameter tube side, wastewater or sludge is pumped at a fixed flowrate. The smallest diameter column has the highest upflow velocity and thus only the fastest particles will settle. Conversely, the largest diameter column has the slowest upflow velocity and therefore the slowest particles will settle.

Mineral precipitates and sludge particles have different settling velocities due to their different densities and molecular structures. Thus, if a sample of sludge and mineral precipitates is passed through a settleometer, these compounds are expected to separate in different settling tubes. Samples from the settling tube can be tested for metals, N and P to determine the polyP and mineral precipitate concentrations. However, there are two limitations to this method. Firstly, it is likely that the mineral precipitates are enmeshed in the sludge flocs and thus they will settle together. Secondly, the use of the settlometer requires a large volume of WAS. As the sample needs to be fresh (to prevent premature release of polyP), the WAS has to be sourced from the lab-scale NDEBPR WAS system. Lab-scale system usually generates a low waste volume due to small reactor sizes. Consequently, the fresh WAS has to be highly diluted to reach this target volume, resulting in the dissolution of mineral precipitates present in the sample.

2.6.9 Closure

An array of potential base methods was identified in the literature review, including physical, chemical and microscopy methods. The advantages and challenges of these methods with respect to characterizing inorganic solids were also highlighted. It was found that one of the common challenges of the identified methods was the potential formation of mineral precipitates when the polyP P and counter-ions are released into the bulk solution. The base methods were evaluated in Section 3.3 and the ICT (and data-modelling procedure) was developed using the chosen method.

3 Methodology

3.1 General overview

To accomplish the objectives of this research, a sequence of logical steps was followed. The ISS characterisation procedure was made up of two major components: a laboratory test protocol (from this point onward this will be referred to ISS characterisation test (ICT)) and a DMP. The former is a laboratory test that can be applied to sludge or wastewater sample to provide input data to a DMP for the characterisation of ISS. The output of the DMP was then evaluated. The following points outlines the development of these two components:

- The approach taken towards the development of the ICT was to identify base methods from previous literature, and thereafter modifying them to provide the required analytical measurements to the DMP. Several potential base methods for the ICT were identified in Section 2.6.
- The next step was a critical assessment in the form of a multicriteria decision analysis on the potential base methods for the ICTs. The assessment was described in Section 3.3.
- The third step involved the modification of the selected base method into an ICT.
- Once the ICT was developed, a sample pool was defined. This step was critical as it identified the samples used for the evaluation of the ISS characterisation procedure.
- A data modelling procedure, described in Section 3.6, was developed to fully characterise ISS into its different component concentrations.
- The next step was the collection of data from the application of the ICT and DMP on the defined sample pool. The results are presented and evaluated in Chapter 4. Figure 14 shows a schematic of the methodology.

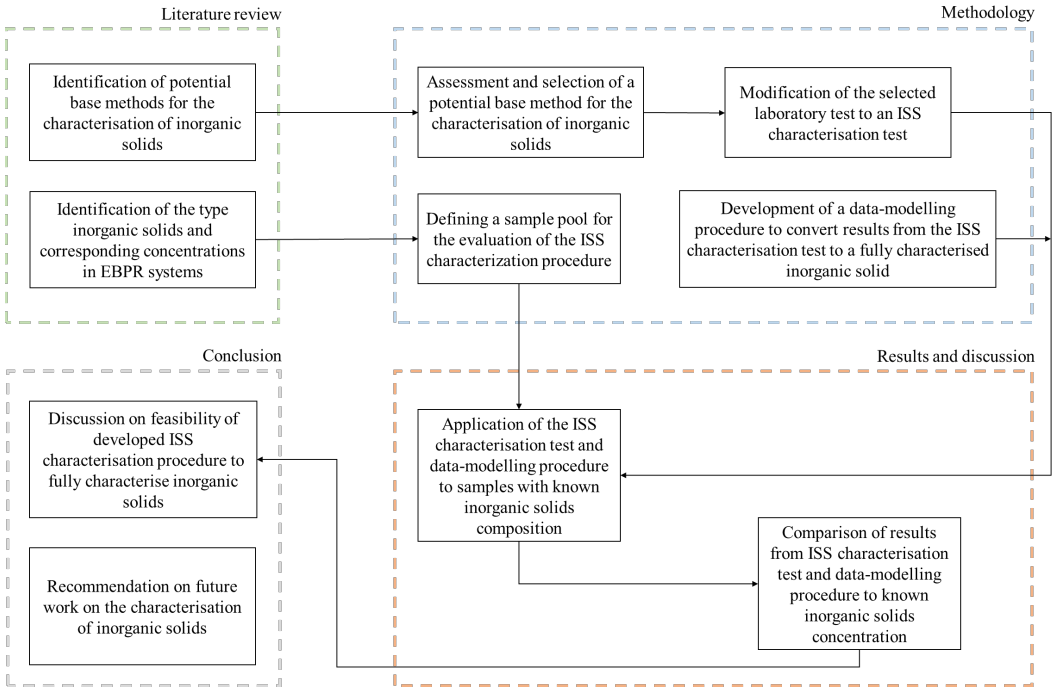

Figure 14. Schematic showing a general overview of the methodology and the interrelation between the different chapters

3.2 Experimental background and approach

Total suspended solids of NDEBPR WAS is generally considered to comprise of active biomass, endogenous residue, reactor-accumulated inorganic sediments (e.g., clay, silt and sand), and reactor-accumulated influent unbiodegradable particulate organics (UPO). The ISS is made up of the reactor-accumulated influent ISS, biomass ISS and polyP (Ekama and Wentzel (2004); see Section 2.2). Mineral precipitates have also been observed in some experimental studies, although their formation is currently included in very few AS system models (e.g., ASM2-3P; Ikumi and Harding, 2020) without any validation base. The contribution of accumulated influent ISS to NDEBPR WAS ISS can be determined using Wentzel *et al.* (1990) steady state model (see Section 2.4.1), according to the approach of Ekama and Wentzel (2004). The biomass ISS, which is only a consequence of the total solids test procedure, is based on a validated ratio of 0.15 mgISS/mgVSS and can thus be calculated using the concentration of biomass generated (Ekama and Wentzel, 2004).

In NDEBPR AS system, polyP is calculated assuming a maximum uptake of 0.38 mgP/mgPAOVSS (Wentzel *et al.*, 1990). This value has generally shown high correlation of model predictions with measured values on P removal (Ikumi *et al.*, 2015). However, depending on several factors such as anoxic P uptake, availability of metal cations and phosphate ions, PAOs might not achieve this maximum P removal. The uptake of metal cations has also seen to vary considerably and the factors driving the metal cations uptake are currently unknown. Furthermore, as PAOs move from the aerobic zone of the AS reactor to the subsequent units, they could experience environments that would favour the release of polyP (Ikumi and Ekama, 2019; Ikumi and Harding, 2020). As already noted, mineral precipitates have rarely been modelled in activated sludge system. It is typically assumed that the ionic strength is too low for precipitation to occur. Precipitation, albeit low concentrations, have been observed in EBPR WAS in the past, especially in membrane reactors. Furthermore, as the sludge is thickened in DAF reactors, CO_2 stripping causes the pH to rise and could possibly favour mineral precipitation. It can thus be deduced that in a sample of EBPR WAS, there are two forms of ISS that carry the most uncertainty in their concentrations: polyP and mineral precipitates.

Due to these uncertainties, analytical measurements taken directly on a sludge or sewage sample containing polyP and mineral precipitates do not yield meaningful results that can be used as input in a DMP. For instance, total magnesium, calcium, or phosphorus measurements on a EBPR sludge sample could be originating from struvite, ACP or polyP as all three can be potentially present. The aim of the ICT is to distinguish between polyP and mineral precipitates, such that the subsequent analytical measurements can then be used in a DMP to characterise the inorganic solids.

3.3 Assessment of potential base methods for the ISS characterisation test

A base method was selected among the potential tests identified in literature based on a multi-criteria decision analysis. The criteria for this assessment are: (i) complexity and robustness of the subsequent DMP, (ii) availability of literature that supports the likelihood of test being successful, (iii) complexity in carrying out the test (by the experimenter) in the Water Quality Laboratory, (iv) expected accuracy of the test results, (v) expected reproducibility of the test

results, (vi) amount of data processing required before data modelling, (vii) availability of equipment and (viii) expected expenditure in carrying out the test. Each criterion was given a weightage based on their relative importance to the context of this study. The scoring system and the results of the multi-criteria analysis are shown in Appendix F. The highest score was achieved by the cold PCA fractionation procedure by De Haas *et al.* (2000) (described in Section 2.6.4). The cold PCA fractionation procedure is relatively straightforward to perform, and results in a simple DMP. Furthermore, there is established literature supporting the reliability of this method in distinguishing polyP from mineral precipitates.

3.4 Experimental set up

3.4.1 UCT AS system

To obtain the polyP compound, a biological system with EBPR was required. As part of a parallel research project, a 62.5 L UCT AS system with membranes (for physical separation) was set-up (see Figure 15) and operated at a 12-day sludge age. This AS system was operated to promote growth of an enhanced PAO biomass culture, which was achieved by gradually increasing the ratio of synthetic feed wastewater (made up of high concentration of propionate) to real wastewater. Through the parallel study, propionate was found to be a favourable substrate for PAOs to sequester anaerobically. With a large portion of the influent substrate utilised anaerobically by PAOs, the other AS system biomass would be limited in competing for organic substrate because the anaerobic zone was the first to be exposed to the influent feed. Together with the provision of sufficient macronutrient and micronutrient quantities as part of the feed (i.e., metals such as Mg, K and Ca and nutrients such as P) provided PAOs with the competitive advantage in the system required for their enhanced growth. The set-up and the operation of the UCT AS system towards promoting the growth of enhanced PAO biomass was based on the study by Wentzel *et al* .(1988). The anaerobic reactor was operated at a volume of 30.5 L, the anoxic at 4.4 L and the aerobic at 29.0 L with the mass repartition between the anaerobic: anoxic: aerobic zones as 0.21:0.06:0.72. The inoculum of biomass used to start the AS reactors was obtained from Bellville wastewater treatment works in Western Cape, South Africa.

An influent wastewater of 1000 mgCOD/L was fed continuously to the UCT AS system, with the percentage of synthetic wastewater gradually increasing. The system was initially fed with a 1:1 ratio of settled wastewater to synthetic wastewater. As the PAOs grew accustomed to the feed, the percentage of settled wastewater was decreased in intervals of 10-20%. The final percentage of synthetic and settled COD were 76% and 24%, respectively. In addition to the propionate, the final synthetic feed also consisted of the following macronutrients: 50 mg/L of magnesium chloride hexahydrate ($MgCl_2.6H_2O$), 120 mg/L of dipotassium hydrogen phosphate (K_2HPO_4) and 0.5 g of yeast for metabolic purposes. The selection of these specific compounds is explained in the study by Thela & Ikumi (2022). The temperature was maintained at 20 ºC and the pH between 7.3-7.5 by dosing sodium hydroxide pellets to the anaerobic zone and hydrochloric acid to the aerobic zone. At steady state, 4 L of AS was wasted per day. Tests such as COD, TKN, TP, and total solids were carried out from samples extracted at various points (influent, anaerobic reactor, aerobic reactor, reaeration tank, and effluent) to determine if steady state has been reached, as well as evaluating the P-removal performance. The results of the tests

are available in the parallel study (Thela & Ikumi, 2022). The measured data was used as input in the Wentzel *et al.*(1990) steady state model (see Appendix C) to characterise the WAS. The characterisation of the steady state WAS is shown in Section 4.1. The WAS was immediately used in the ICT.

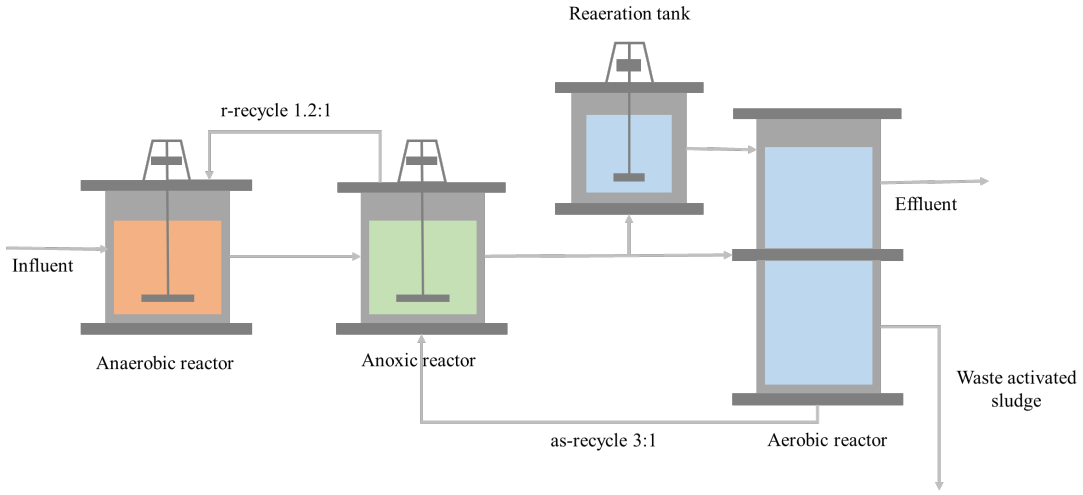

Figure 15. A 62.5 L NDEBPR AS system operated at the University of Cape Town at a 12-day sludge age

3.4.2 Sequencing batch reactor

As part of this project, a sequencing batch reactor (SBR) was set-up as another means to obtain an enhanced culture of PAO. This was run in conjunction with the UCT AS system. However, it was found that the UCT AS system achieved a steady state enhanced culture before the SBR system and hence the WAS was obtained from the UCT AS system for the ICT. The SBR system will nonetheless be used for a parallel research and a brief description of the system is given in Appendix B and may be used for future reference.

3.4.3 ISS characterisation test

In Section 3.3, it was deduced that the cold fractionation procedure by De Haas *et al.* (2000) was the most suitable base method for the ICT. De Haas *et al.* (2000) has concluded that this method, as described in Section 2.6.4, can be used to broadly fractionate EBPR sludge P content into mineral precipitate P and polyP P. It was also shown that the cold PCA acid can effectively dissolve mineral precipitate with negligible hydrolysis of polyP. In these circumstances, the ISS components exist in phases that are distinguishable in analytical measurements (see Figure 16).

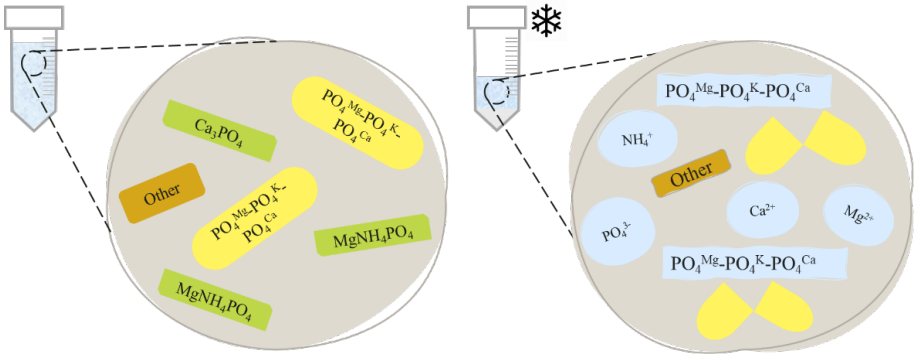

Figure 16. Effect of cold PCA extraction of NDEBPR WAS. Left: Original NDBER WAS. Right: PCA extract

In addition to dissolving mineral precipitates, the cold PCA also lyses the bacteria cell wall and therefore all cell contents, including polyP, are released into the bulk solution. However, as the extraction is carried out at a low temperature, the hydrolysis of polyP is negligible in a short timespan (<5 minutes). Hence, the dissolved ion concentrations in the PCA extract should theoretically correspond to the mineral precipitate ions. The difference between the total soluble and dissolved ion concentration should correspond to the polyP ions concentrations (taking into account the ions from the hydrolysis of biomass). In this study, the influent to the UCT AS system was largely synthetic and soluble with a small proportion (25%) of filtered raw wastewater. It is therefore assumed that there is negligible hydrolysis of UPOs.

Figure 17 shows a schematic of the cold fractionation procedure. The experimental procedure adopted in this study is similar to De Haas *et al.* (2000), although additional analytical measurements were taken on the extractants as shown in Table 5. The cold fractionation procedure, together with the additional analytical measurements is referred to as the ICT.

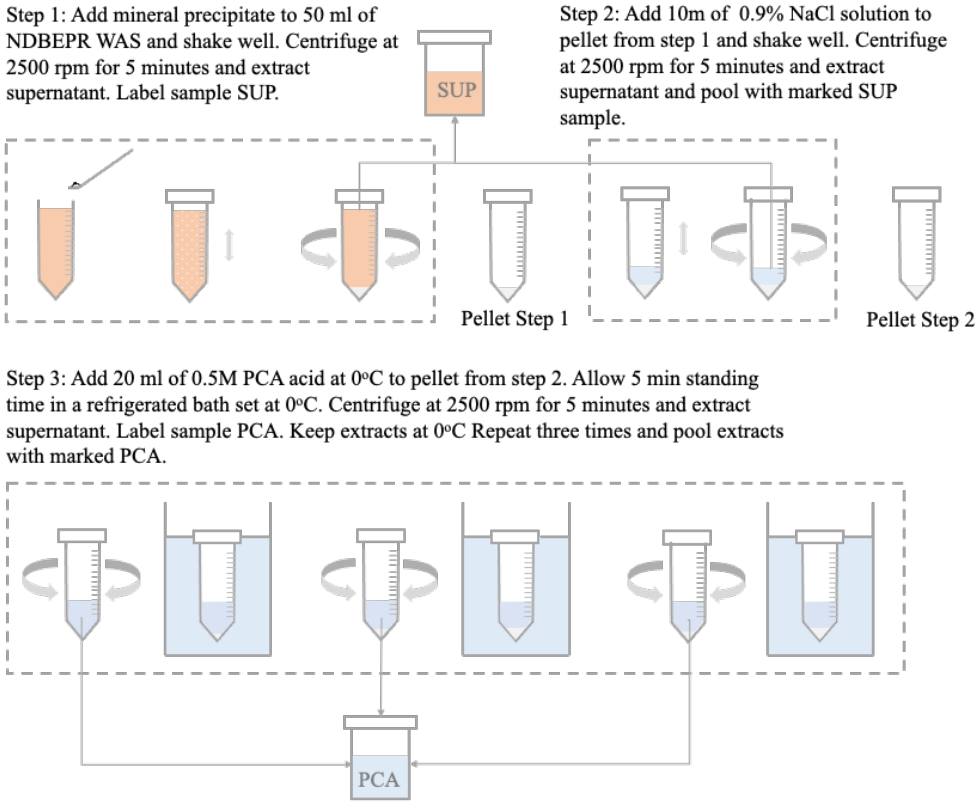

Figure 17. Schematic diagram of the ISS characterization test (ICT)

First, a 50 ml sample (as defined in Table 7) was centrifuged at 2500 rpm for five minutes. The supernatant was extracted and transferred to a sampling flask. To the pellet (solid residue) from this first step, 10 ml of 0.9% NaCl solution was added. The NaCl wash extracts any loose ions attached to the sludge. The supernatant was then extracted after centrifugation. The extract was pooled together in the sampling flask. For each test case the supernatant was analysed for soluble ion concentrations as outlined in Table 5. This step was aimed at determining the concentrations of soluble or loosely bound ions inherently present in the sample.

Table 5. Analytical measurements on the different extracts of the cold fractionation procedure

Test Case	Supernatant	Perchloric acid extract (PCA)	Residual extract
A	Mg^{2+} FSA OP	Mg_T Mg^{2+} TKN FSA TP OP	Mg_T Mg^{2+} TKN FSA TP OP
B	Ca^{2+} OP	Ca^{2+} Ca_T TP OP	Ca^{2+} Ca_T TP OP
C	Mg^{2+} Ca^{2+} FSA OP	Mg^{2+} Mg_T Ca^{2+} Ca_T FSA TKN TP OP	Mg^{2+} Mg_T Ca^{2+} Ca_T FSA TKN TP OP
D - G	Mg^{2+} Ca^{2+} FSA OP K^+	Mg^{2+} Mg_T Ca^{2+} Ca_T FSA TKN TP OP K_T K^+	Mg^{2+} Mg_T Ca^{2+} Ca_T FSA TKN TP OP K_T K^+

Using the pellet from step 2, a 0ºC acid extraction was then carried out. A solution of 0.5 M PCA was made up using a standard concentrated solution of PCA (>98%). The acid solution was allowed to cool at 0 ºC in a freezer. The centrifuge tube containing the pellet from step 2, was placed in a jacketed reactor at 0 ºC. To the pellet, 20 ml of 0.5 M PCA at 0ºC was added. The centrifuge tube was allowed to stand in the jacketed reactor for five minutes. Thereafter, it was centrifuged at 2500 rpm for five minutes in a refrigerated centrifuge; the solution was then extracted and transferred to a sampling flask. The acid extraction step was repeated three times and the solutions were pooled in the same sampling flask. Analytical measurements (see Table 5) were immediately taken on the PCA samples. The residual pellet was re-suspended in 50 ml of deionised water (the same volume as the initial MLSS sampled). Analytical measurements were also performed on the residue.

3.5 Analytical tests

3.5.1 TSS, VSS and ISS concentration

Solid masses of the original samples (NDEBPR WAS and the mixture of NDEBPR WAS and mineral precipitates) were determined using the total solids test (APHA, 1985). A 50 ml sample was centrifuged at 2500 rpm for 10 minutes. The supernatant was discarded, and the pellet was washed from the centrifuge tube into a pre-weighted empty crucible (mass A). The crucible was thereafter allowed to dry in an oven at 105 ^{0}C for 24 hours. After cooling in a desiccator, the crucible with its contents was reweighted (mass B). The difference in mass between mass B and mass A corresponds to the TSS concentration of the sample, as shown in Equation 3.1 below.

To determine the VSS and ISS concentration of the sample, the crucible with its dried contents was then incinerated at 600 ^{0}C for 20 minutes. The crucible was then reweighted (mass C) after cooling in the desiccator. The ISS concentration corresponds to the difference between mass C and mass A as shown in Equation 3.2. The VSS concentration is the difference between TSS and ISS concentration , as shown in Equation 3.3.

$$TSS\ (as\ mg/L) = Mass\ B - Mass\ A \quad (3.1)$$

$$ISS\ (as\ mg/L) = Mass\ C - Mass\ A \quad (3.2)$$

$$VSS\ (as\ mg/L) = TSS - ISS \quad (3.3)$$

3.5.2 Total phosphate (TP) and orthophosphate (OP)

The TP and OP were measured using the molybdate-vanadate colorimetric method (APHA, 1985). For the TP test, a 20 ml sample is first digested to transform the organically bound phosphates, mineral phosphates, and the polyPs into orthophosphates. The digestion procedure consisted of boiling the sample at 97 ºC with a mixture of 0.5 M sulphuric acid (5 ml) and 6% potassium persulphate (5 ml). A solution of molybdate-vanadate is added to 5 ml of the digested mixture and allowed to stand for 30 minutes. The colour reagent is prepared as described by APHA (1985). The intensity of the yellow colour formed is proportional to the concentration of orthophosphate. Standard orthophosphate samples (5, 10, 15 and 20 mgP/L) were also taken through the same steps. A discrete analyser (Gallery™ Discrete Analyzer, Thermofisher™), that performs automated photometric analysis was used to determine the absorbance of each sample and that of the standard OP solutions. By plotting the absorbance versus the OP concentration for standard OP solutions, the concentration of OP for the sample can be found using the sample's absorbance. For the OP test, the digestion step was omitted for both the sample and the standard OP solutions. If concentrations were expected to exceed 100 mgP/L, the samples were diluted before testing. For the ISS characterisation test, water at 0ºC was used for dilution to prevent hydrolysis of polyP at higher temperatures.

3.5.3 Total Kjeldahl Nitrogen (TKN) and Free and Saline Ammonia (FSA)

The TKN (which equals to total nitrogen excluding nitrates and nitrites) and FSA (dissolved NH_3 and NH_4^+) are measured based on the semi-Micro-Kjeldahl Method, 420B (APHA, 1985). For the TKN test, the samples were first digested with a digestion mix containing sulphuric acid solution and potassium sulphate. The digestion mix was prepared as explained in the standard methods for water and wastewater examination (APHA, 1985). The digestion converts the organic N or mineral N into ammonia or ammonium. The sample was then steam distilled using a micro-distillation apparatus with sodium hydroxide. The ammonia from the sample is stripped and condensed into a boric acid solution (APHA, 1985) which turns green or yellow depending on the nitrogen concentration. The sample was then titrated back with 0.001 M sulphuric acid until the original purple colour of boric acid was obtained. For the FSA test, the digestion step was omitted, and the sample was directly steam distilled.

3.5.4 Metal cations

The metal cations namely: Mg^{2+}, K^+, Ca^{2+} were measured using the discrete analyser (Gallery™ Discrete Analyzer, Thermofisher™). This instrument measures the concentration of dissolved ions/compound by measuring the absorbance of specific wavelengths of light passing through a sample. A reagent is added to the filtered sample, which then develops a colour intensity. The intensity of the colour is proportional to the concentration of the compound/ion. The instrument was calibrated with solutions of known concentrations such as to generate a calibration curve. After measuring the absorbance of the sample, its concentration is then determined from the calibration curve. For total metal concentration, the sample was first digested with 0.5 M sulphuric acid and 6% (v/v) potassium persulfate solution, similar to the TKN and TP digestion method.

3.6 Data modelling procedure

3.6.1 Data-modelling procedure I

The DMP I was used to process the results of the ICT into a fully characterised ISS. The following points outlines the development of the DMP I.

- The Mg in struvite (Mg^{2+}_{struv}) is equal to the measured concentration of soluble Mg in PCA extract (Mg^{2+}_{PCA}). This implies that there is negligible interference of Mg from polyP hydrolysis and complete solubilisation of struvite in PCA.
- The polyP Mg is equal to the complex Mg (Mg_{cpx}) as there is negligible concentration of Mg in biomass. To obtain Mg_{cpx}, the sum of Mg in the PCA ($Mg_{T,PCA}$) and residual ($Mg_{T,R}$) has to be determined first, using Equation 3.4. The polyP Mg concentration (Mg_{cpx}) is then obtained by subtracting the soluble Mg in the PCA (Mg^{2+}_{PCA}) from $Mg_{T,PR}$ as shown in Equation 3.5.

$$[Mg_{T,PR}] = [Mg_{T,PCA}] + [Mg_{T,R}] \quad (3.4)$$

$$[Mg_{cpx}] = [Mg_{T,PR}] - [Mg^{2+}{}_{PCA}] \quad (3.5)$$

- The Ca in ACP (Ca^{2+}_{ACP}) is equal to the measured concentration of soluble Ca in the PCA extract (Ca^{2+}_{PCA}). This assumes that there is negligible interference of Ca from polyP hydrolysis and complete solubilisation of ACP in PCA.
- The polyP Ca is equal to the complex Ca (Ca_{cpx}) as there is negligible Ca in biomass. To obtain Ca_{cpx}, the soluble Ca in the PCA (Ca^{2+}_{PCA}) is subtracted from the sum of Ca in the PCA and residual ($Ca_{T,PR}$) as shown in Equation 3.6.

$$[Ca_{cpx}] = [Ca_{T,PR}] - [Ca^{2+}{}_{PCA}] \quad (3.6)$$

- The polyP K is equal to the complex K (K_{cpx}) as there is negligible concentration K in biomass. To obtain K_{cpx}, the soluble K in the PCA (K^{+}_{PCA}) is subtracted from the sum of K in the PCA and residual ($K_{T,PR}$) as shown in Equation 3.7. It was seen in section 2.2. that K-struvite does not precipitate in EBPR systems. As there is no mineral precipitate with K, K^{+}_{PCA} is expected to be close to zero.

$$[K_{cpx}] = [K_{T,PR}] - [K^{+}{}_{PCA}] \quad (3.7)$$

- P is present in polyP, ACP, and struvite. The OP content of the PCA corresponds to the P content of the ACP and struvite provided that all mineral precipitates dissolve and polyP does not hydrolyse. Using the Mg content of struvite (Mg^{2+}_{struv}) and the elemental molar ratio of Mg:P (1:1) (denoted as $M_{P,Struv}$:$M_{Mg,struv}$) in struvite ($MgNH_4PO_4.6H_2O$), its P content (P_{struv}) was determined (see Equation 3.8). By subtracting the struvite P content (P_{struv}) from the PCA extract OP concentration ($PO_4^{3-}{}_{PCA}$), the ACP P content was obtained, as shown in Equation 3.9.

$$[P_{struv}] = [M_{P,struv}: M_{Mg,struv}] \times \frac{[Mg_{struv}]}{24\ mgN/mol} \times 31\ mgP/mol \quad (3.8)$$

$$[P_{ACP}] = [OP_{PCA}] - [P_{struv}] \quad (3.9)$$

- To obtain the complex P (P_{cpx}: polyP P and biomass P), the soluble P in PCA (OP_{PCA}) is subtracted from the sum of P in the PCA and residue (TP_{PR}) as shown in Equation 3.10. The polyP (P_{PP}) was then obtained by subtracting the nucleic P (P_{bio}) from the complex P (P_{cpx}) as shown in Equation 3.11. The nucleic P content of 0.01 mgP/mgVSS was used in the DMP I. It should be noted that this value used by De Haas *et al.* (2000) is different from the f_p value of 0.025 mgP/mgVSS reported by Ekama and Wentzel (2004). However, high correlation with modelled polyP was obtained in De Haas *et al.* (2000) investigation, and was also used in the DMP I.

$$[P_{cpx}] = [\mathrm{TP}_{PR}] - [\mathrm{OP}_{PCA}] \quad (3.10)$$

$$[P_{PP}] = [P_{cpx}] - [P_{bio}] = [P_{cpx}] - f_p\,[X_V] \quad (3.11)$$

- At this point, the elemental composition of the ISS components has been determined. Hence, the ISS concentrations (in terms of mgISS/L) can be calculated as shown in the last column of Table 6.

- The output of the DMP I can be verified by comparing the molar ratio of the different elements from the DMP I to theoretical ratios of the compounds. The molar ratio of Ca:P in ACP can be checked against literature value of 3:4. Similarly, the molar ratio of polyP (Mg:K:Ca:P) can also be verified against literature, although the reported values vary across different studies.

- The N content of struvite (N_{struv}) was obtained by using the elemental molar ratio of Mg:N (1:1) in struvite. Given that there is negligible release of N from biomass in the PCA extract, the FSA of the PCA (FSA_{PCA}) should be equal to N_{struv}. Following this assumption, the N content of the complex fraction should be equal to the N content of the biomass (N_{bio}). Table 6 summarises the DMP I into a matrix.

Table 6. Data modelling procedure I showing the calculations involved in the full characterisation of ISS

	N (mgN/L)	**Mg (mgMg/L)**	**P (mgP/L)**	**Ca (mgCa/L)**	**K (mgK/L)**	**ISS (mgISS/L)**
Soluble (X_{SUP})	FSA_{SUP}	Mg^{2+}_{SUP}	OP_{SUP}	Ca^{2+}_{SUP}	K^{+}_{SUP}	0
Struvite (X_{struv})	$M_{Mg,struv}$: $M_{N,struv}$	Mg^{2+}_{PCA}	$M_{Mg,struv}$: $M_{P,struv}$	0	0	$M_{Mg,struv}$ x MM_{Struv}
ACP (X_{ACP})	0	0	OP_{PCA} - P_{struv}	Ca^{2+}_{PCA}	0	$M_{Ca,ACP}$ x MM_{ACP}
Complex (X_{cpx})	TKN_{PR} - FSA_{PCA}	$Mg_{T,PR}$ - Mg^{2+}_{PCA}	TP_{PR} - OP_{PCA}	$Ca_{T,PR}$ - Ca^{2+}_{PCA}	$K_{T,PR}$ - K^{+}	-
Biomass (X_{bio})	$f_n\,X_V$	0	$f_p\,X_V$	0	0	f_{iPAOBM} x ($X_{BH} + X_{BG}$)
PolyP (X_{PP})	0	Mg_{cpx}	P_{cpx} - P_{bio}	Ca_{cpx}	K_{cpx}	f_{iPAOPP} x P_{PP}

Where:
FSA_{SUP}: FSA concentration in supernatant extract
Mg^{2+}_{SUP}: Soluble Mg concentration in supernatant extract
N_{struv}: N concentration in struvite
TKN_{PR}: Sum of TKN concentration from PCA and residual extract
TKN_{MLSS}: TKN concentration of MLSS
Mg_{cpx}: Total Mg concentration of complex compounds (biomass and polyP)
P_{cpx}: P concentration of complex compounds (biomass + polyP)
P_{bio}: P concentration in biomass (nucleic P concentration)
OP_{PCA}: OP concentration in PCA extract
$M_{Mg,struv}$: Molar concentration of Mg in struvite
f_n: N content of biomass or UPO in terms of mgN/mgVSS
f_p: P content of biomass or UPO in terms of mgP/mgVSS
X_v: Volatile solids concentrations
f_{ipaoPP}: Inorganic mass of polyP = 3.19 mgISS/mgP
f_{iPAOBM} : Inorganic mass fraction of biomass = 0.15 mgISS/mgPAOVSS (or OHOVSS)

3.6.2 Data-modelling procedure II

As discussed later in Section 4.3.1, it was deduced that the DMP I did not yield accurate predictions from the ICT results. Hence, a revised DMP (DMP II) was developed and described in Section 4.3.2.

3.7 Defining the sample pool for evaluation of characterisation procedure

The sample pool is a set of samples that was used to evaluate the feasibility of the ICT and the DMP to characterise the inorganic solids. As discussed previously in Section 2.3, there is a general lack of information on inorganic solids downstream of the AS reactor. The influent wastewater contains inorganic solids mainly in the form of sediments, which can be determined in the total solids test. Therefore, it was only deemed necessary to develop the ISS characterisation procedure for NDEBPR sludge and its digestate. In the scope of this study, the characterisation procedure was evaluated with NDEBPR WAS sample only. Mineral precipitates in EBPR WAS occur predominantly in the form of ACP and struvite. Other precipitates such as calcite or magnesite occur in very low concentrations (<1 mg/L) and were thus assumed to be negligible (see Section 2.2.3). Hence, the samples used for the evaluation of the ICTs were made up of NDEBPR WAS, struvite and ACP. The NDEBPR WAS was obtained from the UCT AS system, as described in Section 3.4.1. Table 7 defines the different test cases that were used for the evaluation.

Table 7. Samples tested for the evaluation of the ISS characterisation procedure

Test Case	Sample
A	Struvite
B	ACP
C	Struvite & ACP
D	NDEBPR WAS
E	NDEBPR WAS & Struvite
F	NDEBPR WAS, Struvite & ACP
G	NDEBPR WAS, Struvite & ACP

Each test case constitutes of a specific objective towards the evaluation of the ISS characterisation procedure. For test cases A and B, the samples were made up by adding a known amount of struvite (approximately 1000 mg/L) and ACP (approximately 200 mg/L) to deionised water, respectively. These test cases were mainly carried out to evaluate if the maximum concentrations of mineral precipitates typically present in EBPR systems (see section 2.6.1) were fully soluble in conditions imposed by ICTs. The concentration of mineral precipitates in the samples were based on the maximum observed concentrations in weak acid/base modelling. It should be noted that the struvite used in this study had a state of hydration of three ($MgNH_4PO_4.3H_2O$), which is different to the typical hydration state of struvite ($MgNH_4PO_4.6H_2O$). Thus, the approximate maximum observed concentration of 1300 mg/L was adjusted to 1000 mg/L. The objective of test case D was to evaluate the effect of the ICT on a NDEBPR WAS sample. Test cases E, F and G were carried out to evaluate the effect of the ISS characterisation test on the mixture of NDEBPR WAS and mineral precipitate. The analytical measurements from test case F and G were used as input to the DMP. The output from the DMP were then assessed against the known concentrations of the inorganic solids.

3.8 Experimental error and uncertainty

All experimental measurements recorded carried some error. The errors in the laboratory involve both systematic errors, which can occur due to poorly maintained instruments, and random error due to instrument resolution (Gaszynski, 2020). The measurement uncertainties in this study were reported in percentage error, mean and standard deviation (Carlson, 2002).

The percentage error was calculated as follows:

$$\%\ error\ = \frac{|Measured\ value - True\ value|}{True\ value}\% \tag{3.12}$$

The mean represents the central value for a set of measurements taken for a particular datapoint. The standard deviation represents the amount of variation of all measured values from the central value. In Chapter 4, instead of reporting the measured values, the mean values accompanied by their corresponding standard deviations were used to represent each datapoint, as shown in Equation 3.12. The mean and standard deviation were calculated according to Equation 3.13 and 3.14, respectively. The standard error (represented by error bars) were calculated as shown in Equation 3.12.

$$< \chi >= \frac{1}{N}\sum_{i=1}^{N} \chi_i \tag{3.13}$$

$$\sigma_\chi = \sqrt{\frac{1}{N-1}\sum_{i=1}^{N}(\chi_i - < \chi >)} \tag{3.14}$$

$$\chi =< \chi > +\sigma_\chi \tag{3.15}$$

$$SE = \frac{\sigma_\chi}{\sqrt{N}} \tag{3.16}$$

$$Where,$$

$$< \chi > \;=\; Mean\ reading$$

$$N \;=\; Number\ of\ readings$$

$$\chi_i \;=\; Reading\ i$$

$$\sigma_\chi \;=\; Standard\ deviation$$

$$SE \;=\; Standard\ error$$

4 Results and discussion

The purpose of this chapter is to present and discuss the trends in the analytical measurements of the ICT and the output of the DMP. The evaluation of the procedure was carried out through the comparison of the output of the DMP with the known ISS concentrations.

4.1 NDEBPR WAS characteristics

The NDEBPR WAS was characterised by calibrating the experimental data generated from the UCT AS system against the mass balanced Wentzel *et al.* (1990) steady state equations (see Appendix C). Table 8 shows the results of the characterisation. Details on the system performance, as well as further characterisation is provided in Appendix G.

Table 8. NDEBPR WAS characteristics from the operation of UCT AS system at steady state

Component	OHO[a]	End. OHO[b]	PAO[a]	End PAO[b]	UPO	PolyP	USO	Effluent	Total
VSS (mgVSS/L)	578	336	2967	359	528	0	45	-	4812
N (mgN/L)	47.2	33.6	296.7	35.9	52.8	0.0	1.3	0.3	466
P (mgP/L)	14.4	8.4	74.2	9.0	13.2	310.1	0.1	57.7	487

a: Active biomass concentration
b: Endogenous biomass concentration

It is beyond the scope of this thesis to discuss all the results from operation of the NDEBPR WAS. The focus of this discussion is on the polyP, VSS and ISS concentrations generated by the UCT AS system as these parameters will be used extensively in this research. According to the predictions of the steady state model of Wentzel *et al.* (1990), which was used to calibrate the UCT AS system, 75% of the live biomass was made up of PAOs. The active PAOs constituted of about 62% of the total sludge concentration. The ratio of polyP P:PAO VSS varies and can reach a maximum of 0.38 mgP/mgPAOVSS (Wentzel *et al.*, 1990). In this sludge, the model predicted ratio was 0.11, which is a third of the maximum concentration. This was however deemed satisfactory to perform the ICT as the polyP concentration was high enough to conduct the evaluation. The polyP concentration of 310.1 mgP/L was determined using Equation 4.1:

$$PolyP\ P\ (in\ mgP/L) = TP_{MLSS} - P_{te} - f_p(X_V) \quad (4.1)$$

$$\begin{aligned} Where, & \\ TP_{MLSS} &= TP\ concentration\ of\ mixed\ liquor \\ P_{te} &= Effluent\ TP\ concentration \\ f_p &= 0.025\ mgP/mgVSS \\ X_V &= Volatile\ solids\ concentration \end{aligned}$$

The total reactor ISS concentration was calculated from the difference between the total solids concentration (X_T) and total VSS concentration (X_V). According to the total solids test, carried out on the NDEBPR WAS, an ISS concentration of 1985 mgISS/L was obtained.

4.2 ISS characterisation test

With the aim to evaluate the feasibility of the ICT and DMP to characterise the inorganic solids, the test cases outlined in Section 3.7 were carried out. Test case A, B and C were performed to evaluate the effect of the ICT on mineral precipitates (i.e., struvite and ACP) whilst test case D was carried out to determine the effect of the ICT on NDEBPR WAS samples. Test case E, F and G were conducted to evaluate the effect of the ICT on a mixture of NDEBPR WAS and mineral precipitate. The analytical measurements for test cases F and G were used as an input to the DMP. The following paragraphs discusses the analytical measurements from the test cases.

4.2.1 Test case A, B and C

Test cases A, B and C were carried out to determine the solubility of known amounts of mineral precipitates under the conditions set by the ICT. For test case A, 50 mg of struvite was added to 50 ml of deionised water to make up a target concentration of 1000 mg/L. The test case A was carried out in triplicate and the average struvite concentration added was 1064 ± 8 mg/L. As noted in Section 2.6.4 and Section 3.4.3, the cold PCA is expected to dissolve the mineral precipitates. For this struvite concentration, the expected concentration of soluble Mg, P and N in the PCA extract (based on the molar fractions of the various elements and the chemical formula of struvite and atomic masses of component elements) are 134 ± 1 mgMg/L, 172 ± 2 mgP/L and 78± 1 mgN/L, respectively (see Appendix H for equations). Figure 18 shows the measured soluble Mg, P and N concentrations for the different extracts of ICT. The soluble concentrations of the residue extract were negligible and not shown in Figure 18.

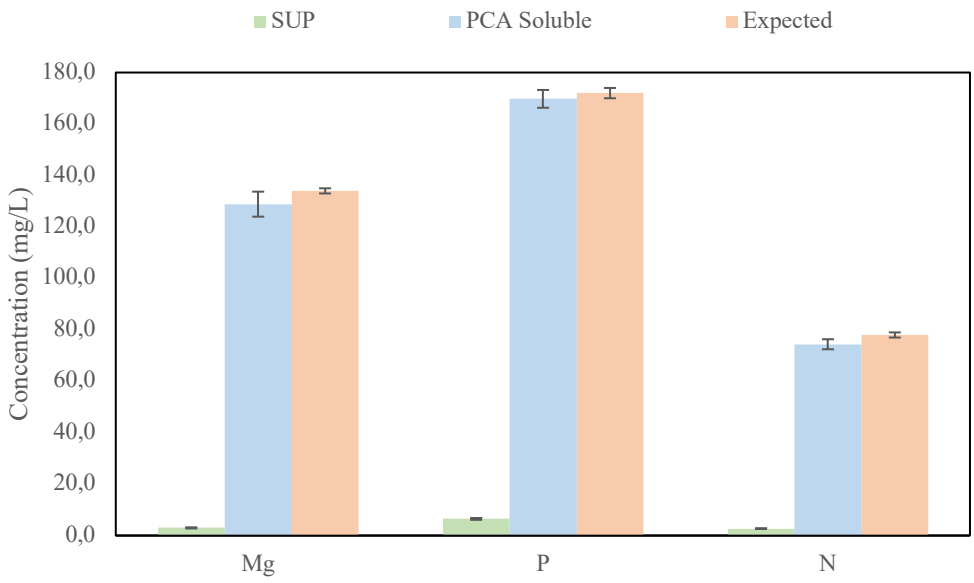

Figure 18. Soluble Mg, OP and FSA concentration in the supernatant and PCA extract of the ICT for test case A

The supernatant extract contained very low soluble concentration of Mg (2.2% of total expected Mg), P (3.8% of total expected P) and N (3.5% of total expected N). This demonstrates that only a trivial amount of struvite dissolved in the deionised water and NaCl solution. The PCA extract contained the majority of the Mg (96% of total expected Mg), P (99% of total expected P) and N (96% of total expected N). The residual extract concentration of all elements was negligible (<0.5%). Thus, it can be assumed that three 0.5 M cold PCA (0 ºC) extractions is suitable to fully dissolve 1000 mg/L struvite.

Typically, a satisfactory recovery, as calculated using Equation H6 in Appendix H would lie in the range of 90–110%. Considering all three extracts, the recovery for the three elements was within this range. The molar ratio Mg:P:N in the PCA extract (1:1.02:1.04) was close to the struvite theoretical molar ratio of 1:1:1 and provides further confidence in the experimental results.

For test case B, approximately 10.5 mg of ACP was added to 50 ml of deionised water to make up a target concentration of 200 mg/L. The test case B was carried out in triplicate and the average ACP concentration was 210 ± 7 mg/L. For this ACP concentration, the expected concentrations of Ca and P in the PCA extract are 81 ± 3 mgCa/L and 42 ± 2 mgP/L, respectively (see Appendix H for calculations). Figure 19 shows the measured soluble Ca and P concentrations for the different extracts of the ICT.

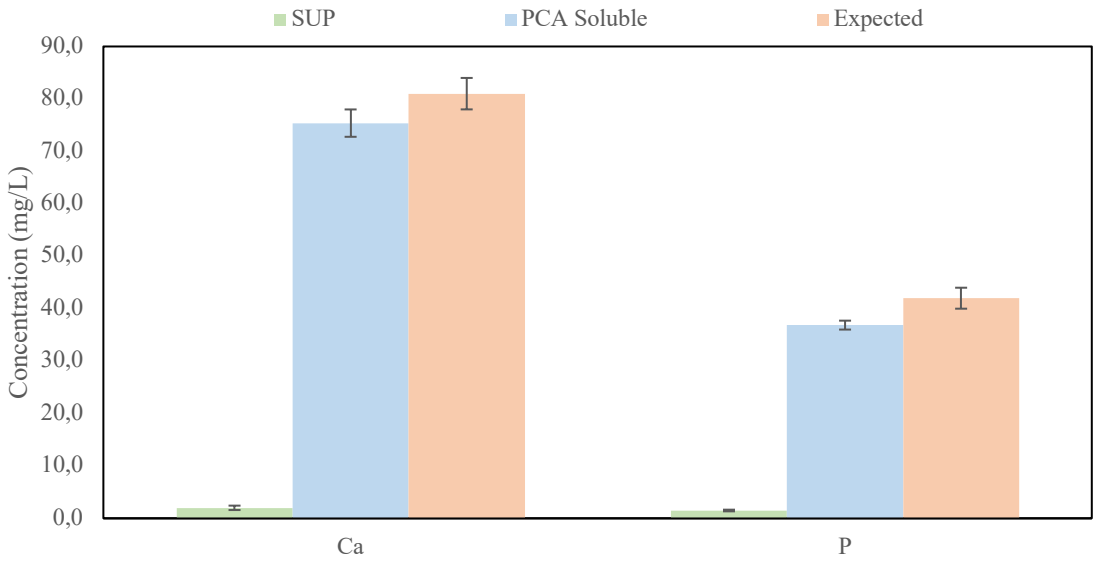

Figure 19. Soluble Ca and OP concentration in the supernatant and PCA extract of the ICT for test case B

The supernatant extract contained low soluble concentrations of Ca (2.5% of total expected Ca) and P (3.6% of total expected P). This demonstrates that only a small amount of ACP dissolved in the supernatant. The PCA contained the majority of the Ca (93% of total expected Ca) and P (88% of total expected P). The residual extract concentration of all elements was therefore very low (< 9%). Thus, it can be assumed that three 0.5 M cold PCA (0 ºC) extractions are suitable to fully dissolve 200 mg/L ACP. Considering all three extracts, the recovery of each three elements was within acceptable margin (see Appendix C).

For test case C, approximately 50 mg of struvite and 10.5 mg of ACP was added to 50 ml of deionised water to make up a target struvite concentration of 1000 mg/L and 200 mg/L of ACP. The experiment was carried out in triplicate and the average concentrations of struvite and ACP were 1048 ± 8 mg/L and 210 ± 9 mg/L, respectively. For this ACP concentration, the expected concentrations of Mg, Ca, P and N are 132 ± 1 mgMg/L, 81 ± 4 mgCa/L, 213 ± 3 mgP/L and 77 ± 1 mgN/L, respectively (see Appendix H for calculations). Figure 20 shows the measured Mg, Ca, P and N concentrations of the different extracts of ICT.

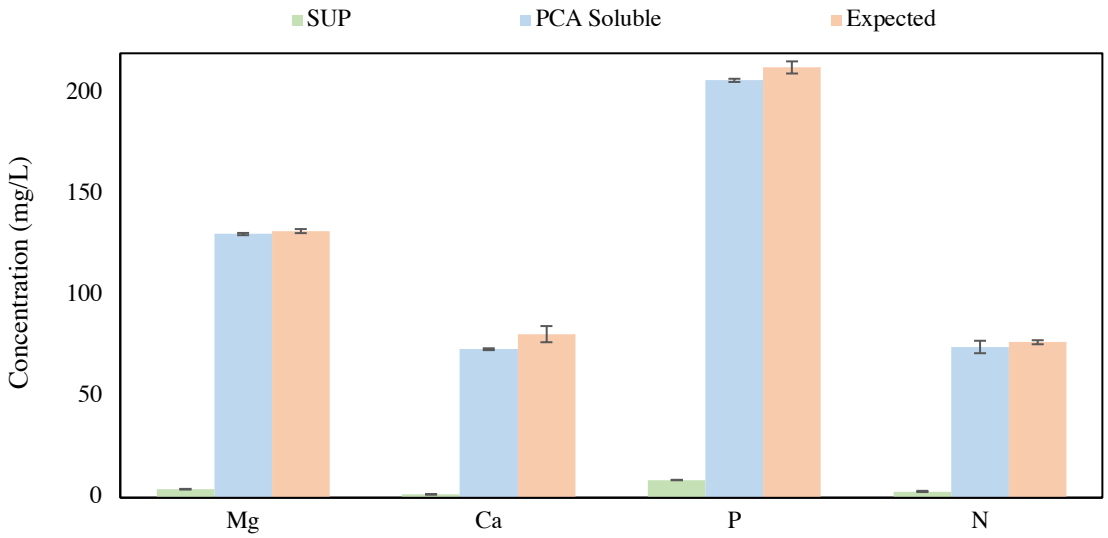

Figure 20. Soluble Mg, Ca, OP and FSA concentration in the supernatant and PCA extract of the ICT for test case C

The supernatant extract contained low soluble concentration of Mg (3.2% of total expected Mg), Ca (2.1% of total expected Ca) P (4.2% of total expected P) and nitrogen (4% of total expected N). Similarly, to test case A and B, this demonstrates that only a trivial amount of struvite and ACP dissolved in the supernatant extract. The PCA contained the majority of the Mg (98% of total expected Mg), Ca (91% of total expected Ca), P (91% of total expected P) and nitrogen (97% of total expected N). The residual extract concentration of all elements was therefore very low (<10%). Thus, it can be assumed that three 0.5 M cold PCA (0°C) extractions are suitable to fully dissolve up concentrations of struvite and ACP up to concentrations of 1000 mg/L and 200 mg/L, respectively. Considering all three extracts, the recovery of each of the three elements was within an acceptable range (see Appendix C).

4.2.2 Test case D

For test case D, the ICT was performed on the NDEBPR WAS sample without the addition of chemical precipitates. The NDEBPR WAS was obtained from the UCT AS system as described in Section 3.4.1. The characteristic of the WAS sample is presented in Table 8. The main aim of test case D was to determine the effect of the cold PCA fractionation procedure on the NDEBPR WAS (containing polyP stored by the enhanced culture of PAO biomass).

4.2.2.1 Presence of mineral precipitates

It was first necessary to determine if mineral precipitates were already present in the NDEBPR WAS sample. This is because ACP was seen to precipitate on the membrane of the reactor in the previous operation of UCT AS system, subsequently affecting the measurements on the extracts. The experimental results from a diluted sample were compared to the original NDEBPR WAS. The presence of ACP or struvite was identified by comparing the concentration of Ca, Mg, and phosphate in the supernatant. In the presence of mineral precipitates, it is expected that the supernatant (dissolved) concentrations of Mg, Ca and P all increase due to the dissolution of mineral precipitates (ACP or struvite). Figure 21 shows these concentrations in the diluted and undiluted NDEBPR WAS sample.

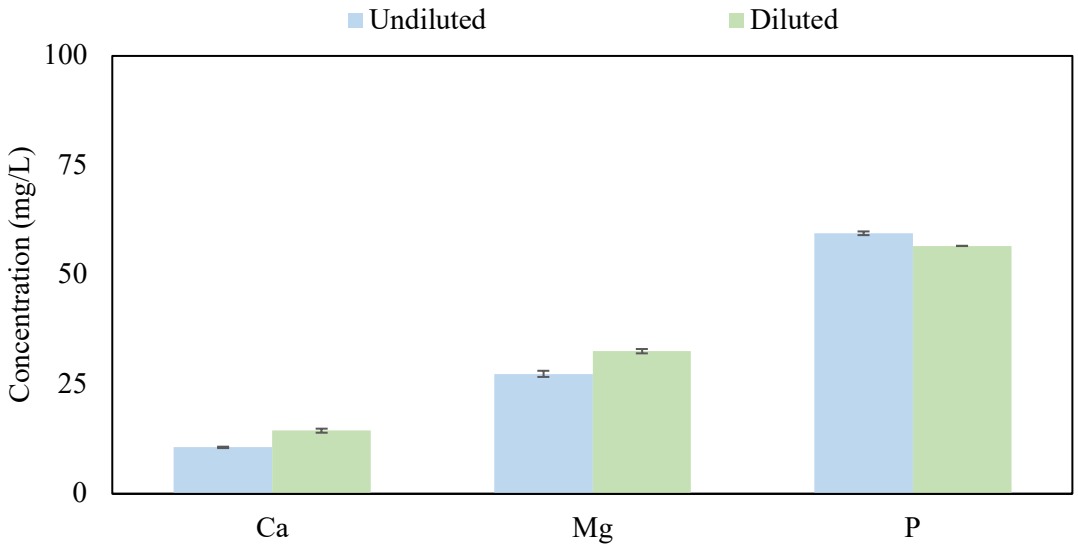

Figure 21. Comparing Ca, Mg and P concentrations to determine the presence of mineral precipitate.

As seen from Figure 21, the Mg and Ca concentrations increased slightly in the diluted sample (by 3.8 ± 0.6 mgCa/L and 5.2 ± 1.2 mgMg/L, respectively), whilst the phosphate concentration decreased slightly. It should be noted that in the presence of ACP, the soluble concentration of Ca and P would both increase in the supernatant of the diluted sample. In the presence of struvite, the concentration of Mg, N and P would increase in the diluted NDEBPR WAS supernatant. The concentration of soluble N was negligible in the diluted samples. Hence, it can be deduced that the slight increase in Mg and Ca in the supernatant of the diluted NDEBPR WAS is not due to the solubilization of ACP or struvite. As the sample was diluted with tap water, it was expected that the slight increase in Mg and Ca was due to the inherent hardness of the tap water. From this conclusion, it was deemed safe to carry out test cases E, F and G, assuming that the only precipitate present in the sample will be equal to the known amount of precipitate added.

4.2.2.2 Effect of cold PCA on NDEBPR WAS

As mentioned in Section 2.6.4, during the PCA extraction, De Haas *et al.* (2000) showed that polyP was released into the PCA solution but did not hydrolyse into OP due to the cold temperature and short extraction times. On the other hand, mineral precipitates were shown to dissolve well in cold PCA acid. Hence, for a mixture of both mineral precipitate and NDEBPR

WAS, soluble concentrations in the PCA extract would correspond to the mineral precipitate ions. However, in De Haas *et al.* (2000) experiment, no measurements were taken on the metal ion concentrations in the extracts. Hence, the effect of cold PCA extraction on counter-metal ions is not known. The DMP I (see Section 3.6.1) assumes that the counter-ions are not released in the cold PCA extract. If there is significant release of counter-ions in the PCA extract, the predictions of the DMP I will be inaccurate. As there is no mineral precipitate in test case D, the release of counter-ions in the PCA extract can be identified. Figure 22 shows the soluble and total concentrations of Mg, K, Ca, P and N in the different extracts.

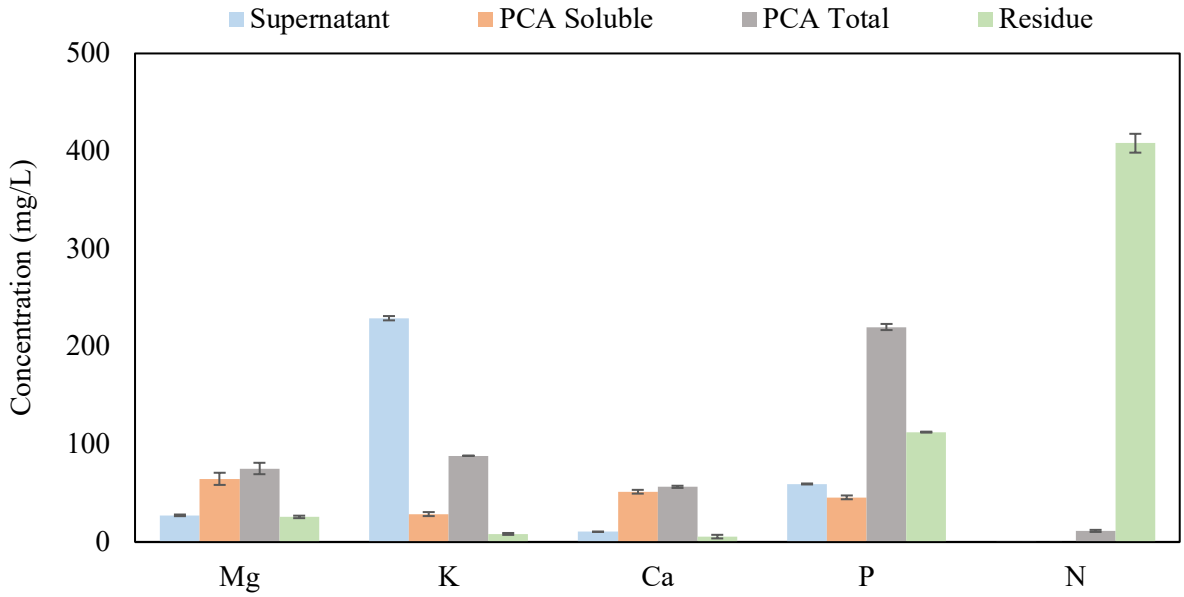

Figure 22. Concentrations of soluble and total ions in PCA extract

It can be observed from Figure 22 that the PCA extract contains soluble concentration of Mg, K, Ca, and P. With regards to the OP concentration in the PCA extract, there are several possible sources for this ion from the sludge: (i) hydrolysis of biomass cells (ii) redissolution of mineral precipitates (iii) breakdown of polyPs. The approximate formula for biomass (OHO or PAO) is $C_5H_7O_2N_{0.1}P_{0.025}$ (Henze *et al.*, 2008). When hydrolysed, the P and nitrogen are released as phosphate and ammonium ions (Brouckaert *et al.*, 2010; Ikumi *et al.*, 2014). As the FSA concentration in the PCA soluble extract is negligible, it is unlikely that the phosphate ions originated from the biomass. In the previous section, it was concluded that the presence of mineral precipitates in the original NDEBPR WAS sample was insignificant. Hence, it can be deduced that the presence of phosphate in the soluble extract originated from the hydrolysis of polyP. Moreover, the high concentrations of Mg, K and Ca in the soluble extract also point towards hydrolysis of polyP molecules, as this would result in the release of counter-ions. This would contradict the findings of De Haas *et al*. (2000). However, one study has shown that there is up to 25 % of polyP hydrolysis in cold PCA extracts (Müssig-Zufika *et al.*, 1994). In Section 4.2.2.4, the proportion of polyP hydrolysed in the PCA extract is determined.

As the concentrations of metals in other wastewater compounds (USO, UPO and biomass) are very low and no mineral precipitate was present in the sample, the soluble concentrations of Mg, K and Ca in the PCA extract were also attributed to the hydrolysis of polyP. As the counter-ions

are hydrolysed in the cold PCA extract, they are released as free ions. It is interesting to note that the ratio of Mg:K:Ca:P in the soluble extract was 1.82:0.50:0.87:1 which is significantly different from the approximate molar ratio of counter-ions in polyP found in literature (i.e., 0.3:0.3:0.03:1 (Harding & Ekama, 2009). There are potentially two reasons for this discrepancy: (i) the release of polyP counter-ions in PCA acid were varied for each one of the counter-ion, (ii) the polyP molecules in the PAOs are significantly different in this study. Although literature has shown a range of ratios for polyP counterion (see Section 2.2.2), the abovementioned ratio is significantly off from these values. Thus, the latter reason is not likely correct.

4.2.2.3 Overall recovery

The overall recovery of each element was defined as the ratio of the sum of elemental concentration in each extract to the total MLSS elemental concentrations, as shown in Equation H7 (see Appendix H). Typically, in the wastewater modelling environment, a satisfactory recovery would be in the range of 90–110%. This range is acceptable as obtaining 100% balance under experimental conditions is challenging to achieve due to possible influence of systematic and random errors (e.g., cumulative error due from minor calibration problems with the various instrumentation used). The overall recovery for Mg, K, Ca, P and N in test case D were 91%, 114%, 103%, 90%, and 90%, respectively. The recovery was deemed satisfying for Mg, Ca, P and N for test case D. Across all readings (for all test cases), it was found that the total measurement for K in the residual and PCA extract was not satisfactory. It is likely that the high concentration of K from the digestion mixture (see section 3.5.4 for metal cation analytical test procedure), negatively affects the accuracy of the discrete analyser through interference. In future, with K measurements, it is thus recommended to switch the potassium sulphate with sodium sulphate in the digestion mixture for more accurate K measurements.

4.2.2.4 Recovery of polyP

The polyP P concentration determined by calibrating the experimental data of the UCT AS system against the mass balanced steady state model of Wentzel *et al.* (1990), was compared against the polyP P concentration using the ICT. The polyP concentration from the ICT was determined using the De Haas *et al.* (2000) approach, shown in Equation 4.2. The same equation was used in the DMP I.

$$PolyP\ P\ (mgP/L) = (TP_{PCA} + TP_{RES}) - OP_{PCA} - Nucleic\ Acid\ P \quad (4.2)$$

$$Where,$$

$$TP_{PCA} = TP\ concentation\ of\ PCA\ extract$$

$$OP_{PCA} = OP\ concentration\ of\ PCA\ extract$$

$$TP_{RES} = TP\ concentration\ of\ Residual\ extract$$

As seen from Equation 4.2, the polyP concentration is obtained from the sum of P from the solids (which is equal to the sum of P from the PCA and residue extract), subtracting the soluble P concentration in the PCA (which accounts for the dissolved mineral precipitates) and the biomass P (nucleic acid P). The soluble P concentration in the PCA extract accounts for P from the solubilization of phosphate minerals. The nucleic acid P (or biomass P) is obtained by a ratio of

0.01 mgP/mgVSS (De Haas *et al.*, 2000). The modelled VSS concentration is shown in Table 8. The polyP concentration was calculated for two scenarios. It was first calculated using the actual concentration from the PCA extract, i.e. with polyP hydrolysis. The second scenario assumes that the PCA OP concentration is zero i.e., there is no hydrolysis of polyP. The result of this analysis is shown in Table 9.

Table 9. PolyP determination with/without polyP hydrolysis

Scenario	PCA TP (mgP/L)	PCA OP (mgP/L)	Residual TP (mgP/L)	BioP (mgP/L)	PolyP (mgP/L)
With polyP hydrolysis	220.1 ± 3.8	45.8 ± 1.9	112.5 ± 0.4	48.1	238.7 ± 6.1
With no polyP hydrolysis	220.1 ± 3.8	0.0	112.5 ± 0.4	48.1	284.5 ± 4.2
Modelled polyP using Equation 4.2					310.1

With polyP hydrolysis in the PCA extract, the polyP concentration was 238.7 ± 6.1 mgP/L. Assuming no hydrolysis in the PCA extract, the polyP concentration was 284.6 ± 4.2 mgP /L. The modelled polyP concentration was 310.1 mgP/L (see Section 4.1). In the first scenario, 77% of the polyP P was recovered whilst in the second scenario, 92% of polyP P was recovered assuming no polyP hydrolysis. Accounting for the hydrolysed polyP in the PCA extract improves the recovery by 15%. It can be deduced that 15% of the polyP is hydrolysed in the PCA extract. This is relatively close to the 25% polyP hydrolysis reported by Mussig-Zufika *et al.* (1994).

4.2.3 Test case E

In test case E, a known amount of struvite was added to the NDEBPR WAS. The characteristic of the NDEBPR WAS was similar as in test case D as the UCT AS system was operated at steady state. A concentration of 1030 ± 6 mg/L of struvite was added to 50 ml of the NDEBPR WAS. The aim of this test case was to determine the effect of the cold PCA fractionation procedure on a mixture of NDEBPR WAS and struvite. At several instances, reference to test case D and A provides a clear illustration of how the addition of struvite alters the concentrations in the different extract.

4.2.3.1 Supernatant concentrations (first extract)

Table 10 below shows a comparison in the increased supernatant concentrations attributed to the addition of struvite in test case E (where NDEBPR WAS was present in the sample) and test case A (whereby struvite only was added to the sample, with no NDEBPR WAS present). Relative to the supernatant concentrations in test case D, there was a slight increase in Mg and N in the test case E supernatant. The increase in these concentrations corresponded very well with the increase in supernatant concentrations in test case A (ICT on struvite only). This demonstrates that the slight increase in Mg and N concentrations is due to the dissolution of some struvite. Conversely, the increase in phosphate concentration was significantly higher than P concentration in the test case A supernatant. It is uncertain as to why the concentration of P was high in the supernatant. The possibility of sample contamination was eliminated as all triplicates showed a high increase in P concentrations as compared to test case D supernatant. The possibility of some polyP release

after the first centrifugation was also eliminated as the test on the supernatant was done immediately after the centrifugation. Furthermore, the concentration of counter-ions did not increase accordingly to support the release of polyP. The spike in OP concentrations could be related to the operation of the reactor. However, not enough information is available to be able to determine the root cause for this spike in OP concentration in the supernatant.

Table 10. Supernatant concentration comparison

Supernatant concentrations	Test case E - Test Case D	Test Case A
Mg (in mgMg/L)	2.1 ± 4.2	2.9 ± 0.2
N (in mgN/L)	2.6 ± 0.2	2.8 ± 0.2
P (in mgP/L)	17.6 ± 0.9	6.5 ± 0.8

4.2.3.2 Effect of cold PCA on NDEBPR WAS and struvite

The addition of struvite to the sample in test case D is expected to increase the soluble concentration of Mg, N and P in the cold PCA extract. The experiments in test case A have shown that the cold PCA was effective in dissolving struvite. Approximately, the same concentration of struvite (1000 mg/L) was added to a 50 ml NDEBPR WAS in test case E. It is thus expected to observe the same increase as in test case A for the same concentration of Mg, N and P in the PCA extract if the struvite dissolves fully.

Figure 23 shows the soluble PCA concentration of test case E in comparison to the expected concentration as calculated using Equation H1-H5 (see Appendix H). The FSA concentration of the PCA extract is the same as the expected N concentration of struvite (Test case E: 76.6 ± 1.4 mgN/L, expected concentration: 76 ± 1 mgN/L), thereby demonstrating that all struvite has dissolved. It was observed that the increase in concentrations of Mg and P in the PCA extract was higher than the expected concentrations. Using Equation H6 in Appendix H, the recovery for Mg and P were 161% and 125%, respectively. It was seen in Section 4.2.2.2 that a portion of polyP was hydrolysed with the PCA test, resulting in P and counter-ions being released into the PCA extract as free ions. Hence, it can be deduced that the extra Mg, Ca and P in the PCA extract are from the release of polyP counter-ion.

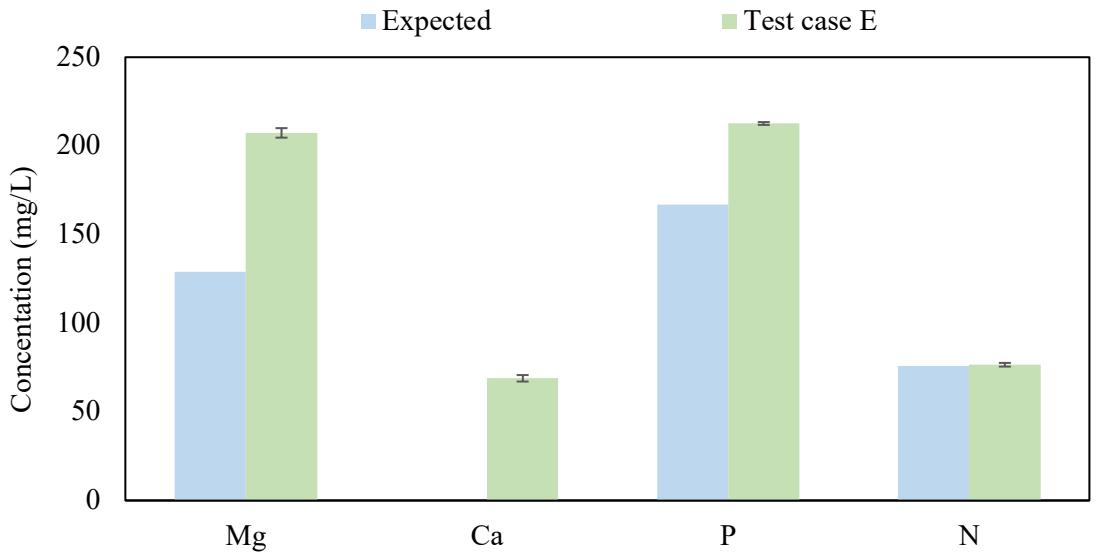

Figure 23. Actual and expected soluble concentrations in PCA extract for test case E

Interestingly, the total soluble Mg and OP concentrations in the PCA extract of test case E was roughly equal to the soluble Mg and OP concentrations from the PCA extract of test case A and D combined, as illustrated in Figure 24. From this, it can be inferred that the extent of Mg and P release did not change significantly from test case D (i.e., the same concentrations of polyP P and Mg were released in test case D and E).

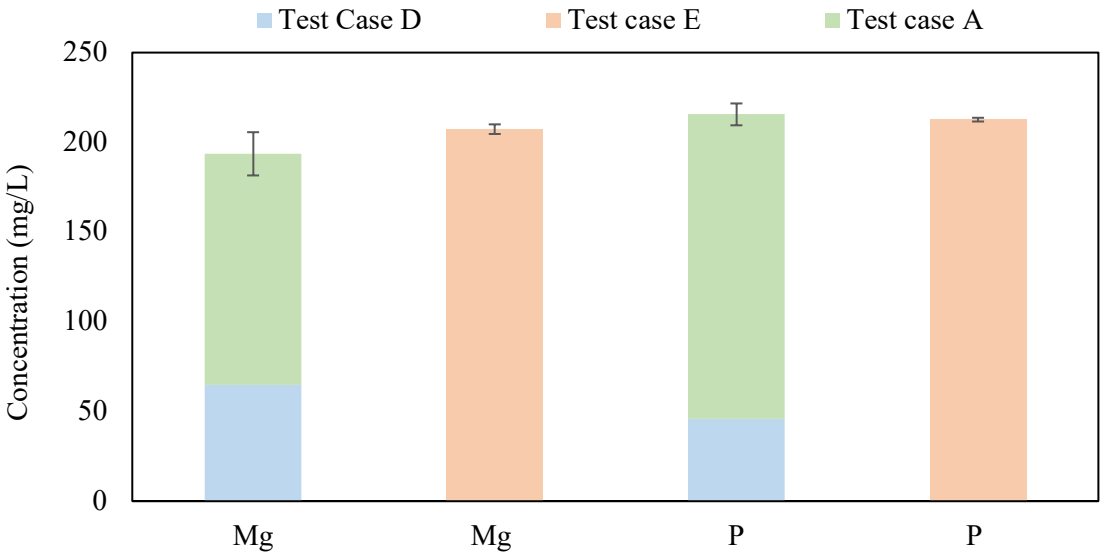

Figure 24. Comparison of PCA extract concentrations between test case A, D and E

The ratio of soluble Mg:N:P in the PCA extract of test case E should be equal to 1:1:1 if only struvite dissolves. The ratio of soluble Mg:N:P in the PCA extract of test case E was 1:0.79:0.63. Considering the soluble Mg and P release from polyP, this ratio changes to 1:0.92:0.98. The latter is closer to the Mg:N:P ratio in struvite and thus further demonstrates that the extent of polyP hydrolysis did not significantly vary from test case D.

The extent of Ca and K release from polyP can also be determined by comparing the soluble K and Ca concentrations of test case E with test case D. The addition of struvite to the NDEBPR

WAS is not expected to change the concentration of soluble of K and Ca in the PCA extract. The overall recovery (sum of extracts versus MLSS) of test case E was deemed satisfactory for Mg, Ca, N and P and is illustrated on Table 39D. However, the overall K recovery was unsatisfactory and was not used in the analysis due to a low confidence in the measured K concentrations. The soluble Ca concentration in the PCA extract increased by 33% from test case D. As the only other source of Ca in test case E is from polyP (it was seen in Section 2.2.3, that the NDEBPR WAS sludge has negligible concentration of calcite), it can be deduced that there was an increase in the Ca release from polyP. Hence, this does not align with the trend observed for Mg and P, which was seen to be constant in test case D and E.

At this point it is worth noting the importance in determining the extent of polyP hydrolysis, and how consistent it is in the cold PCA extraction. The DMP I was based on findings by De Haas *et al.* (2000), who found that there was no hydrolysis of polyP. However, in test case D, an increase in OP and soluble Mg, N, Ca and K showed the occurrence of hydrolysis. Therefore, the DMP I is not likely to yield accurate results, as discussed later in Section 4.3.1. Given that the extent of polyP hydrolysis stays relatively constant, this can potentially be integrated in an altered DMP (referred as DMP II).

4.2.3.3 Recovery of polyP

A similar analysis as in Section 4.2.3.3 was performed for test case E. Table 11 presents the results of this analysis. In the second scenario, it was assumed that 45.8 mgP/L was hydrolysed, as determined in test case D. The modelled polyP was 310.1 mgP/L and was obtained according to Equation 4.1. Not considering polyP hydrolysis, the polyP concentration is 265.5 ± 5.3 mgP/L. The percentage recovery is 86%. Conversely, accounting for polyP hydrolysis, the polyP concentration is determined as 311.4 ± 8.3 mgP/L, therefore achieving 100% recovery. This improvement of 14% is approximately the same as in test case D. Hence, this further demonstrates that the release of polyP P was fairly consistent in test cases D and E.

Table 11. Analysis of polyP concentration assuming hydrolysis in PCA extract

Scenario	PCA TP (mgP/L)	PCA OP (mgP/L)	Residual TP (mgP/L)	BioP (mgP/L)	PolyP (mgP/L)
With polyP hydrolysis	359.8 ± 1.4	212.6± 1.0	166.5 ± 2.8	48.1	265.5 ± 5.3
With no polyP hydrolysis	359.8 ± 1.5	166.8 ± 1.0	166.5 ± 2.8	48.1	311.4 ± 8.3
Modelled polyP using Equation 4.1					310.1

4.2.4 Test case F

In test case F, 207 ± 4 mg/L ACP and 1054 ± 10 mg/L struvite were added to the characterised NDEBPR WAS in Section 4.1. The characteristic of the NDEBPR WAS was similar as in test case D since it was sourced from the same UCT AS system that operated at steady state. The aim of this test case was to determine the effect of the cold PCA fractionation procedure on a mixture of NDEBPR WAS, struvite and ACP. The results from test case F are also used as an input to the DMP.

4.2.4.1 Supernatant concentrations

In the supernatant extract of the ICT, a slight increase in soluble Ca and Mg concentrations showed that there was insignificant dissolution of ACP and struvite. It was thus expected that the mineral precipitate ion concentrations were measured in the PCA extract. Table 31D in Appendix D shows the supernatant concentration in test case F. The spike in OP concentration was not observed in the supernatant of test case F, as opposed to test case E.

4.2.4.2 Effect of cold PCA on NDEBPR WAS, struvite and ACP

With the addition of ACP and struvite in test case F, it is expected to observe an increase in the soluble Mg, Ca, P and N concentrations in the PCA extract provided that the mineral precipitate dissolves. The expected soluble Mg, Ca, P and N concentrations in the PCA extract were compared to the actual concentrations of the PCA extract (see Appendix H for calculations), as shown in Figure 25.

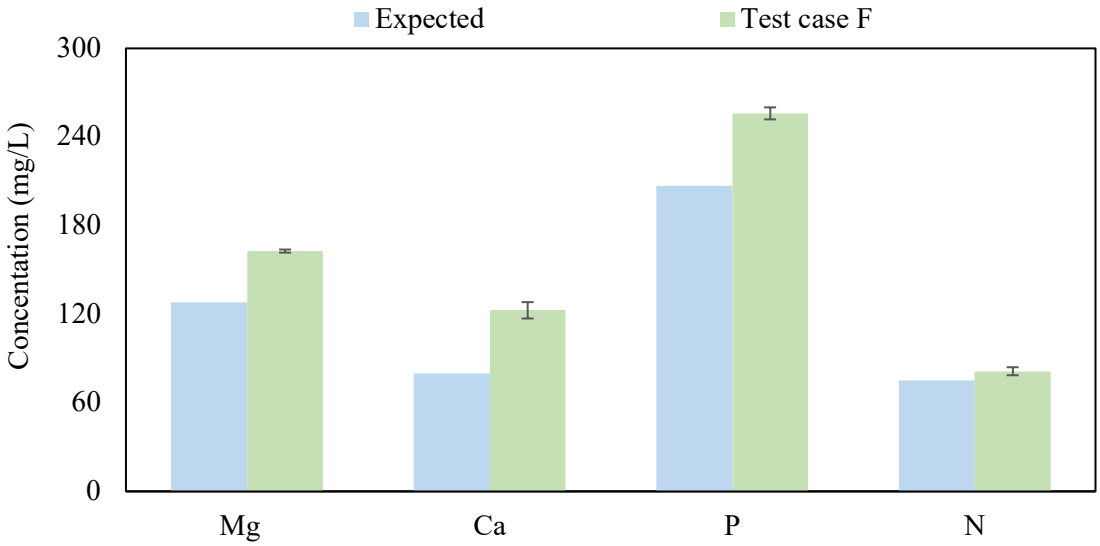

Figure 25. Actual and expected soluble concentrations in PCA extract for test case F

It can be clearly observed that the concentrations of Mg, Ca and P were higher than the expected corresponding concentrations in the PCA extract. The percentage difference between the expected and actual concentrations for Mg, Ca, P and N are 21%, 35%, 19% and 8%, respectively. Firstly, it is worth mentioning that the soluble N concentration is close to the expected N concentration. The difference is likely due to the hydrolysis of a low concentration of biomass, resulting in the release of N in the PCA extract. This demonstrates that all struvite dissolved in test case F. For Mg, Ca and P the percentage differences are relatively high. In test case E (Section 4.2.3.2) a similar trend was observed where concentrations of Mg and P were more than the expected soluble concentrations of the PCA extract. This was attributed to the release of polyP P and the counter-ions. It can thus be deduced that the differences between the expected and actual soluble concentrations in the PCA extract of test case F were also linked to the release of polyP P and counter-ions.

To determine the effect of the PCA extract on ACP and struvite, the following steps were followed:

- It was first required to assume that the extent of polyP hydrolysis to OP remained constant as in test case D at 15% of the total polyP concentration (see Section 4.2.2.4).
- The difference between the OP concentration in the PCA extract (256.0 ± 2.7 mgP/L) and the sum of P from struvite (171 ± 2 mgP/L) and hydrolysed polyP OP concentration (45.8 ± 1.9 mgP/L), was determined as shown in Equation 4.3. From this equation, it was determined that the OP from ACP was 39 ± 7 mgP/L. As this value is very close to the expected concentration of ACP OP (41 ± 1 mgP/L), it can be deduced that all ACP dissolved and the polyP P hydrolysis indeed remained constant as in test cases D and E.

$$OP_{ACP} = OP_{PCA} - (P_{Struv} + OP_{hyd.\ polyP}) = 40\ mgP/L \quad (4.3)$$

$$Where,$$

$$OP_{PCA} = OP\ concentation\ of\ PCA\ extract$$

$$P_{Struv} = P\ content\ of\ struvite$$

$$OP_{hyd.\ polyP} = OP\ concentration\ released\ from\ hydrolysed\ polyP$$

From the previous test cases, it was observed that the counter-ion release from polyP was constant for Mg, whilst Ca showed some variation. It was determined that all struvite dissolved by analysing the FSA concentration in PCA extract. The Mg concentration in the PCA extract should theoretically be 132 ± 2 mgMg/L. Therefore, the concentration of Mg released from polyP is obtained from the difference between the measured soluble Mg in the PCA extract and 132 ± 2 mg/L. This yields 31 ± 3 mgMg/L, which is different from what was released in test case D (64.8 ± 6.2 mgMg/L). Hence, the extent of counter-ion Mg release was not the same as in test cases D and E.

Conversely, the counter-ion Ca release in test case F was seen to be relatively consistent with test case D. The expected increase in Ca concentration (from test cases D and E) due to the solubilization of ACP is 80 ± 2 mgCa/L, as demonstrated through the equations in Appendix H. The measured soluble Ca concentration in the PCA extract was 123 mgCa/L. The concentration of Ca released from polyP in test case F is 43 mgCa/L. The measured Ca release in the PCA extract from test cases D and E was 52 mgCa/L and 69 mgCa/L, respectively. It can thus be deduced that the release of polyP Ca in test case F varied slightly from test case D, but is considerably less than the release in test case E. In conclusion, the hydrolysis of polyP to OP in the PCA extract was observed to be consistent for test cases D, E and F. However, the release of Mg and Ca was not always constant for test cases D, E and F.

4.2.4.3 Overall recovery

The overall recovery of the elements for test case F (sum of extracts versus MLSS) was within acceptable range, except for K measurement. The overall recovery is illustrated in Table 40D in Appendix D. The polyP recovery was discussed in Section 4.3.

4.2.5 Test case G

In test case G, 207 ± 5 mg/L ACP and 500 ± 4 mg/L struvite was added to the characterised NDEBPR WAS of Section 4.1. The characteristic of the NDEBPR WAS was similar to that of test case D as the UCT AS system was at steady state. The aim of this test case was to determine the effect of the cold PCA fractionation procedure on a mixture of NDEBPRWAS, struvite and ACP. The results from test case G were used as an input to the DMP.

4.2.5.1 Supernatant concentrations

As observed in previous test cases with mineral precipitates, there is negligible dissolution of mineral precipitates in the supernatant extract. It is thus expected to recover all the mineral precipitates in the PCA extract. In test case G, half of the amount of struvite precipitate was used as compared to test case F. Figure 26 shows the supernatant concentrations in test case G in comparison with test cases F and D.

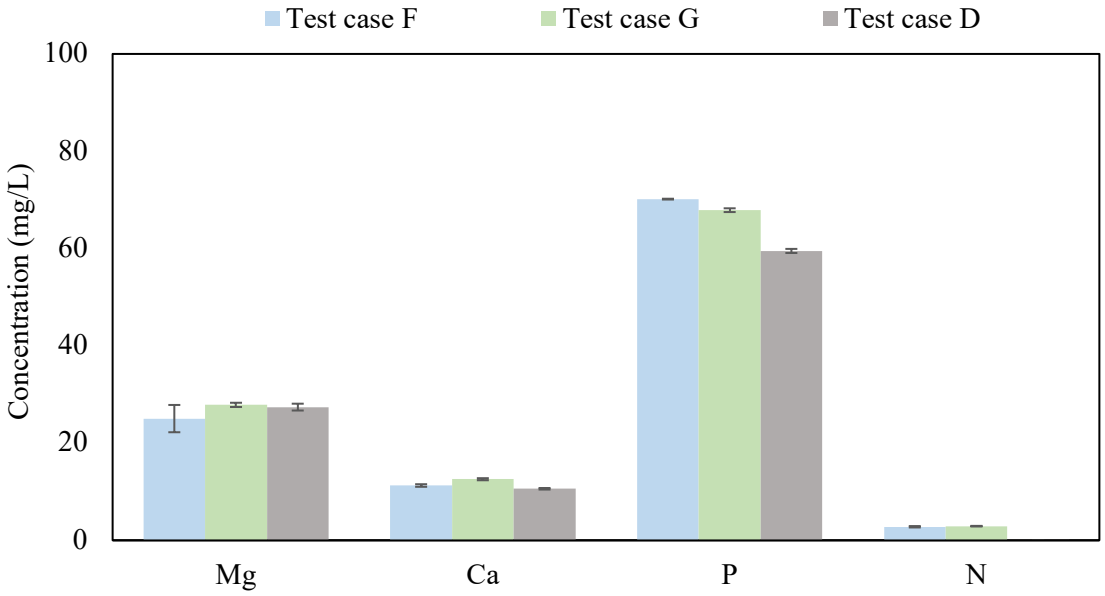

Figure 26. Supernatant concentration for Test case F, G and D

There is a negligible difference in supernatant concentrations between test cases F and G, due to the fact that the soluble concentrations originated mostly from the sludge. The sludge had the same characteristics as in test cases D-G. The dissolution of mineral precipitates into the supernatant was also insignificant in test case G, as also observed in previous test cases.

4.2.5.2 Effect of cold PCA on NDEBPR WAS, struvite and ACP

The effect of the cold PCA extract on the mineral precipitates and polyP was also determined for test case G. Figure 27 shows the measured soluble concentrations and the expected concentrations of Mg, Ca, P and N in the PCA extract. It can be clearly observed that the measured concentrations are higher than the expected concentrations for Mg, Ca and P.

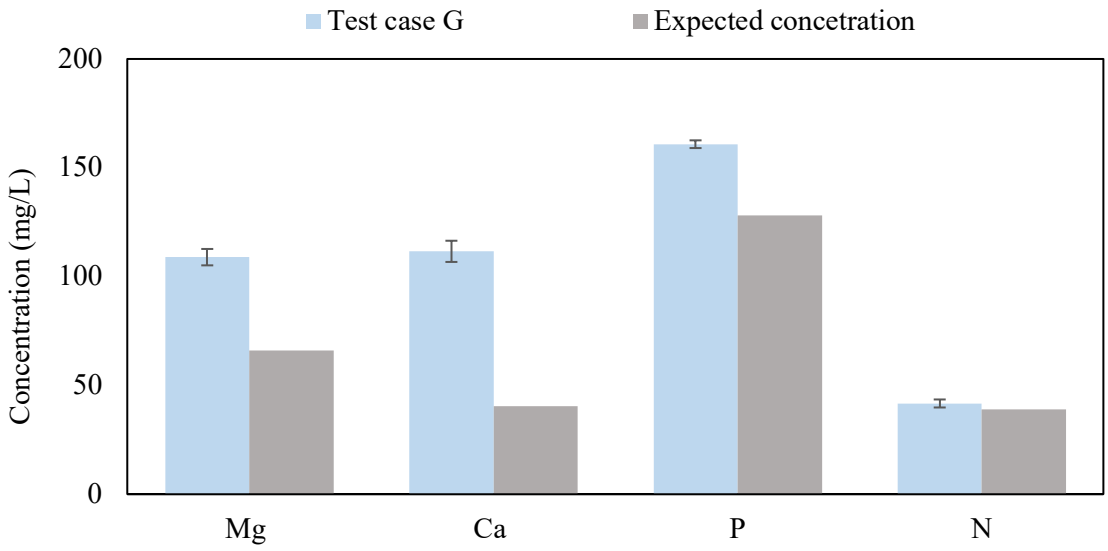

Figure 27. Actual and expected soluble concentrations in PCA extract for test case G

In test cases D, E and F it was shown that the hydrolysis of polyP resulted in the release of Mg, Ca, and P release into the PCA extract. Three deductions were made from the analysis of the results from these cases:

a) the release of polyP P in the PCA extract was seen to be approximately constant at 15% of the total polyP concentration
b) the release of polyP counter-ions Mg and Ca was varied amongst the test cases, and
c) all mineral precipitates dissolved in the PCA extract

To further verify (a) and (b), the difference between the measured ion concentration in the PCA extract of test cases G and D was compared to the expected ion concentration of the mineral precipitates (as calculated in Appendix H), as presented in Table 12. In the case where the polyP hydrolysis extent was similar to test case D, these two parameters should be equal.

Table 12. Actual and expected soluble concentrations in PCA extract of test case G

Soluble PCA concentration		
	Test case G – Test case D	Expected concentration
Mg (mgMg/L)	44.2 ± 10.0	62.8 ± 0.5
Ca (mgCa/L)	60.0 ± 11.0	80.1 ± 2.0
P (mgP/L)	115.0 ± 8.1	122.6 ± 2.3
N (mgN/L)	41.7 ± 9.2	36.6 ± 0.3

The percentage error (as calculated from Equation 3.8) for Mg, Ca, and P is 33%,48%, and 10% respectively. For Mg and Ca, the percentage error is relatively significant. With the same extent of polyP hydrolysis as in test case D, it can be observed that Mg concentration from struvite was 44.2 ± 10.0 mgMg/L. As the expected Mg concentration from struvite is 62.8 ± 0.5 mgMg/L, it is likely that an additional 18 mgMg/L was released from polyP (as compared to test case D).

Similarly, the percentage error in Ca could be ascribed to a higher release of Ca from polyP (by approximately 20 mgCa/L). The release of P from polyP was fairly consistent as the percentage error was low. It is worth noting that the FSA concentration in the PCA extract is equal to the N concentration in struvite. This was also observed in previous test cases and demonstrates that all struvite dissolved, and hydrolysis of biomass N to form ammonia is negligible in the cold PCA extract.

4.2.5.3 Overall recovery

The overall recovery of the elements for test case G (sum of extracts versus MLSS) was deemed satisfactory, except for K measurements. The overall recovery is illustrated in Table 41D in Appendix D. The polyP recovery is discussed in the next section.

4.3 Data-modelling procedure

4.3.1 Application and evaluation of data-modelling procedure I

4.3.1.1 Output of data-modelling procedure I

The data modelling procedure, developed in Section 3.6.1, was applied to the results of test case F. This section aims to discuss and evaluate the output from the DMP I, summarized in Table 13.

Table 13. Output of DMP I using results from test case F

	N (mgN/L)	Mg (mgMg/L)	P (mgP/L)	Ca (mgCa/L)	K (mgK/L)	ISS (mgISS/L)
Soluble (S_{oluble})	2.8	25.0	70.2	11.3	268.5	-
Struvite (X_{struv})	95.0	162.8	210.2	0	0	1661.7
ACP (X_{ACP})	0	0	45.8	122.7	0	457.5
Complex (X_{cpx})	192.5	86.6	277.6	-3.6	196.6	-
Biomass (X_{bio})	340.0	0	34.8	0	0	536.1
PolyP (X_{PP})	0	86.6	242.8	-3.6	196.6	774.5

The aim of this paragraph is to discuss the procedure followed in Section 3.6.1 to obtain the concentration of the different ISS components. As observed in Table 13, the concentration of struvite, ACP and polyP predicted from the DMP I for test case F were 1661 mgISS/L, 457 mgISS/L and 242 mgP/L, respectively. The calculation process is outlined below:

- The struvite concentration is predicted from the measured Mg concentration in the PCA extract (162.8 mgMg/L) using the formula shown in Table 6.
- The polyP Mg concentration was determined using Equation 3.1 and yielded 86.6 mgMg/L. The P content of struvite was calculated using a Mg:P molar ratio in struvite, as shown in Equation 3.4. The struvite P concentration was thus 210 mgP/L.
- The ACP P concentration was determined from the difference between the PCA OP concentration and the struvite P concentration, as shown in Equation 3.5. The ACP P concentration was 45.8 mgP/L.

- The ACP Ca concentration was determined from the soluble Ca concentration in the PCA extract (122.7 mgCa/L). The ACP concentration (as mgISS/L) was then determined using its Ca concentration, as shown in Table 6.
- The Ca concentration of polyP was determined using Equation 3.2. The polyP Ca concentration was calculated to be a negative value. This is further explained in the next section. It was observed during these experiments that K measurements were inconclusive and inaccurate using the chosen method. Hence the output for polyP K content (186.6 mgK/L) from the DMP I is also incorrect.

4.3.1.2 Model predictions

First, the accuracy of the DMP I was discussed by comparing its output with the known concentrations of mineral precipitates and polyP. Figure 28 shows the predicted and actual concentrations of mineral precipitates.

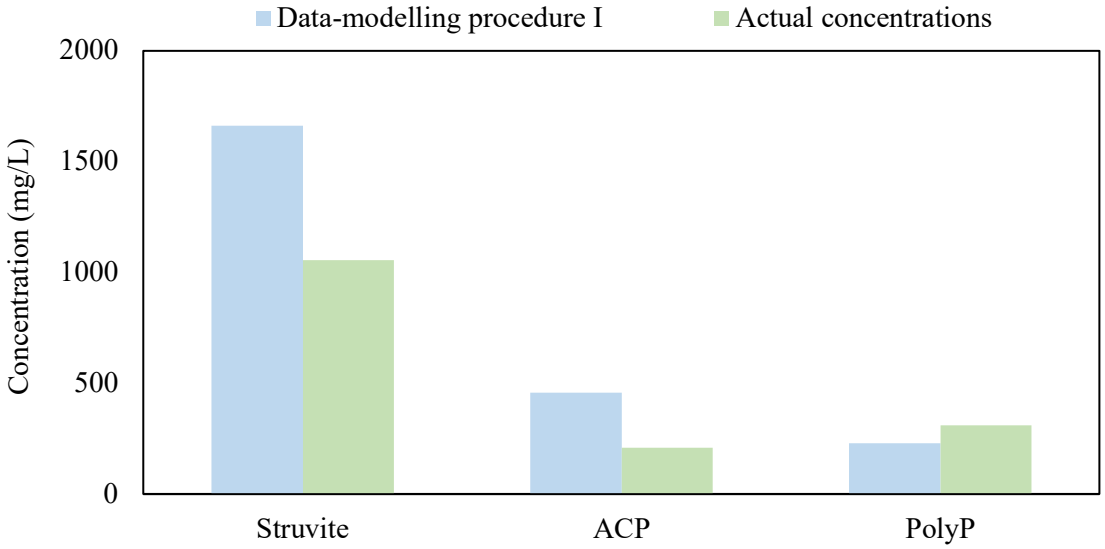

Figure 28. Comparison between DMP I output and actual ISS concentrations

From Figure 28, it can be observed that the concentration of mineral precipitates has been overestimated, whilst the concentration of polyP is underestimated. The percentage error in prediction for struvite and ACP were 66% and 129%, respectively. These values are high and are a result of the hydrolysis of polyP in the PCA extract. The DMP assumes no polyP hydrolysis in the PCA extract, and thus all ions measured in the PCA extract are attributed to the mineral precipitates. Due to polyP hydrolysis, the Mg and Ca concentrations in the PCA extract (162.77 mgMg/L and 122.68 mgCa/L, respectively, as seen from Table 31D) were higher than the concentrations of Mg and Ca dissolved from struvite (132 mgMg/L) and ACP (81 mgCa/L), respectively. As the concentration of struvite and ACP were calculated from the soluble Mg and Ca concentrations in the PCA extract, these values were also overestimated.

The concentration of polyP P as well as the counter-ions are output of the DMP I. The percentage error in the prediction of polyP P was 28%. The polyP P concentration in the DMP was calculated following De Haas *et al.* (2000) approach. Figure 29 shows the output from the determination of

polyP, with and without hydrolysis (for more details, a similar analysis was carried out in Section 4.2.2.4).

Assuming no polyP hydrolysis, the percentage error in polyP prediction decreases from 28% to 7%. Hence, it can be deduced that the under-prediction of polyP P is related to the hydrolysis of polyP in the PCA extract. The DMP I also allowed for the determination of polyP counter-ion concentrations and the polyP formula in terms of $Mg_aK_bCa_cP_d$ as outlined in Section 3.6.1.

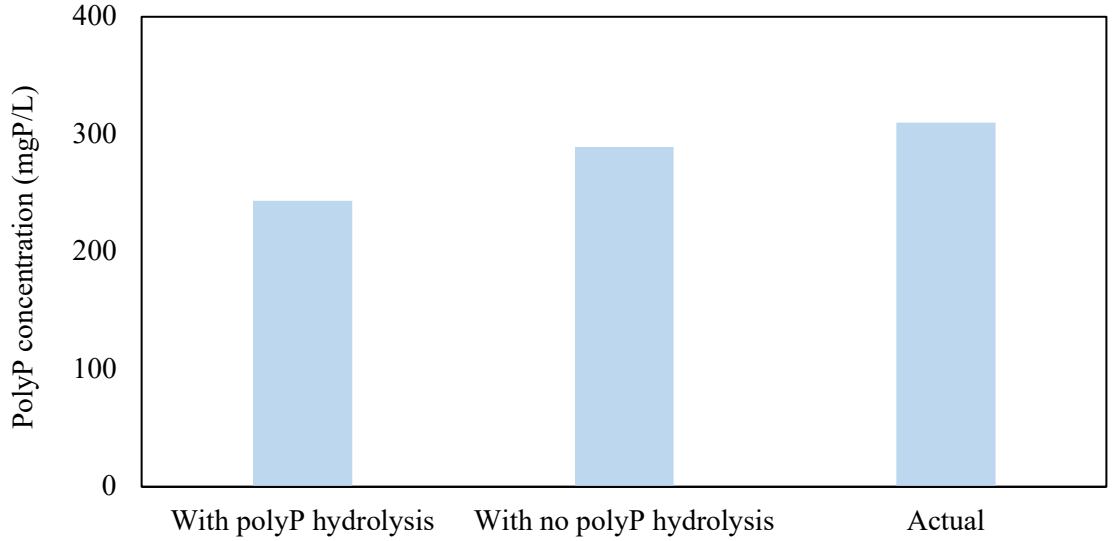

Figure 29. DMP I output with and without polyP hydrolysis

Due to the release of polyP counter-ions and polyP P, the data-modelling output for the concentration of the counter-ions is invalid. It can be observed that the polyP Ca concentration is negative. This was obtained from the difference between the total Ca in the PCA and residual extract and the soluble PCA extract, as shown in Equation 3.2. However, it was seen that polyP Ca is released into the PCA extract as a soluble ion. This consequently increases the soluble Ca concentration and makes the polyP Ca concentration calculated as a negative value.

4.3.1.3 ISS recovery

To further evaluate the DMP I, the measured ISS concentrations can be compared to sum of the ISS concentrations from the output of the DMP I. Figure 30 shows a breakdown of the modelled ISS concentrations, as well as the measured ISS concentrations.

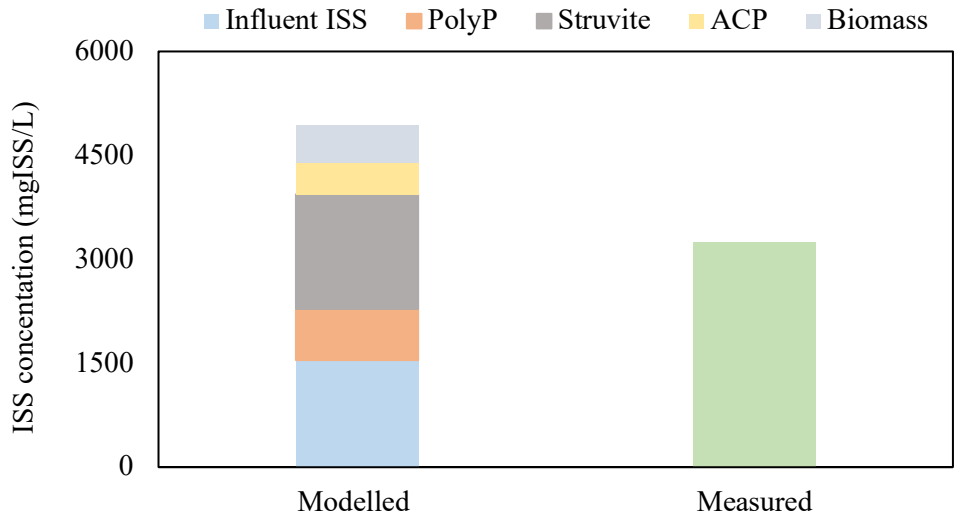

Figure 30**. Comparison between DMP I modelled ISS concentration and measured ISS concentration**

It can be clearly observed that the modelled ISS concentration is significantly higher than the measured ISS concentration. There are two possible causes behind this. First, the influent ISS concentration was measured as 109 mgISS/L but typically, concentrations of ISS in settled wastewater are in the range of 15-30 mgISS/L (see Section 2.2.1). It is currently speculated that this high concentration is because the feed to the reactors was taken from the bottom of the storage tank, where a significant amount of sand has settled and accumulated. Second, the solids concentration in the influent wastewater is diluted with the synthetic WW, as the latter has no solids content. Using Equation 4.4, the accumulated ISS (only due to influent ISS) concentration was calculated for an influent ISS concentration of 109 mgISS/L and 30 mgISS/L.

$$MX_{Io,influent} = \frac{(X_{io} \times R_s \times Q_i)}{V_p} \quad (4.4)$$

$$Where,$$

$$MX_{Io,influent} = Accumulated\ ISS\ mass\ due\ to\ influent\ ISS$$

$$X_{Io} = Reactor\ ISS\ concentration$$

$$R_s = Sludge\ age$$

$$Q_i = Influent\ flow$$

$$V_p = Volume\ of\ reactor$$

Using the system characteristics (R_s, Q_i and V_p) given in Section 3.4.1, it was found that the accumulated ISS concentration for influent concentration of 109 mgISS/L and 30 mgISS/L were 1547 mgISS/L and 425 mgISS/L, respectively. The high influent ISS concentration measured is significantly contributing to the total ISS and could potentially be the major source of error. Secondly, it was determined that the modelled ISS concentration of struvite and ACP were overestimated due to the hydrolysis of polyP into the PCA extract. Struvite and ACP are contributing to an overprediction of 850 mgISS/L, whilst the influent ISS could potentially be contributing to a surplus of 1100 mgISS/L. Furthermore, it should be noted that the polyP concentration is underpredicted by 68 mgP/L. This consequently results in an underprediction of polyP ISS concentration of 220 mgISS/L. The net error amounts to approximately 1800 mgISS/L

(55% error), which is the difference between the prediction of DMP and the measured ISS. Hence, it can be deduced that the hydrolysis of the polyP in the extract affects the total modelled ISS concentrations.

From the evaluation of the DMP I, it was clear that the hydrolysis of polyP molecules in the PCA extract had considerable impact on its predictions. The mineral precipitates concentrations were overpredicted whilst the polyP concentration was underpredicted. The measured ISS concentration did not agree with the modelled ISS concentration. A second DMP was thus developed to account for the hydrolysis of polyP.

4.3.2 Data-modelling procedure II

Due to the hydrolysis of polyP in the PCA extract, it was deemed necessary to develop DMP II, to investigate if better predictions can be obtained from the results of the ICT. The following sections described the development of the DMP II and discusses the application of the DMP II to the results of the ICT.

4.3.2.1 Development

The DMP I was developed to allow for a rigorous and robust characterisation. At certain points in the model, stoichiometric relations could be verified, such as the polyP counter-ion molar ratios, or the Ca:P in ACP. This verification provided confidence in the DMP. Due to the release of polyP counter-ions (Mg, Ca and P) in the PCA extract, the DMP robustness decreases as the same stoichiometric relationship has to be used to characterise the inorganic solids. The development of the DMP II is explained below. Table 14 shows the matrix for the DMP II.

The following points give the rationale behind the DMP II:

- Due to the release of polyP counter-ions in the PCA extract, the measurement of soluble Mg in the PCA extract does not correspond only to the Mg from struvite. The analysis of the results for test cases D and E, F and G showed that FSA in the PCA extract was solely from struvite, and negligible contribution to FSA from biomass was observed. This has two positive implications for the DMP. Firstly, the concentration of struvite can be obtained from the N measurements directly. Secondly, using the molar ratio of Mg:N (denoted as $M_{Mg,struv}$:$M_{N,struv}$ in equations below) in struvite (1:1), the soluble concentration of Mg (also P) corresponding to struvite (Mg_{struv}) can be obtained. Equation 4.5 and 4.6 are used to calculate Mg_{struv} and P_{struv}.

$$[Mg_{struv}] = [M_{Mg,struv}: M_{N,struv}] \times \frac{[N_{struv}]}{14\ mgN/mol} \times 24\ mgMg/mol \quad (4.5)$$

$$[P_{struv}] = [M_{P,struv}: M_{N,struv}] \times \frac{[N_{struv}]}{14\ mgN/mol} \times 31\ mgP/mol \quad (4.6)$$

- The Mg content of polyP (or complex Mg, Mg_{cpx}) is given from the difference between the total Mg in the PCA and residue extract ($Mg_{T,PR}$) and the struvite Mg concentration (Mg_{struv}), as shown in Equation 4.7. It should be noted that the soluble Mg in the PCA extract cannot be used in this step (as in DMP I) due to the release of the counter-ion Mg in the PCA extract.

$$[Mg_{cpx}] = [\mathrm{Mg}_{T,PR}] - [\mathrm{Mg}_{\mathrm{struv}}] \quad (4.7)$$

- Due to the release of OP in the PCA extract, the determination of polyP P as carried out in the DMP I was not possible. In the DMP II, using the molar ratio of P:Mg (denoted as $M_{P,PP}$:$M_{Mg,PP}$) in the approximate formula of polyP (see Section 2.2.2), the P content of polyP was determined. The P:Mg ratio used in this research was 1:0.35. This value lies on the upper range of Mg:P values reported in previous literature. For lower values of Mg:P, inaccurate predictions from the DMP II were obtained. It should be noted that this value will likely vary for a different system and has to be parametrised or calibrated for each experimental investigation. However, up to now, it is not known what drives the uptake of counter-ions by PAOs. The P content of polyP is obtained using Equation 4.8.

$$[P_{PP}] = [\mathrm{M}_{P,\mathrm{PP}}: \mathrm{M}_{Mg,\mathrm{PP}}] \times \frac{[\mathrm{Mg}_{\mathrm{cpx}}]}{24\ mgN/mol} \times 31\ mgP/mol \quad (4.8)$$

- The contribution of P from ACP in the PCA extract was determined by subtracting the P contribution from struvite and polyP. It was previously concluded that approximately 15% of polyP is hydrolysed to orthophosphates in the PCA extract, and hence this proportion was included in the formula as shown in Equation 4.9. Although the rate of polyP P hydrolysis was observed to be fairly consistent in this study, it can potentially vary as sludge properties such as polyP concentration change. De Haas et al. (2000) showed that there was negligible polyP hydrolysis in the cold PCA extract, whilst Müssig-Zufika et al.(1994) showed that there was up to 25% of polyP hydrolysis. Hence, the degree of polyP hydrolysis needs to be parametrised or calibrated for each experimental investigation.

$$[P_{ACP}] = [\mathrm{OP}_{\mathrm{PCA}}] - [\mathrm{P}_{struv}] - 0.15\,[P_{PP}] \quad (4.9)$$

- The Ca concentration of ACP (CaACP) was determined by using the molar ratio of Ca:P in ACP [Ca3(PO4)2], as shown in Equation 4.10. As there is release of Ca2+ from polyP in the PCA extract, the approach used in DMP I was not possible.

$$[Ca_{ACP}] = [\mathrm{M}_{Ca,\mathrm{ACP}}: \mathrm{M}_{P,\mathrm{ACP}}] \times \frac{[P_{ACP}]}{31\ mgP/mol} \times 40\ mgCa/mol \quad (4.10)$$

- The Ca content of polyP (or complex Ca, Cacpx) is given from the difference between the total Ca in the PCA and residue extract (CaT,PR) and the ACP Ca concentration (CaACP), as shown in Equation 4.11. Similarly, the K content of the polyP is obtained using Equation 4.12.

$$[Ca_{cpx}] = [Ca_{T,PR}] - [Ca_{ACP}] \quad (4.11)$$

$$[K_{cpx}] = [K_{T,PR}] - [K_{ACP}] \quad (4.12)$$

- The ISS concentrations (as mgISS/L) of the different ISS constituents can be obtained as shown in the last column of Table 14.

Table 14. Data-modelling procedure II

	N (mgN/L)	Mg (mgMg/L)	P (mgP/L)	Ca (mgCa/L)	K (mgK/L)	ISS (mgISS/L)
Soluble ($X_{soluble}$)	FSA_{SUP}	Mg^{2+}_{SUP}	OP_{SUP}	Ca^{2+}_{SUP}	K^{+}_{SUP}	-
Struvite (X_{struv})	FSA_{PCA}	$M_{Mg,struv}$: $M_{N,struv}$	$M_{P,struv}$: $M_{N,struv}$	0	0	$M_{N,struv}$ x MM Struvite
ACP (X_{ACP})	0	0	OP_{PCA} - P^{-}_{struv}- $0.15P_{PP}$	$M_{Ca,ACP}$:$M_{P,ACP}$	0	M_{Ca} x MM ACP
Complex (X_{cpx})	TKN_{PR} - FSA_{PCA}	$Mg_{T,PR}$ - Mg^{2+}_{struv}	$P_{PP} + P_{bio}$	$Ca_{T,PR}$ -Ca_{ACP}	$K_{T,PR}$ - K^{+}	-
Biomass (X_{bio})	$f_n X_V$	0	$f_p X_V$	0	0	f_{iPAOBM} x ($X_{BH} + X_{BG}$)
PolyP (X_{PP})	0	Mg_{cpx}	$M_{Mg,PP}$: $M_{P,PP}$	Ca_{cpx}	K_{cpx}	f_{iPAOPP} x P_{PP}

Where:
FSA_{SUP}: FSA concentration in supernatant extract
Mg^{2+}_{SUP}: Soluble Mg concentration in supernatant extract
N_{struv}: N concentration in struvite
TKN_{PR}: Sum of TKN concentration from PCA and RES extract
TKN_{MLSS}: TKN concentration of MLSS
Mg_{cpx}: Total Mg concentration of complex compounds (biomass + polyP)
P_{cpx}: P concentration of complex compounds (biomass + polyP)
P_{bio}: P concentration in biomass (nucleic P concentration)
OP_{PCA}: OP concentration in PCA extract
$M_{Mg,struv}$: Molar concentration of Mg in struvite
f_n: N content of biomass or UPO in terms of mgN/mgVSS
f_p: P content of biomass or UPO in terms of mgP/mgVSS
X_v: Volatile solids concentrations
f_{ipaoPP}: Inorganic mass of polyP = 3.19 mgISS/mgP
f_{iPAOBM} : Inorganic mass fraction of biomass = 0.15 mgISS/mgPAOVSS (or OHOVSS)

4.3.2.2 Application and evaluation of data-modelling procedure II

Test case F

Output of data-modelling procedure II

In test case F, 1054 mg/L of struvite and 207 mg/L of ACP were added to the characterised NDEBPR WAS, as described in Section 4.1. The results shown in Appendix D, was used as input to the DMP II. The output of the DMP II is shown in Table 15.

Table 15. Output from DMP II for test case F (NA: Not Applicable)

	N (mgN/L)	Mg (mgMg/L)	P (mgP/L)	Ca (mgCa/L)	K (mgK/L)	ISS (mgISS/L)
Soluble ($X_{soluble}$)	2.8	25.0	70.2	11.3	268.5	-
Struvite (X_{struv})	81.4	139.6	180.3	0.0	0	1146
ACP (X_{ACP})	0	0	15.0	28.9	0	150
Complex (X_{cpx})	95.7	109.8	453.3	90.1	196.6	NA
Biomass (X_{bio})	481.4	0	48.1	0.0	0	536.8
PolyP (X_{PP})	0	109.8	405.2	90.1	196.6	1293.0
Where NA is Not Applicable						

As observed from Table 15, the concentration of struvite, ACP and polyP predicted from the DMP II for test case F were 1146 mgMg/L, 405 mgP/L and 150 mgP/L, respectively. The struvite concentration is predicted from the measured FSA concentration of 81.4 mgN/L in the PCA extract. The Mg concentration from polyP was determined using Equation 4.7 and yielded 109.8 mgMg/L. The ratio of P: Mg of 1:0.35 was then used to calculate the P concentration of polyP (as shown in Equation 4.8) and a concentration of 405.2 mgP/L was obtained. Using Equation 4.9, the concentration of P from ACP was 15 mgP/L. The elemental Ca:P ratio of ACP was then used to obtain the Ca concentration of ACP. The Ca content of polyP of 90.1 mgCa/L was obtained using Equation 4.11.

Accuracy of data-modelling procedure II

The output concentration from the DMP II was compared to the actual concentrations of the inorganic solids. This is illustrated in Figure 31. The actual concentration of struvite and ACP were 1054 mg/l and 207 mg/l, respectively. The modelled concentration of polyP, using steady state equations, was 310.1 mgP/L. The percentage error (calculated using Equation 3.8) in the prediction of struvite, ACP and polyP were 15%, 25% and 31%, respectively. All three predictions have a high percentage error (>10%).

Struvite has the least percentage error as its measurement is directly linked to the FSA concentration in the PCA extract. It was observed in the test cases that the N concentration in the PCA extract was consistently close to the concentration of N in struvite. However, as identified in Section 4.3.1, the struvite concentration is overpredicted due to the release of small concentrations of biomass N in the PCA extract.

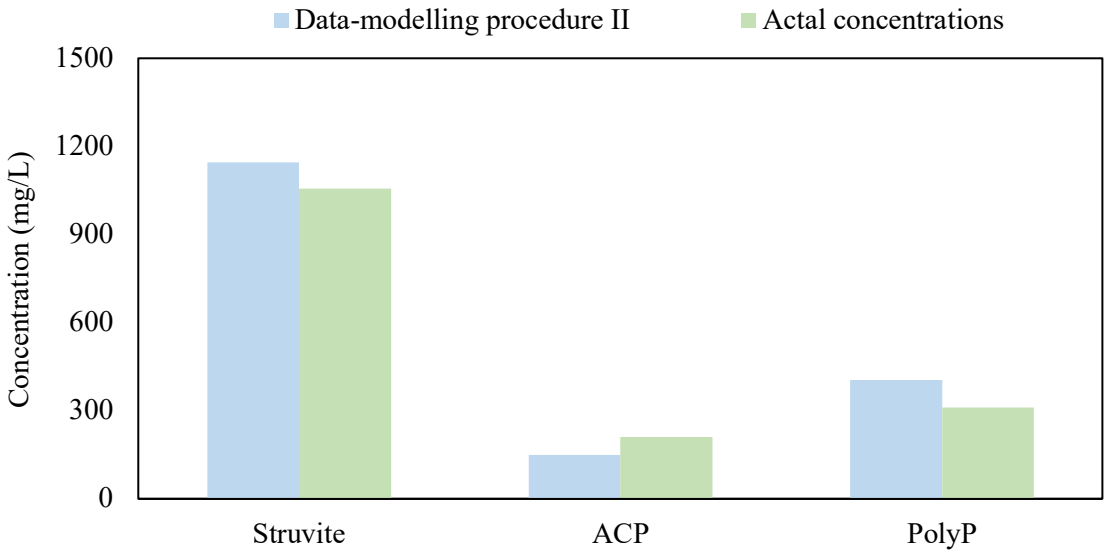

Figure 31. DMP II output and actual ISS concentrations for test case F

The polyP concentration had a significant percentage error. As discussed in 4.3.2.1, the concentration of polyP is obtained using the molar ratio of Mg:P ratio in polyP. There are two sources of error in this calculation. First, the Mg concentration of polyP is derived from the struvite Mg concentration (determined using Equation 4.5). The calculated struvite Mg concentration already has a percentage error of 15% due to the release of biomass N. Secondly, the ratio of Mg;P in the NDEBPR WAS polyP is not necessarily equal to 0.35. Hence, as previously mentioned in the development of the DMP II, it is first required to parametrise the Mg:P ratio in the polyP.

The concentration of ACP is underpredicted by 25% in the DMP II. The ACP ISS concentration is determined from its P concentration. The ACP P is determined using the difference between the PCA OP concentration and the struvite P and hydrolysed polyP P concentration, as shown in Equation 4.9. As the struvite P concentration is overestimated, this error is carried over and concentration of ACP is consequently underestimated. There is also some error induced from the assumption that polyP P hydrolysis stays constant as 15% of total polyP P. As previously mentioned in the development of the DMP II, it is first required to parametrise the extent of hydrolysis of polyP in the PCA extract. Given that accurate K measurements are taken, the extent of polyP hydrolysis can be determined using the K concentration in the PCA extract.

Recovery of ISS

The reconciliation of the modelled and measured ISS is a critical aspect of the DMP since it provides confidence in the results obtained from the DMP. Figure 32 shows the measured ISS versus the modelled ISS. In Section 4.3.1.3, it was deduced that the influent ISS measurement was possibly incorrect and thus the accumulated influent ISS in the sludge was recalculated (using Equation 4.4) assuming an influent ISS of 30 mgISS/L. It can be observed that the modelled ISS concentration is slightly higher than the measured ISS concentration. The percentage error in the modelled ISS concentration is 9% and was within the acceptable range (<10%).

The overprediction of the ISS from the DMP II is clearly related to the overprediction of struvite and ACP. The concentration of struvite and polyP was overpredicted by 90 mgISS/L and 300 mgISS/L, respectively. The polyP ISS concentration was obtained using a ratio of 3.19 mgISS/mgP-polyP. The ACP concentration was underpredicted by 50 mgISS/L. The net error is an overprediction of 340 mgISS/L (a percentage error of 10%). The difference between the modelled ISS and measured ISS is roughly 300 mgISS/L.

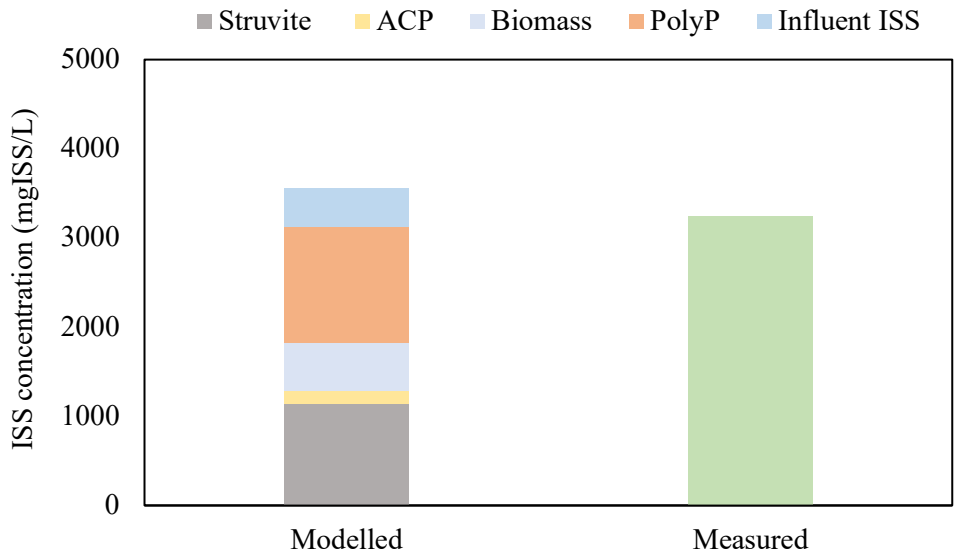

Figure 32. DMP II modelled ISS concentration and actual ISS concentration for test case F

Test case G

Output of data-modelling procedure II

In test case G, 500 mg/L of struvite and 207 mg/L of ACP were added to the characterised NDEBPR WAS, as described in Section 4.1. The results, shown in Appendix D, was used as input to the DMP II, (see Section 4.3.2). The output of the DMP II is shown in Table 16.

Accuracy of data-modelling procedure II

From the DMP II, it was predicted that the concentrations of struvite, ACP and polyP were 587 mg/L, 170 mg/L and 355.5 mgP/L, respectively. Comparatively, the initial concentrations of struvite and ACP used in test case G were 507 mg/L and 200 mg/L, respectively. The modelled polyP concentration was 310.10 mgP/L. These values are illustrated in Figure 33. The percentage error in the prediction of struvite, ACP and polyP is thus 17%, 32% and 15%, respectively.

Table 16. Output of DMP II for test case G

	N (mgN/L)	Mg (mgMg/L)	P (mgP/L)	Ca (mgCa/L)	K (mgK/L)	ISS (mgISS/L)
Soluble ($X_{soluble}$)	2.9	27.9	67.9	12.6	277.4	-
Struvite (X_{struv})	41.7	71.5	92.4	0.0	0	587.0
ACP (X_{ACP})	0	0	15.2	29.3	0	152
Complex (X_{cpx})	396.0	96.3	403.6	87.4	180.3	-
Biomass (X_{bio})	481.4	0	48.1	0.0	0	536.8
PolyP (X_{PP})	0	96.3	355.5	87.4	0	1134

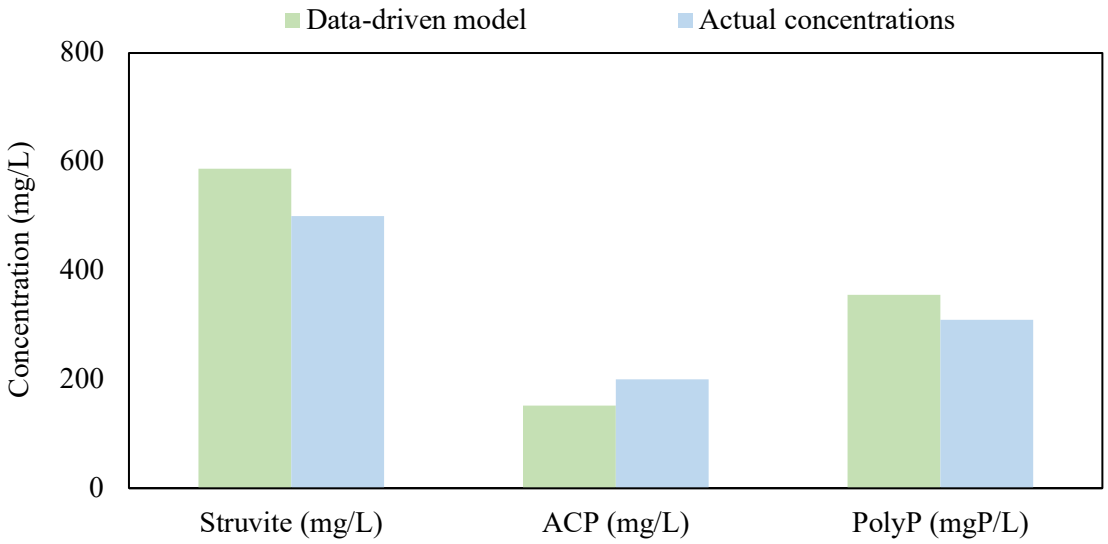

Figure 33. DMP II output and actual ISS concentrations for test case G

As observed in test case F, the struvite concentration was overpredicted. The overprediction is also likely ascribed to the breakdown of small concentrations of biomass in the cold PCA extract. The struvite ISS concentration (as mgISS/L) is sensitive to the concentration of N. An extra N concentration of 5 mgN/L causes the ISS to be overpredicted by 87 mgISS/L (12%). For high concentration of struvite in the wastewater, as in test cases F and G, the percentage error is low, but the output can be used to approximate the struvite concentration with high confidence. However, if the sample contains low concentration of struvite, the output of the modelling procedure is not reliable as the N measurement will be significantly affected by FSA from hydrolysed biomass.

A similar trend (to test case F) in the prediction of ACP and polyP concentration was observed in test case G. The concentration of polyP is overpredicted in test case G, as seen in test case F. It can be deduced that the overprediction is also due to the error carried over from the

determination of struvite Mg, as well as the approximation of 1:0.35 used for the P:Mg ratio in polyP. Nonetheless, there is a significant improvement in the prediction of polyP. The ACP concentration is also underpredicted for test case G. As discussed above, this underprediction is related to the overprediction of struvite which is carried over into the calculation for ACP P.

Recovery of ISS

The reconciliation of the modelled ISS with the measured ISS can provide confidence to the output of the DMP II. Figure 34 shows the measured ISS versus the modelled ISS.

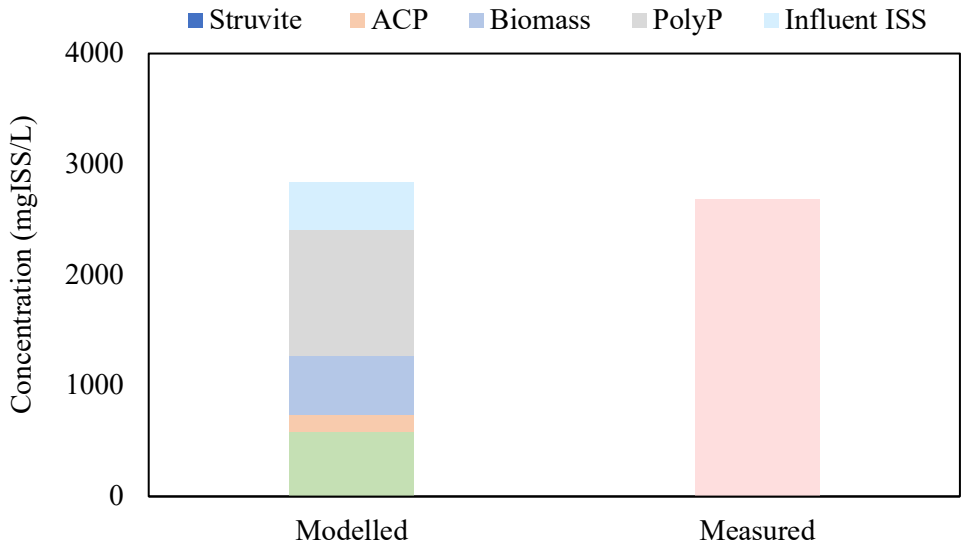

Figure 34. DMP II modelled ISS concentration and actual ISS concentration for test case G

In Section 4.3.1.3, it was deduced that the influent ISS measurement was incorrect and thus the accumulated influent ISS in the sludge was recalculated (using Equation 4.4) assuming an influent ISS of 30 mgISS/L (see Section 2.2.1). The modelled ISS concentration is slightly higher than the measured ISS concentration. The source of this discrepancy is similar as determined in test case F i.e., the mispredictions of the struvite, ACP and polyP concentration. However, the percentage error for test case G (5%) is lower than test case F (9%). The prediction of the polyP concentration was more accurate in test case G. As each polyP P corresponds to an ISS of 3.19 mgISS/P, it has a significant impact on the ISS concentration. In this case the percentage error was reduced by 4%.

5 Conclusion

This research was focused on developing and evaluating a characterisation procedure for inorganic solids found in EBPR systems. The characterisation procedure, which was subdivided into an ISS characterisation procedure (ICT) and a data-modelling procedure (DMP) can help towards the tracking of inorganic solids across EBPR systems. This chapter aims at concluding on the ability of the developed procedure to characterise inorganic solids in EBPR systems.

5.1 ISS Characterisation test

The purpose of the ICT was to subject a sample of EBPR WAS sludge to a condition such that either mineral precipitates or polyP dissolve, exclusively. Consequently, analytical tests carried out on the filtrate or filtered out solids can yield meaningful results that can be used in a DMP. Through a multi-criterion analysis, it was found that the cold PCA fractionation procedure by De Haas *et al.* (2000) was the most suitable base method. The following paragraphs conclude on the applicability of the ICT (based on the De Haas *et al.* (2000) cold PCA fractionation procedure) to characterise inorganic solids.

The ICT was carried out on a known concentration of struvite, ACP and a combination of both. In the past, the cold PCA fractionation procedure was shown to be effective in dissolving mineral precipitates (De Haas, 1998). However, a longer extraction time (30 minutes) was used, which consequently allowed more time for the precipitates to dissolve. In this experiment it was shown that three consecutive short extraction times of five minutes were sufficient to dissolve the expected maximum concentration of mineral precipitates.

The ICT procedure on NDEBPR WAS has shown that during the cold PCA extraction, polyP was hydrolysed into OP. Counter-ions (Mg, K and Ca) were also released into the PCA extract as free ions. Consequently, in the presence of mineral precipitates such as struvite or ACP, analytical measurements cannot distinguish between the ions from the mineral precipitates and polyP. This does not align with the observations made by De Haas *et al.* (2000), who reported negligible hydrolysis of polyP into OP.

The ICT was carried out on samples of NDEBPR WAS and mineral precipitates. The test yielded results in line with the tests carried out on the mineral precipitate and sludge separately. It was seen that the cold PCA extraction was effective in dissolving mineral precipitates, even in the presence of sludge. However, it was deduced that polyP molecules were again hydrolysed partially in the PCA extract. Thus, in a sample with unknown amount of polyP and mineral precipitates, the output of DMP I based on the analytical measurements of the ICT would yield incorrect outputs. The polyP P hydrolysis was consistent in all test cases with NDEBPR sludge, with 15% of the polyP P released as OP. Conversely, this was not the case for the release of counter-ions which was erratic. The soluble measurement in the PCA extract demonstrated that the majority of soluble N originated from struvite. There was negligible release of biomass N in the PCA extract.

5.2 Data-modelling procedure

The DMP is a set of arithmetic equations, that processes the results obtained from the ICT to characterise the inorganic solids. In Section 3.6.1, the DMP I was developed assuming no polyP hydrolysis in the PCA extract. The DMP I was applied to the results of test case F (a mixture of NDEBPR WAS, struvite and ACP). The hydrolysis of polyP caused the output of the DMP I to be significantly inaccurate. The release of polyP P and counter-ions into the cold PCA extract caused the concentration of the mineral precipitates to be overpredicted by more than 100% (66% and 129% for struvite and ACP respectively). The concentration of polyP P was underpredicted by 28%. Hence, it was concluded that the DMP I with the analytical measurements of the ICT was not suitable to characterise inorganic solids.

The DMP II was developed to account for the hydrolysis of polyP. The DMP II used the elemental ratio of the compounds to characterise the inorganic solids. As compared to the DMP I, the DMP II has several limitations. First, the DMP II output depends extensively on the measured FSA concentration in the PCA extract. The struvite, polyP and ACP concentrations all depend on this measurement. Secondly, the elemental ratio of P:Mg is used in the DMP II to determine the polyP P concentration. In this study, the ratio used was based on previous literature, but it varies for different systems. Up until now the factors driving the counter-ion uptake by PAOs is not well established, thus the P:Mg ratio could not be parametrised in the DMP II. Lastly, it was necessary to assume that the extent of polyP P hydrolysis to characterise the sludge using the DMP II. In this project, the hydrolysis of polyP to OP is roughly equal to 15% of the total polyP P concentration. However, this value has not been validated and further investigations are required to determine the factors affecting the extent of polyP hydrolysis. These factors can then be parametrised into the DMP to yield the polyP P concentration.

The results of test cases F and G were used as input to the DMP II. There was a significant improvement in the prediction of the mineral precipitate concentrations using DMP II. Better predictions were obtained for the struvite concentration as it was determined based on FSA concentration in the PCA extract, which was not affected by polyP hydrolysis. The FSA of the PCA extract was from the dissolved struvite and negligible hydrolysed biomass. Although the prediction of ACP improved from the DMP I, the percentage error was still high. The errors were likely induced from the assumed percentage of polyP P hydrolysed and P:Mg ratio of polyP. The accuracy of the prediction of polyP concentration did not improve in the DMP II. Likewise, the polyP P concentration depends on the P:Mg ratio of polyP, and thus parametrising this value can potentially improve the prediction of ACP and polyP in the DMP II.

The release of polyP P and counter-ions in the PCA extract negatively impacts the ability to use the cold PCA fractionation procedure and the DMPs (I and II) in accurately characterising inorganic solids in an NDEBPR WAS sample. The DMP II relies on the polyP molecular formula and extent of polyP hydrolysis. Hence, to improve the accuracy of the ISS characterisation procedure, future research needs to focus on these two parameters (outlined in the next chapter).

5.3 Closure

The ISS characterisation procedure developed in this research needs to be further developed and improved before it can be validated. The ICT (based on the De Haas *et al.* (2000) cold fractionation procedure) is not an ideal method as it does not effectively separate polyP and mineral precipitates. The DMP can be modified to account for polyP hydrolysis in the ICT (DMP II). However, there are two major limitations to this modification, namely: the dependency on a single analytical measurement and the requirement to parametrise the Mg:P ratio in polyP and polyP P hydrolysis for each experiment.

6 Future work

This project has pioneered the research into the characterisation of inorganic solids. Whilst achieving the objectives outlined in Section 1.4, it has also paved the way for upcoming work in this field. The aim of this chapter is to provide some guidance on future research, such that a complete, rigorous, and comprehensive ISS characterisation procedure is obtained.

6.1 Evaluation of alternative base methods for the ISS characterisation test

In this research, several potential experiments or conditions were identified as a method to separate and/or distinguish between polyP and mineral precipitates. Since the cold PCA fractionation procedure by De Haas *et al.* (2000) did not effectively separate polyP and mineral precipitates, other potential methods identified in this research can be evaluated.

6.2 Degree of polyP hydrolysis in cold PCA extract

Around 15% of polyP was hydrolysed in the PCA extract which was found to be fairly consistent in all cases. The ratio of polyP hydrolysed was integrated in the DMP II. However, further tests are required to validate this ratio. Future research can investigate the release of K with the polyP hydrolysis in the PCA extract and determine if there is any correlation. This relationship can then be implemented to parametrise polyP hydrolysis using accurate K measurements. Furthermore, it has been identified that the counter-ions Mg, K and Ca were released erratically in test cases with polyP, and there is no explicit trend or factors identified at this stage. Future research can determine the factors affecting the release of these counter-ions, and potential parametrisation in the DMP.

6.3 Determination of the molecular formula of polyP in PAOs

Although there is literature that approximates the polyP molecular formula in the form of $Mg_aK_bCa_cP_d$, it is currently not known what drives the uptake of counter-ions by polyP, and the consequent molecular formula of polyP. A research study on the factors affecting polyP counter-ion uptake can help to parametrise the uptake of Mg, K and Ca in EBPR systems, and this can be easily included in the DMP. As the DMP II relies on the molecular formula of polyP, more accurate results can potentially be obtained once the polyP molecular formula is known.

7 References

Aage, H.K., Andersen, B.L., Blom, A. & Jensen, I. 1997. The solubility of struvite. *Journal of Radioanalytical and Nuclear chemistry*. 223(2):213–215. DOI: 10.1016/S0022-5347(17)66025-7.

Abbona, F., Lundager Madsen, H.E. & Boistelle, R. 1982. Crystallization of two magnesium phosphates, struvite and newberyite: Effect of pH and concentration. *Journal of Crystal Growth*. 57(1):6–14. DOI: 10.1016/0022-0248(82)90242-1.

APHA. 1985. *Standard method for examination of water and wastewater*. 16th ed. A. Greenberg, R. Trussel, & C. Lenore, Eds. Washington: American Public Health Association.

Arvin, E. & Holm Kristensen, G. 1985. Exchange of Organics, Phosphate and Cations between Sludge and Water in Biological Phosphorus and Nitrogen Removal Processes. *Water Science and Technology*. 17(11–12):147–162. DOI: 10.2166/wst.1985.0229.

Asensi, E., Alemany, E., Duque-Sarango, P. & Aguado, D. 2019. Assessment and modelling of the effect of precipitated ferric chloride addition on the activated sludge settling properties. *Chemical Engineering Research and Design*. 150:14–25. DOI: 10.1016/j.cherd.2019.07.018.

Balaban, R.S. 1984. The application of nuclear magnetic resonance to the study of cellular physiology. *American Journal of Physiology-Cell Physiology*. 246(1):10–19. DOI: 10.1152/ajpcell.1984.246.1.C10.

Barat, R., Bouzas, A., Martí, N., Ferrer, J. & Seco, A. 2009. Precipitation assessment in wastewater treatment plants operated for biological nutrient removal: A case study in Murcia, Spain. *Journal of Environmental Management*. 90(2):850–857. DOI: 10.1016/j.jenvman.2008.02.001.

Batstone, D.J., Kazadi, C., Tait, S. & Flores-Alsina, X. 2015. A generalised chemical precipitation modelling approach in wastewater treatment applied to calcite. *Water Research*. 68:342–353. DOI: 10.1016/j.watres.2014.10.011.

Bhuiyan, M.I.H., Mavinic, D.S. & Beckie, R.D. 2007. A solubility and thermodynamic study of struvite. *Environmental Technology*. 28(9):1015–1026. DOI: 10.1080/09593332808618857.

Blackall, L.L., Crocetti, G.R., Saunders, A.M. & Bond, P.L. 2002. A review and update of the microbiology of enhanced biological phosphorus removal in wastewater treatment plants. *Antonie van Leeuwenhoek, International Journal of General and Molecular Microbiology*. 81(1–4):681–691. DOI: 10.1023/A:1020538429009.

Blonda, M., Brunetti, A., Morrone, S., Ramadori, R. & May, J.W. 1994. Determination of orthophosphate in activated sludges from wastewater-treatment systems showing enhanced biological phosphate removal. *Water Research*. 28(1):155–159. DOI: 10.1016/0043-1354(94)90129-5.

Brouckaert, C.J., Ikumi, D.S. & Ekama, G.A. 2010. A 3-phase anaerobic digestion model. *In Proceedings from the 12th IWA Anaerobic Digestion Conference (AD12)*. 3(3).

Carlson, G.A. 2002. *Experimental Errors and Uncertainty*.

Choi, J.N., Seung-Woo, J. & Chung, Y. 2006. Enhanced anaerobic gas production of waste activated sludge pretreated by pulse power technique. *Bioresource technology*. 3(2):198–213. DOI: 10.1016/j.biortech.2005.02.023.

Comeau, Y., Hall, K.J., Hancock, R.E.W. & Oldham, W.K. 1986. Biological model for enhanced biological phosphorus removal. *Water Research*. 20(12):1511–1521.

Cordell, D. 2010. The Story of Phosphorus. Department of Water annd Environmental studies, University of Technology Sydney.

Crocetti, G.R., Hugenholtz, P., Bond, P.L., Schuler, A., Keller, J., Jenkins, D. & Blackall, L.L. 2000. Identification of polyphosphate-accumulating organisms and design of 16S rRNA-directed probes for their detection and quantitation. *Applied and Environmental Microbiology*. 66(3):1175–1182. DOI: 10.1128/AEM.66.3.1175-1182.2000.

Daims, H., Ramsing, N.B., Schleifer, K.H. & Wagner, M. 2001. Cultivation-Independent, Semiautomatic Determination of Absolute Bacterial Cell Numbers in Environmental Samples by Fluorescence in Situ Hybridization. *Applied and Environmental Microbiology*. 67(12):5810–5818. DOI: 10.1128/AEM.67.12.5810-5818.2001.

Danen-Louwerse, H.J., Lijklema, L. & Coenraats, M. 1995. Coprecipitation of phosphate with calcium carbonate in Lake Veluwe. *Water Research*. 29(7):1781–1785. DOI: 10.1016/0043-1354(94)00301-M.

Dromgoole, E.L. & Walter, L.M. 1990. Iron and manganese incorporation into calcite: Effects of growth kinetics, temperature and solution chemistry. *Chemical Geology*. 81(4):311–336. DOI: 10.1016/0009-2541(90)90053-A.

Ekama, G.A. & Wentzel, M.C. 2004. A predictive model for the reactor inorganic suspended solids concentration in activated sludge systems. *Water Research*. 38(19):4093–4106. DOI: 10.1016/j.watres.2004.08.005.

Ekama, G.A., Wentzel, M.C. & Lowenthal, R.E. 2006. Integrated chemical-physical processes kinetic modelling of multiple mineral precipitation problems. *Water Science and Technology*. 53(12):65–73. DOI: 10.2166/wst.2006.407.

Ekama, G.A., Wentzel, M.C. & Sötemann, S.W. 2006. Tracking the inorganic suspended solids through biological treatment units of wastewater treatment plants. *Water Research*. 40(19):3587–3595. DOI: 10.1016/j.watres.2006.05.034.

Fernandez, E.J. & Clark, D.S. 1987. NMR spectroscopy: A non-invasive tool for studying intracellular processes. *Enzyme and Microbial Technology*. 9(5):259–271. DOI: https://doi.org/10.1016/0141-0229(87)90001-9.

Gaszynski, C., Ikumi, D.S. & Ekama, G.A. 2020. Identification of wastewater primary sludge composition using augmented batch tests and mathematical models. University oF Cape Town.

Green, D.W. & Perry, R.H. 2007. *Perry's Chemical Engineers' Handbook*. 8th ed. New York: McGraw-Hill Education. Available: https://www.accessengineeringlibrary.com/content/book/9780071422949.

van Groenestijn, J.W., Vlekke, G.J.F.M., Anink, D.M.E., Deinema, M.H. & Zehnder, A.J.B. 1988. Role of Cations in Accumulation and Release of Phosphate by Acinetobacter Strain 210A. *Applied and Environmental Microbiology*. 54(12):2894–2901. DOI: 10.1128/aem.54.12.2894-2901.1988.

Günther, S., Trutnau, M., Kleinsteuber, S., Hause, G., Bley, T., Röske, I., Harms, H. & Müller, S. 2009. Dynamics of polyphosphate-accumulating bacteria in wastewater treatment plant microbial communities detected via DAPI (4′,6′-diamidino-2- phenylindole) and tetracycline labeling. *Applied and Environmental Microbiology*. 75(7):2111–2121. DOI:

10.1128/AEM.01540-08.

De Haas, D.W. 1989. Chemical Fractionation of Activated Sludge with special reference to enhanced Biological Phosphate removal. University of Johannesburg.

De Haas, D.W. 1991. Significance of fractionation methods in assessing the chemical form of phosphate accumulated by activated sludge and an Acinetobacter pure culture. *Water SA*. 17(1).

De Haas, D.W. 1998. The use of simultaneous chemical precipitation in modified activated sludge systems exhibiting biological enhanced phosphate removal. University of Cape Town.

De Haas, D.W. & Greben, H.A. 1991. Phosphorus fractionation of activated sludges from modified Bardenpho processes with and without chemical precipitant supplementation. *Water Science and Technology*. 23(4–6):623–633. DOI: 10.2166/wst.1991.0512.

De Haas, D.W., Wentzel, M.C. & Ekama, G.A. 2000. The use of simultaneous chemical precipitation in modified activated sludge systems exhibiting biological excess phosphate removal. Part 2: Method development for fractionation of phosphate compounds in activated sludge. *Water SA*. 26(4):453–466.

Han, Y., Zhang, C., Wu, L., Zhang, Q., Zhu, L. & Zhao, R. 2018. Influence of alternating electromagnetic field and ultrasonic on calcium carbonate crystallization in the presence of magnesium ions. *Journal of Crystal Growth*. 499(April):67–76. DOI: 10.1016/j.jcrysgro.2018.07.037.

Harding, T. & Ekama, G.A. 2009. A steady state stoichiometric model describing the anaerobic digestion of enhanced phosphorus removal waste activated sludge. University of Cape Town.

Harold, F.M. 1962. Depletion and replenishment of the inorganic polyphosphate pool in Neurospora crassa. *Journal of bacteriology*. 83:1047–1057. DOI: 10.1128/JB.83.5.1047-1057.1962.

Harold, F.M. 1966. Inorganic polyphosphates in biology: structure, metabolism, and function. *Bacteriological reviews*. 30(4):772–94.

Henze, M., Gujer, W., Mino, T., Matsuo, T., Wentzel, M.C. & Marais, G. v. R. 1995. The Activated Sludge Model No. 2: Biological phosphorus removal. *Water Science and Technology*. 31(2):1–11. DOI: 10.1016/0273-1223(95)00175-M.

Henze, M., Amy, G., Brdjanovic, D., Comeau, Y., Ekama, G.A., Garcia, J.H.O., Gerba, C.P., Hooijmans M., C., et al. 2008. *Biological Wastewater Treatment: Principles, Modelling and Design*. 1st ed. M. Henze, M. van Loosdrecht, G.A. Ekama, & D. Brdjanovic, Eds. London: IWA Publishing.

Hu, P., Liu, J., Bao, H., Wu, L., Jiang, L., Zou, L., Wu, Y., Qian, G., et al. 2018. Enhancing phosphorus release from waste activated sludge by combining high-voltage pulsed discharge pretreatment with anaerobic fermentation. *Journal of Cleaner Production*. 196:1044–1051. DOI: 10.1016/j.jclepro.2018.06.153.

Ikumi, D.S. 2015. The Development of a Three Phase Plant-Wide Mathematical Model for Sewage Treatment. University of Cape Town.

Ikumi, D.S. & Harding, T.H. 2020. Kinetics of biological and chemical processes in anoxic-aerobic digestion of phosphorus rich waste activated sludge. *Water Research*. 170:115333. DOI: 10.1016/j.watres.2019.115333.

Ikumi, D.S., Harding, T.H. & Ekama, G.A. 2014. Biodegradability of wastewater and activated sludge organics in anaerobic digestion. *Water Research*. 56:267–279. DOI: 10.1016/j.watres.2014.02.008.

Ikumi, D.S., Ekama, G.A., Mebrahtu, M.K., Brink, I.C. & Wentzel, M.C. 2015. *Mass Balances and Modelling Over Wastewater Treatment Plants*.

Ikumi, D.S., Ekama, G.A. & Brouckaert, C.J. 2019. Plant-wide modelling of Anaerobic digestion of waste sludge from parent nutrient (N&P) removal system. *Unpublished*.

Iorhemen, O.T., Hamza, R.A. & Tay, J.H. 2016. Membrane bioreactor (Mbr) technology for wastewater treatment and reclamation: Membrane fouling. *Membranes*. 6(2):13–16. DOI: 10.3390/membranes6020033.

Jardin, N. & Popel, J. 1994. Phosphate release of sludges from enhanced biological P-removal during digestion. *Water Science & Technology*. 30(6):281–292.

Jenne, R., Banadda, E.N., Smets, I.Y., Bamelis, A., Verdickt, L. & Van Impe, J.F. 2005. Activated sludge image analysis system: monitoring settleability and effluent clarity. *Water science and technology : a journal of the International Association on Water Pollution Research*. 52(10–11):193–199.

Jenné, R., Banadda, E.N., Smets, I.Y., Gins, G., Mys, M. & Van Impe, J.F. 2004. Optimization of an Image Analysis Procedure for Monitoring Activated Sludge Settleability. *IFAC Proceedings Volumes*. 37(3):345–350. DOI: 10.1016/s1474-6670(17)32605-8.

Kawaharasaki, M., Tanaka, H., Kanagawa, T. & Nakamura, K. 1999. In situ identification of polyphosphate-accumulating bacteria in activated sludge by dual staining with rRNA-targeted oligonucleotide probes and 4',6-diaimidino-2-phenylindol (DAPI) at a polyphosphate-probing concentration. *Water Research*. 33(1):257–265. DOI: 10.1016/S0043-1354(98)00183-3.

Kawaharasaki, M., Manome, A., Kanagawa, T. & Nakamura, K. 2002. Flow cytometric sorting and RFLP analysis of phosphate accumulating bacteria in an enhanced biological phosphorus removal system. *Water Science and Technology*. 46(1–2):139–144. DOI: 10.2166/wst.2002.0469.

Kazadi, C., Tait, S., Flores-Alsina, X. & Batstone, D.J. 2015. A systematic study of multiple minerals precipitation modelling in wastewater treatment. *Water Research*. 85:359–370. DOI: 10.1016/j.watres.2015.08.041.

Kazadi, C., Flores-alsina, X., John, D. & Tait, S. 2016. Validation of a plant-wide phosphorus modelling approach with minerals precipitation in a full-scale WWTP. *Water Research*. 100:169–183. DOI: 10.1016/j.watres.2016.05.003.

Kerdachi, D.A. & Healey, K.J. 1987. The reliability of cold perchloric acid extraction to assess metal bound phosphates. *Biological Phosphate Removal from Wastewaters*. (January, 1):339–342. DOI: 10.1016/B978-0-08-035592-4.50040-7.

Kezia, K., Lee, J., Zisu, B., Chen, G.Q., Gras, S.L. & Kentish, S.E. 2017. Solubility of Calcium Phosphate in Concentrated Dairy Effluent Brines. *Journal of Agricultural and Food Chemistry*. 65(20):4027–4034. DOI: 10.1021/acs.jafc.6b05792.

Koutsoukos, P., Amjad, Z., Tomson, B. & Nancollas, G.H. 1980. Crystallization of Calcium Phosphates. A Constant Composition Study. *Journal of the American Chemical Society*. 102(5):1553–1557. DOI: 10.1021/ja00525a015.

Kuroda, A., Takiguchi, N., Gotanda, T., Nomura, K., Kato, J., Ikeda, T. & Ohtake, H. 2002. A simple method to release polyphosphate from activated sludge for phosphorus reuse and recycling. *Biotechnology and Bioengineering*. 78(3):333–338. DOI: 10.1002/bit.10205.

Liu, W.T., Nielsen, A.T., Wu, J.H., Tsai, C.S., Matsuo, Y. & Molin, S. 2001. In situ identification of polyphosphate- and polyhydroxyalkanoate-accumulating traits for microbial populations in a biological phosphorus removal process. *Environmental Microbiology*. 3(2):110–122. DOI: 10.1046/j.1462-2920.2001.00164.x.

Loewenthal, R.E., Ekama, G.A. & Marais, G. v. R. 1989. Mixed weak acid/base systems. Part 1 - mixture characterisation. *Water SA*. 15(1):3–24.

Louvet, J.N., Giammarino, C., Potier, O. & Pons, M.N. 2010. Adverse effects of erythromycin on the structure and chemistry of activated sludge. *Environmental Pollution*. 158(3):688–693. DOI: 10.1016/j.envpol.2009.10.021.

Maake, V. & Ikumi, D.S. 2021. Using Augmented batch tests to quantify kinetics of anaeerobic breakdown of waste sludge containing Enhanced cultures of breakdown of Waste Sludge containng enhanced cultures of polyphosphate accumulating organisms. University of Cape Town.

Mamais, D., Pitt, P.A., Cheng, Y.W., Loiacono, J., Jenkins, D., Mamais, D., Pitt, P.A., Cheng, Y.W., et al. 2019. Determination of ferric chloride dose to control struvite precipitation in anaerobic sludge digesters. 66(7):912–918.

Maqueda, C., Pérez Rodríguez, J.L. & Lebrato, J. 1994. Study of struvite precipitation in anaerobic digesters. *Water Research*. 28(2):411–416. DOI: 10.1016/0043-1354(94)90278-X.

Mcdowell, H., Brown, W.E. & Sutter, J.R. 1971. Solubility Study of Calcium Hydrogen Phosphate. Ion-Parr Formation. *Inorganic Chemistry*. 10(8):1638–1643. DOI: 10.1021/ic50102a020.

Mesquita, D.P. & Amaral, A.L. 2013. Activated sludge characterization through microscopy: A review on quantitative image analysis and chemometric techniques. *Analytica Chimica Acta*. 802:14–28. DOI: 10.1016/j.aca.2013.09.016.

Mesquita, D.P., Amaral, A.L. & Ferreira, E.C. 2011. Identifying different types of bulking in an activated sludge system through quantitative image analysis. *Chemosphere*. 85(4):643–652. DOI: 10.1016/j.chemosphere.2011.07.012.

Mesquita, D.P., Leal, C., Cunha, J.R., Oehmen, A., Amaral, A.L., Reis, M.A.M. & Ferreira, E.C. 2013. Prediction of intracellular storage polymers using quantitative image analysis in enhanced biological phosphorus removal systems. *Analytica Chimica Acta*. 770(June 2012):36–44. DOI: 10.1016/j.aca.2013.02.002.

Miyamoto-Mills, J., Larson, J., Jenkins, D. & Owen, W. 1983. Design and Operation of a Pilot-Scale Biological Phosphate Removal Plant at Central Contra Costa Sanitary District. *Water Science and Technology*. 15(3–4):153–179. DOI: 10.2166/wst.1983.0113.

Da Motta, M., Pons, M.N. & Roche, N. 2003. Monitoring filamentous bulking in activated sludge systems fed by synthetic or municipal wastewater. *Bioprocess and Biosystems Engineering*. 25(6):387–393. DOI: 10.1007/s00449-003-0323-3.

Müssig-Zufika, M., Kornmüller, A., Merkelbach, B. & Jekel, M. 1994. Isolation and analysis of intact polyphosphate chains from activated sludges associated with biological phosphate removal. *Water Research*. 28(8):1725–1733. DOI: 10.1016/0043-1354(94)90244-5.

Musvoto, E. V., Loewenthal, R.E., Wentzel, M.C. & Ekama, G.A. 2000. Integrated chemical physical processes modelling - Development of a kinetic-based model for mixed weak acid / base systems. *Water SA*. 34(6).

Musvoto, E. V., Wentzel, M. & Ekama, G.A. 2000. Integrated chemical-physical processes modelling. Simulating aeration treatment of anaerobic digester supernatants. *Water S. A*. 34(6):1868–1880.

Nielsen, A.E. & Toft, J.M. 1984. Electrolyte crystal growth kinetics. *Journal of Crystal Growth*. 67(2):278–288. DOI: 10.1016/0022-0248(84)90188-X.

Pastor, L., Mangin, D., Ferrer, J. & Seco, A. 2010. Struvite formation from the supernatants of an anaerobic digestion pilot plant. *Bioresource Technology*. 101(1):118–125. DOI: 10.1016/j.biortech.2009.08.002.

Piyadasa, C., Yeager, T.R., Gray, S.R., Stewart, M.B., Ridgway, H.F., Pelekani, C. & Orbell, J.D. 2017. The influence of electromagnetic fields from two commercially available water-treatment devices on calcium carbonate precipitation. *Environmental Science: Water Research and Technology*. 3(3):566–572. DOI: 10.1039/c7ew00060j.

Poinapen, J., Wentzel, M.C. & Ekama, G.A. 2009. Biological sulphate reduction with primary sewage sludge in an upflow anaerobic sludge bed (UASB) reactor -part 1: Feasibility study. *Water SA*. 35(5):525–534. DOI: 10.4314/wsa.v35i5.49178.

Quevauvilliers, M. & Ikumi, D.S. 2021. Improved Tracking of Phosphorus in Wastewater Treatment Works through Anaerobic Digestion of P-rich sludge. University of Cape Town.

Ramphao, M., Wentzel, M.C., Merritt, R., Ekama, G.A., Young, T. & Buckley, C.A. 2004. Impact of Membrane Solid – Liquid Separation on Design of Biological Nutrient Removal Activated Sludge Systems. *Biotechnology and Bioengineering*. 89(6):630–646. DOI: 10.1002/bit.20311.

Van Rensburg, P., Musvoto, E. V., Wentzel, M.C. & Ekama, G.A. 2003. Modelling multiple mineral precipitation in anaerobic digester liquor. *Water Research*. 37(13):3087–3097. DOI: 10.1016/S0043-1354(03)00173-8.

Rice, G., Barber, A., O'Connor, A., Stevens, G. & Kentish, S. 2009. Fouling of NF membranes by dairy ultrafiltration permeates. *Journal of Membrane Science*. 330(1–2):117–126. DOI: 10.1016/j.memsci.2008.12.048.

Roberts, J.K.M. & Jardetzky, O. 1981. Monitoring of cellular metabolism by NMR. *Biochimica et Biophysica Acta (BBA) - Reviews on Bioenergetics*. 639(1):53–76. DOI: https://doi.org/10.1016/0304-4173(81)90005-7.

Rouina, M., Kariminia, H.R., Mousavi, S.A. & Shahryari, E. 2016. Effect of electromagnetic field on membrane fouling in reverse osmosis process. *Desalination*. 395:41–45. DOI: 10.1016/j.desal.2016.05.009.

Salerno, M.B., Lee, H., Parameswaran, P. & Rittmann, B.E. 2012. Using a Pulsed Electric Field as a Pretreatment for Improved Biosolids Digestion and Methanogenesis. *Proceedings of the Water Environment Federation*. 2008(15):2005–2018. DOI: 10.2175/193864708788733675.

Serafim, L.S., Lemos, P.C., Levantesi, C., Tandoi, V., Santos, H. & Reis, M.A.M. 2002. Methods for detection and visualization of intracellular polymers stored by polyphosphate-accumulating microorganisms. *Journal of Microbiological Methods*. 51(1):1–18. DOI: 10.1016/S0167-7012(02)00056-8.

Seviour, R.J., Mino, T. & Onuki, M. 2003. The microbiology of biological phosphorus removal in activated sludge systems. *FEMS Microbiology Reviews*. 27(1):99–127. DOI: 10.1016/S0168-6445(03)00021-4.

Shu, L., Schneider, P., Jegatheesan, V. & Johnson, J. 2006. An economic evaluation of phosphorus recovery as struvite from digester supernatant. *Bioresource Technology*. 97(17):2211–2216. DOI: 10.1016/j.biortech.2005.11.005.

Sotemann, S.J., Ristow, N., Wentzel, M.C. & Ekama, G.A. 2005. A steady state model for anaerobic digestion of sewage sludges. *Water S.A*. 31(4):511. DOI: 10.4314/wsa.v31i4.5143.

Streichan, M., Golecki, J.R. & Schön, G. 1990. Polyphosphate-accumulating bacteria from sewage plants with different proceses for biological phosphorus removal. *FEMS Microbiology Letters*. 73(2):113–124. DOI: 10.1016/0378-1097(90)90657-C.

Takács, I., Patry, G.G. & Nolasco, D. 1991. A dynamic model of the clarification-thickening process. *Water Research*. 25(10):1263–1271. DOI: 10.1016/0043-1354(91)90066-Y.

Tao, X. & Xia, H. 2007. Releasing characteristics of phosphorus and other substances during thermal treatment of excess sludge. *Journal of Environmental Sciences*. 19:1153–1158.

Thela, N. & Ikumi, D.S. 2022. Growing an enhanced culture of Polyphosphate Accumulating organisms using a University of Cape Town Membrane Bioreactor (UCTMBR) System. Department of Civil Engineering, University of Cape Town.

Tijssen, J.P.F., Beekes, H.W. & Van Steveninck, J. 1982. Localization of polyphosphates in Saccharomyces fragilis, as revealed by 4′,6-diamidino-2-phenylindole fluorescence. *Biochimica et Biophysica Acta (BBA) - Molecular Cell Research*. 721(4):394–398. DOI: https://doi.org/10.1016/0167-4889(82)90094-5.

Vogts, M., Ikumi, D.S. & Ekama, G.A. 2015. The Removal of Nitrogen and Phosphorus in Anoxic-Aerobic Digestion of Waste Activated Sludge from Biological Nutrient Removal Systems. *Creative Commons Atrribution Licence*. 41(2):1–3.

Wang, L. & Nancollas, G.H. 2008. Calcium orthophosphates: Crystallization and Dissolution. *Chemical Reviews*. 108(11):4628–4669. DOI: 10.1021/cr0782574.

Wentzel, M., Loewenthal, R., Ekama, G.A. & Marais, G. v. R. 1988. Enhanced polyphosphate organism cultures in activated sludge systems - part 1: enhanced culture development. *Water S. A*. 14(2):81–92.

Wentzel, M.C., Ekama, G.A., Dold, P.L. & Marais, G. v. R. 1990. Biological excess phosphorus removal. Steady state process design. *Water SA*.

Wentzel, M.C., Ubisi, M.F., Lakay, M.T. & Ekama, G.A. 2002. Incorporation of inorganic material in anoxic/aerobic-activated sludge system mixed liquor. *Water Research*. 36(20):5074–5082. DOI: 10.1016/S0043-1354(02)00053-2.

WRC. 1984. *Theory , Design and Operation of Nutrient Removal Activated Sludge Processes*.

Appendix A: Cold PCA fractionation procedure

The following table outlines the steps followed by De Haas *et al.* (2000).

Table 17A. Cold PCA fractionation procedure. Adapted from De Haas *et al.* (2000)

Step	Procedure	Analysis	Interpretation
1	A 50 ml sample of activated sludge was transferred to a centrifuged tube with screw lid.	The original activated sludge sample was tested for TP and total solids test (VSS, ISS and TSS)	
2	The sample was centrifuged at 3000 g for 5 min. The supernatant was collected.		Original supernatant corresponding to "effluent" at point of sampling
3	A solution of 0.9% (m/v) NaCl (10 ml) was added to the pellet in step 1 and shake well, with cap.		
4	The sample was then centrifuged at 3 000 r/min (max. 2000 *g*) for 5 min. The supernatant in step 3 was pooled to the SUP sample. *(Step 2).*	Half of the SUP sample was filtered. The SUP and filtered SUP (fSUP) were analyzed for • orthoP immediately • total P The analytical measurements were correct ed by a factor of 1.2i.e., 60 ml extract per 50 ml original mixed liquor.	"Interstitial" loosely bound phosphate pooled with that present in the original supernatant.
5	A volume of 20 ml of 0.5 M cold perchloric acid was added to the pellet of step 4. The extraction was carried in a refrigerated water bath at 0^0C. Three consecutive extraction of 5 minutes were carried. The extracts were pooled together and stored at 0^0C.	The PCA extract was analyzed for: orthoP immediately**;** total P Correct by a factor of 1.2 i.e., 60 m*l* extract per 50 m*l* original mixed liquor.	Acid-soluble complex P (polyP and nucleic acids) extracted as well as chemical precipitates (orthoP).
6	The pellet of step 5 was resuspended in distilled water.	The residue was analyzed for total P	Non acid-extractable P compounds grouped.

Appendix B: Sequencing batch reactor

The sequencing batch reactor was set up as another means to obtain an enhanced cultures of PAO at steady state. Due to the fact that the MBR system has yielded an enhanced culture of PAOs ahead of this one, the sludge from this reactor was not used. However, this reactor was used in a parallel study to determine the effect of mineral precipitate on EBPR. Hence, for future references, a description of how this system was set up and rationale behind design decisions, is hereby provided. Figure 35B provides a schematic of the set-up of the SBR reactor.

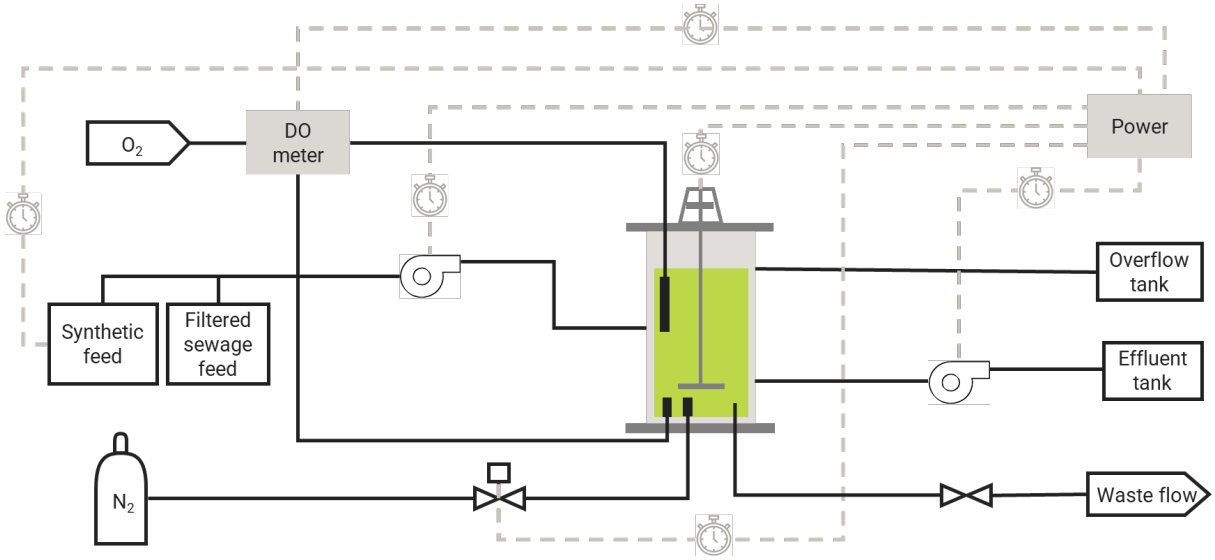

Figure 35B. Sequencing batch reactor schematic

The reactor is operated in a sequence of feeding, anaerobic phase, aerobic phase and settling. This was based on similar SBR reactors operated in the past in other studies [insert reference]. The total cycle time was 6 hours. Hence, 4 cycles were operated per day. Each phase was controlled by timers, except for wasting which was manually carried out. The cycles with the operational conditions and time period are shown in Table 18B. The reactor was a 10 L Perspex cylinder, with 9L effective volume. Similarly, to the MBR reactor, the reactor was fed a percentage of synthetic feed (propionate) and settled wastewater. As the bacteria grew accustomed to synthetic feed, the percentage of synthetic feed was increased gradually from 0 to 75%. The content of the synthetic and filtered raw wastewater feed was kept identical to the UCT AS system (see section 3.4.1). The feed from the synthetic and filtered raw wastewater tanks were pumped, using peristatic pumps, over the anaerobic phase. The anaerobic phase was roughly 3 hours (excluding settling time, which is also anaerobic). During the anaerobic phase, the aerators were turned off and nitrogen gas was pumped for the first 10 minutes, to kick out any oxygen remaining from the previous phase [insert reference]. Feeding slowly over the three hours of anaerobic phase, favoured the growth of PAOs over GAOs. During all phases, except settling, the mixer was turned on. The mixer was controlled by a motor installed on top of the reactor as depicted in Figure 35B.

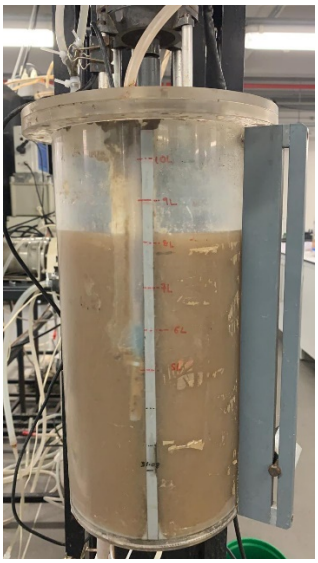

Figure 36B. Sequencing batch reactor anaerobic phase

The aeration phase was 1.6 hours. During aeration the aerators were turned on. The aerator was essentially compressed air being pumped into a diffuser, installed [give specific name] at the bottom of the reactor. The level of oxygen was controlled at 3 mgO/l by a DO meter. The oxygen level was measured using a DO probe as depicted in Figure 35B. During the settling phase, the aerator and mixer were turned off for an hour. After one hour, a peristatic pump was turned on and drew out half of the supernatant volume. The settling time was considered anaerobic and thus the total anaerobic time was four hours. Approximately 0.9 L of sludge was wasted every day to keep a sludge age of 10 days. At this low sludge age, nitrification is prevented and thus prevents the growth of denitrifying PAOs. The reactor was designed, constructed, and operated by the author for a period of two months before it was passed on to the next experimenter.

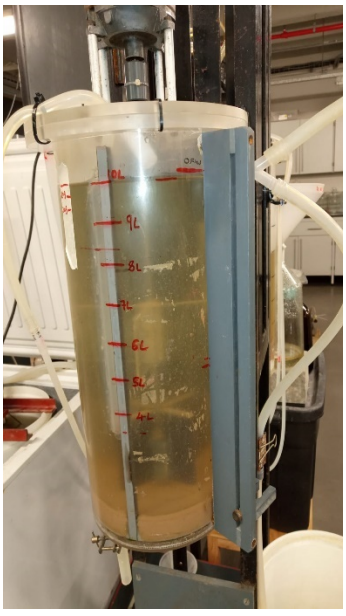

Figure 37B. Sequencing batch reactor settling phase

Table 18B. Schedule of sequencing batch reactor

Cycle	Time	Operation	Duration (mins)	DO Pump	Mixer	Nitrogen Gas	Effluent pump	Feed pump
Cycle 1	11:00:00	Feeding; N_2 pumping	150	OFF	ON	ON	OFF	ON
	13:30:00	Anaerobic Reaction	170	OFF	ON	OFF	OFF	OFF
	13:50:00	Aerobic reaction	100	ON	ON	OFF	OFF	OFF
	15:30:00	Settling	60	OFF	OFF	OFF	OFF	OFF
	16:30:00	Decanting supernatant	30	OFF	OFF	OFF	ON	OFF
Cycle 2	17:00:00	Feeding; N_2 pumping	150	OFF	ON	ON	OFF	ON
	19:30:00	Anaerobic Reaction	170	OFF	ON	OFF	OFF	OFF
	19:50:00	Aerobic reaction	100	ON	ON	OFF	OFF	OFF
	21:30:00	Settling	60	OFF	OFF	OFF	OFF	OFF
	22:30:00	Decanting supernatant	30	OFF	OFF	OFF	ON	OFF
Cycle 3	23:00:00	Feeding; N_2 pumping	150	OFF	ON	ON	OFF	ON
	01:30:00	Anaerobic Reaction	170	OFF	ON	OFF	OFF	OFF
	01:50:00	Aerobic reaction	100	ON	ON	OFF	OFF	OFF
	03:30:00	Settling	60	OFF	OFF	OFF	OFF	OFF
	04:30:00	Decanting supernatant	30	OFF	OFF	OFF	ON	OFF
Cycle 4	05:00:00	Feeding; N_2 pumping	150	OFF	ON	OFF	OFF	ON
	07:30:00	Anaerobic Reaction	170	OFF	ON	OFF	OFF	OFF
	07:50:00	Aerobic reaction	100	ON	ON	OFF	OFF	OFF
	09:30:00	Wasting 0.9L WAS	0	ON	ON	OFF	ON	OFF
	09:30:00	Settling	60	OFF	OFF	OFF	OFF	OFF
	10:30:00	Decanting supernatant	30	OFF	OFF	OFF	ON	OFF

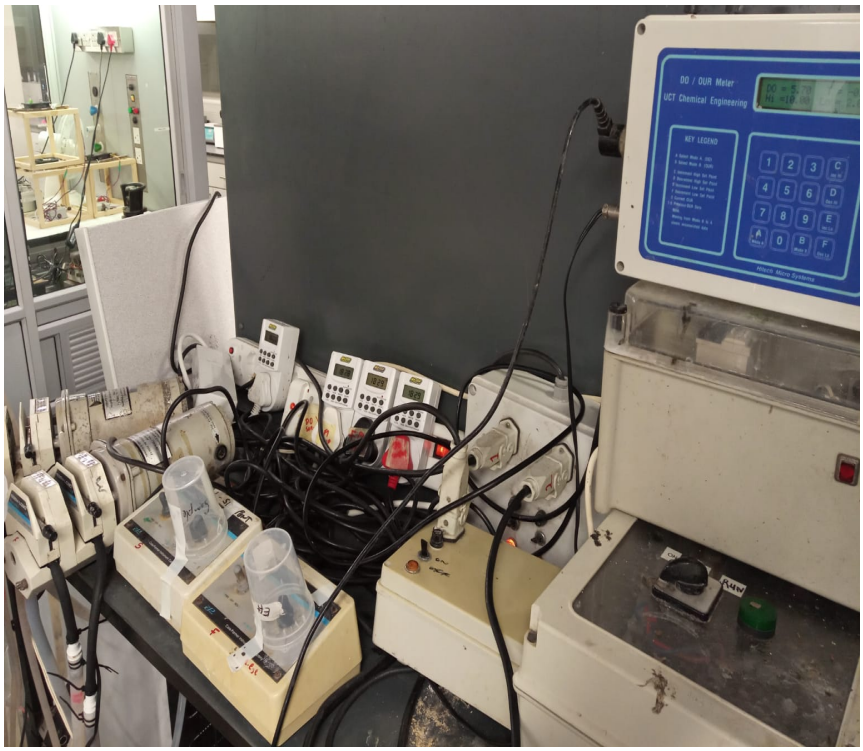

Figure 38B. Instrument control of sequencing batch reactor

Appendix C: NDEBPR WAS characterisation

The NDEBPR WAS was characterised using Wentzel *et al.* (1990) steady state equations. The relevant equations are provided below.

$$X_{BG} = \left(\frac{Q_i S_{ti}}{V_p}\right)(1 - f_{S\prime up} - f_{S\prime us})\left[\frac{\%}{100} f_{S\prime bs} \frac{Y_G R_s}{1 + b_{GT} R_s}\right]_s \quad \text{(C1)}$$

$$X_{BH} = \left(\frac{Q_i S_{ti}}{V_p}\right)(1 - f_{S\prime up} - f_{S\prime us})\left[\left(1 - \frac{\%}{100} f_{S\prime bs}\right)\frac{Y_H R_s}{1 + b_{GT} R_s}\right]_s \quad \text{(C2)}$$

$$X_{EG} = \left(\frac{Q_i S_{ti}}{V_p}\right)(1 - f_{S\prime up} - f_{S\prime us})\left[\left(\frac{\%}{100} f_{S\prime bs}\right) f_{EG} b_G R_s X_{BG}\right]_s \quad \text{(C3)}$$

$$X_{EH} = \left(\frac{Q_i S_{ti}}{V_p}\right)(1 - f_{S\prime up} - f_{S\prime us})\left[\left(\frac{\%}{100} f_{S\prime bs}\right) f_{EH} b_H R_s X_{BH}\right]_s \quad \text{(C4)}$$

$$X_I = \left(\frac{Q_i S_{ti}}{V_p}\right)\frac{f_{S\prime up}}{f_{cv}} R_s \quad \text{(C5)}$$

$$X_V = \left(\frac{Q_i S_{ti}}{V_p}\right)\left[\left(1 - f_{upi} - f_{usi}\right)\left[\left(\frac{\%}{100} f_{SBs}\right)\frac{Y_G R_s}{1 + b_{GT} R_s}(1 + f_{EG} b_{GT} R_s) + \left(1 - \frac{\%}{100} f_{SBs}\right)\frac{Y_H R_s}{1 + b_{GT} R_s}(1 + f_{EH} b_{HT} R_s)\right]_s + \frac{f_{upi}}{f_{cv}} R_s\right] \quad \text{(C6)}$$

Where,

X_{BG} = *VSS concentration of active PAOs*

X_{BH} = *VSS concentration of active OHOs*

$f_{S\prime us}$ = *Fraction of total COD that is unbiodegradable soluble*

$f_{S\prime up}$ = *Fraction of total COD that is unbiodegradable particulate*

$f_{Sb\prime s}$ = *Fraction of biodegradable COD that is soluble*

f_{EH} = *Unbiodegradable fraction of fraction of OHOs* = 0.20

Y_H = *Yield of OHOs* = 0.45 *mgVSS/mgCOD*

$$b_{HT} = Death\ rate\ of\ OHOs$$

$$Y_G = Yield\ of\ PAOs = 0.45\ mgVSS/mgCOD$$

$$b_{GT} = Death\ rate\ of\ PAOs$$

The values obtained from Equations C1-C6 relate to the average concentration across the all the zones (aerobic, anaerobic and anoxic) of the AS system. To obtain the specific concentrations in each zone of the UCT MBR AS system, the Equation C7 given by Ramphao *et al.* (2004) can be used.

$$f_{m(aer)} = \frac{MXv_{aer}}{\overline{MXv}_{sys}} = \frac{Xv_{aer}}{Xv_{sys}} \quad \text{(C7)}$$

$Where,$

$$f_{m(aer)} = Aerobic\ mass\ fraction$$

$$MXv_{aer} = Measured\ VSS\ mass\ of\ the\ aerobic\ zone$$

$$\overline{MXv}_{sys} = Calculated\ VSS\ mass\ of\ MBR\ AS\ system\ using\ equation$$

The aerobic mass fraction is determined as the ratio between the experimentally measured aerobic VSS mass and calculated VSS mass. This fraction is then used to determine the X_{BH}, X_{EH}, X_{BG}, X_{EG}, X_{inert} and X_v concentrations in the aerobic zone. The concentrations of the different components of the WAS are the same as the concentrations in the aerobic zone, given the WAS has not been thickened.

Appendix D: Results of ISS characterisation test

This section provides the results from the analytical measurements of the samples from the ISS characterisation test. The overall recovery is also provided.

Table 19D. Test case A soluble measurement results

Soluble	Test case A: Struvite only									
	SUP					PCA				
	Sample A	Sample B	Sample C	Average	Std dev.	Sample A	Sample B	Sample C	Average	Std dev.
Mg (mgMg/L)	2.23	2.84	3.53	2.87	0.65	123.00	134.68	-	128.84	8.26
K (mgK/L)	NA	NA	NA	-	-	NA	NA	NA	-	-
Ca (mgCa/L)	NA	NA	NA	-	-	NA	NA	NA	-	-
P (mgP/L)	6.623	5.726	7.188	6.512	0.737	174.337	161.473	173.476	169.762	7.191
N (mgN/L)	2.82	2.45	2.98	2.75	0.27	73.51	70.86	78.82	74.40	4.05

Table 20D. Test case A Total measurement results

Total	Test case A: Struvite only									
	PCA					RES				
	Sample A	Sample B	Sample C	Average	Std dev.	Sample A	Sample B	Sample C	Average	Std dev.
Mg (mgMg/L)	127.74	129.98	128.41	128.71	1.15	0.85	0.48	0.38	0.57	0.25
K (mgK/L)	NA	NA	NA	-	-	NA	NA	NA	-	-
Ca (mgCa/L)	NA	NA	NA	-	-	NA	NA	NA	-	-
P (mgP/L)	170.126	171.325	168.878	170.110	1.223	0.319	0.205	0.312	0.279	0.064
N (mgN/L)	74.80	-	-	74.80	-	0.07	0.09	0.13	0.10	0.03

Table 21D. Test case B soluble measurement results

Soluble	Test case B: ACP only									
	SUP					PCA				
	Sample A	Sample B	Sample C	Average	Std dev.	Sample A	Sample B	Sample C	Average	Std dev.
Mg (mgMg/L)	NA	NA	NA	-	-	NA	NA	NA	-	-
K (mgK/L)	NA	NA	NA	-	-	NA	NA	NA	-	-
Ca (mgCa/L)	1.24	2.96	1.88	2.03	0.87	72.25	78.52	-	75.38	4.43
P (mgP/L)	1.862	1.201	1.489	1.518	0.332	37.896	37.885	34.825	36.869	1.770
N (mgN/L)	NA	NA	NA	-	-	NA	NA	NA	-	-

Table 22D. Test case B total measurement results

Total	Test case B: ACP only									
	PCA					RES				
	Sample A	Sample B	Sample C	Average	Std dev.	Sample A	Sample B	Sample C	Average	Std dev.
Mg (mgMg/L)	NA	NA	NA	-	-	NA	NA	NA	-	-
K (mgK/L)	NA	NA	NA	-	-	NA	NA	NA	-	-
Ca (mgCa/L)	80.29	81.76	80.06	80.70	0.92	0.38	0.49	-	0.44	0.08
P (mgP/L)	38.784	37.861	39.661	38.769	0.900	0.192	-	-	0.192	-
N (mgN/L)	NA	NA	NA	-	-	NA	NA	NA	-	-

Table 23D. Test case C soluble measurement results

Soluble	Test case C: Struvite and ACP									
	SUP					PCA				
	Sample A	Sample B	Sample C	Average	Std dev.	Sample A	Sample B	Sample C	Average	Std dev.
Mg (mgMg/L)	4.04	4.45	-	4.25	0.29	131.87	129.89	129.85	130.54	1.15
K (mgK/L)	NA	NA	NA	-	-	NA	NA	NA	-	-
Ca (mgCa/L)	2.04	1.74	1.33	1.70	0.36	73.64	72.56	74.44	73.55	0.94
P (mgP/L)	8.952	8.520	8.928	8.800	0.243	205.657	205.658	208.500	206.605	1.641
N (mgN/L)	3.6	2.4	3.4	3.1	0.6	-	78.3	70.9	74.6	5.2

Table 24D. Test case C total measurement results

Total	Test case C: Struvite and ACP									
	PCA					RES				
	Sample A	Sample B	Sample C	Average	Std dev.	Sample A	Sample B	Sample C	Average	Std dev.
Mg (mgMg/L)	131.78	132.96	130.55	131.76	1.21	-	0.40	-	0.40	-
K (mgK/L)	NA	NA	NA	-	-	NA	NA	NA	-	-
Ca (mgCa/L)	74.29	76.57	72.19	74.35	2.19	0.01	0.53	-	0.27	0.36
P (mgP/L)	207.166	208.981	208.288	208.145	0.916	0.577	0.620	0.935	0.711	0.195
N (mgN/L)	75.67	74.60	-	75.14	0.76	-	0.10	0.01	0.05	0.06

Table 25D. Test case D soluble measurement results

Test Case D: NDEBPR WAS										
Extract	SUP					PCA				
Soluble	Sample A	Sample B	Sample C	Average	Std.dev	Sample A	Sample B	Sample C	Average	Std.dev
Mg	29.09	26.69	26.45	27.41	1.46	55.97	76.76	61.52	64.75	10.77
K	227.68	233.42	226.22	229.11	3.81	25.16	32.26	28.64	28.69	3.55
Ca	11.00	10.43	10.43	10.62	0.33	47.89	54.41	52.38	51.56	3.33
P	59.124	60.508	58.883	59.505	0.877	41.920	47.843	47.657	45.806	3.367
N	0.05	0.07	0.07	0.06	0.01	-0.01	-0.02	-0.01	-0.02	0.01

Table 26D. Test case D total measurement results

Test Case D: NDEBPR WAS										
Extract	PCA					RES				
Total	Sample A	Sample B	Sample C	Average	Std.dev	Sample A	Sample B	Sample C	Average	Std.dev
Mg	72.22	67.16	86.63	75.34	10.11	27.92	23.52	25.97	25.80	2.20
K	111.17	88.38	88.36	88.37	0.01	16.86	2.94	5.34	8.38	1.70
Ca	55.46	-	57.69	56.57	1.58	9.20	3.03	4.70	5.64	3.19
P	190.534	223.952	216.261	220.107	5.439	-	113.040	112.050	112.545	0.700
N	13.57	10.84	10.03	11.48	1.86	420.80	414.40	389.20	408.13	16.71

Table 27D. Test case D Diluted soluble measurement results

Test Case D: NDEBPR WAS Diluted										
Extract	SUP					PCA				
Soluble	Sample A	Sample B	Sample C	Average	Std.dev	Sample A	Sample B	Sample C	Average	Std.dev
Mg	31.46	32.81	33.48	32.58	1.03	73.46	73.25	69.50	72.07	2.23
K	223.49	217.87	218.83	220.06	0.68	40.97	40.22	40.54	40.58	0.22
Ca	13.39	15.29	14.62	14.43	0.96	40.54	44.30	37.75	40.86	3.29
P	56.659	56.659	56.546	56.622	0.065	38.825	41.791	37.286	39.301	2.290
N	0.07	0.07	0.07	0.07	0.00	0.00	0.22	-1.58	-0.46	0.98

Table 28D. Test case D Diluted total measurement results

Test Case D: NDEBPR WAS Diluted										
Extract	PCA					RES				
Total	Sample A	Sample B	Sample C	Average	Std.dev	Sample A	Sample B	Sample C	Average	Std.dev
Mg	77.76	78.95	72.90	76.54	3.20	28.12	13.72	23.58	21.80	7.36
K	176.26	152.68	197.68	175.54	22.51	98.64	115.96	-	107.30	12.24
Ca	53.35	55.94	51.98	53.76	2.01	1.44	6.23	0.97	2.88	2.91
P	222.322	225.349	218.189	221.953	3.594	79.116	82.068	76.896	79.360	2.595
N	14.76	15.26	13.68	14.57	0.81	522.24	553.92	588.48	554.88	33.13

Table 29D. Test case E soluble measurement results

Test Case E: NDEBPR WAS and Struvite										
Extract	SUP					PCA				
Soluble	Sample A	Sample B	Sample C	Average	Std.dev	Sample A	Sample B	Sample C	Average	Std.dev
Mg	34.28	22.98	31.12	29.46	5.83	204.06	212.65	205.26	207.32	4.65
K	215.58	223.34	242.45	227.12	13.83	108.30	113.34	114.11	111.92	3.16
Ca	12.76	11.65	12.26	12.22	0.55	69.14	67.49	70.24	68.96	1.38
P	77.267	76.922	77.084	77.091	0.172	214.307	212.867	210.731	212.635	1.799
N	2.63	2.95	2.35	2.64	0.30	75.05	79.28	75.47	76.60	2.33

Table 30D. Test case E total measurement results

Test Case E: NDEBPR WAS and Struvite										
Extract	PCA					RES				
Total	Sample A	Sample B	Sample C	Average	Std.dev	Sample A	Sample B	Sample C	Average	Std.dev
Mg	229.59	231.55	213.48	224.87	9.92	50.12	36.74	-	43.43	9.46
K	97.45	106.92	85.45	96.61	10.76	55.50	38.33	42.14	40.23	2.69
Ca	72.49	69.86	72.94	71.76	1.66	21.08	15.99	16.47	16.23	2.81
P	359.044	357.808	362.633	359.828	2.507	169.600	169.004	160.880	166.495	4.872
N	77.99	75.58	76.57	76.72	1.21	391.80	375.60	390.20	385.87	8.93

Table 31D. Test case F soluble measurement results

Test Case F: NDEBPR WAS and Struvite + ACP										
Extract	SUP					PCA				
Soluble	Sample A	Sample B	Sample C	Average	Std.dev	Sample A	Sample B	Sample C	Average	Std.dev
Mg	25.55	24.17	25.42	25.04	0.76	233.04	161.47	164.08	162.77	1.84
K	271.38	267.52	266.57	268.49	2.55	125.77	103.91	111.62	113.77	11.09
Ca	11.53	11.26	11.09	11.29	0.22	131.94	116.62	119.50	122.68	8.14
P	69.778	70.099	70.590	70.156	0.409	331.679	214.321	222.002	256.001	5.431
N	3.41	2.42	2.60	2.81	0.52	101.17	82.93	60.13	81.41	20.56

Table 32D. Test case F total measurement results

Test Case F: NDEBPR WAS and Struvite + ACP										
Extract	PCA					RES				
Total	Sample A	Sample B	Sample C	Average	Std.dev	Sample A	Sample B	Sample C	Average	Std.dev
Mg	234.11	157.21	156.42	195.66	44.63	29.00	53.70	53.70	53.70	14.26
K	188.66	155.86	167.44	172.26	8.18	295.40	107.75	11.10	138.08	68.34
Ca	109.69	118.10	133.52	113.90	12.09	5.02	5.03	5.52	5.19	0.29
P	571.662	404.640	413.325	408.983	94.023	100.450	136.760	136.640	124.617	20.929
N	104.49	65.90	72.52	80.97	20.64	352.80	373.20	427.20	384.40	38.44

Table 33D. Test case G soluble measurement results

Test Case G: NDEBPR WAS, Struvite and ACP										
Extract	SUP					PCA				
Soluble	SAMPLE A	SAMPLE B	SAMPLE C	AVERAGE	SD	SAMPLE A	SAMPLE B	SAMPLE C	AVERAGE	SD
Mg	28.78	27.85	26.96	27.86	0.91	112.70	105.17	38.71	108.94	5.33
K	264.80	283.67	283.67	277.38	10.89	106.87	104.70	120.28	110.62	8.44
Ca	13.08	12.46	12.22	12.58	0.45	114.55	111.85	108.42	111.61	3.07
P	68.808	67.368	67.476	67.884	0.802	162.182	163.130	157.194	160.836	3.189
N	2.94	2.80	3.06	2.93	0.13	42.34	46.52	36.28	41.71	5.15

Table 34D. Test case G total measurement results

Test Case G: NDEBPR WAS, Struvite and ACP										
Extract	PCA					RES				
Total	SAMPLE A	SAMPLE B	SAMPLE C	AVERAGE	SD	Reading 1	Reading 2	Reading 3	Average	SD
Mg	123.93	180.74	110.39	117.16	9.57	49.00	51.50	51.50	50.67	1.44
K	186.37	184.00	188.05	186.14	2.04	263.90	106.85	102.70	104.78	2.93
Ca	110.63	114.78	109.34	111.58	2.84	4.88	5.09	5.53	5.17	0.33
P	242.447	245.237	242.444	243.376	1.612	200.250	-	195.680	197.965	3.231
N	41.80	46.78	-	44.29	3.53	400.80	358.80	420.60	393.40	31.56

Table 35D. Overall recovery test case A

Test Case A						
Test case	SUP	PCA	RES	Total	MLSS	% Recovery
Mg	2.87	128.71	0.57	132.15	133.7	99%
K	-	-	-	-	-	-
Ca	-	-	-	-	-	-
P	6.51	170.11	0.28	176.90	172.7	102%
N	2.75	74.80	0.10	77.64	78.0	100%

Table 36D. Overall recovery test case B

Test Case B						
Test case	SUP	PCA	RES	Total	MLSS	% Recovery
Mg	-	-	-	0.00	-	-
K	-	-	-	0.00	-	-
Ca	2.03	80.70	0.44	83.17	81.3	102%
P	1.52	38.77	0.19	40.48	42.0	96%
N	-	-	-	0.00	-	-

Table 37D. Overall recovery test case C

Test Case C						
Test case	SUP	PCA	RES	Total	MLSS	% Recovery
Mg	4.25	131.76	0.40	136.41	133.7	102%
K	-	-	-	0.00	-	-
Ca	1.70	74.35	0.27	76.33	81.3	94%
P	8.80	208.14	0.71	217.66	214.7	101%
N	3.15	75.14	0.05	78.34	78.0	100%

Table 38D. Overall recovery test case D

Test Case D						
Test case	SUP	PCA	RES	Total	MLSS	% Recovery
Mg	27.41	75.34	25.80	128.54	125.11	103%
K	229.11	88.37	8.38	325.86	278.01	117%
Ca	10.62	56.57	5.64	72.83	71.27	102%
P	59.50	220.11	112.55	392.16	403.331	97%
N	0.06	11.48	408.13	419.68	413.41	102%

Table 39D. Overall recovery test case E

Test Case E						
Test case	SUP	PCA	RES	Total	MLSS	% Recovery
Mg	29.46	224.87	43.43	297.76	273.22	109%
K	227.12	96.61	40.23	363.96	262.21	139%
Ca	12.22	71.76	16.23	100.21	100.18	100%
P	77.09	359.83	166.49	603.41	616.150	98%
N	2.64	76.72	385.87	465.23	-	88%

Table 40D. Overall recovery test case F

Test Case F						
Test case	SUP	PCA	RES	Total	MLSS	% Recovery
Mg	25.04	195.66	53.70	274.40	273.22	100%
K	268.49	172.26	138.08	578.83	200.55	289%
Ca	11.29	113.90	5.19	130.38	145.78	89%
P	70.16	408.98	124.62	603.75	650.870	93%
N	2.81	80.97	384.40	468.18	523.27	89%

Table 41D. Overall recovery test case G

Test Case F						
Test case	SUP	PCA	RES	Total	MLSS	% Recovery
Mg	27.86	117.16	50.67	195.69	217.22	90%
K	277.38	186.14	104.78	568.29	218.33	260%
Ca	12.58	111.58	5.17	129.33	137.13	94%
P	67.88	243.38	197.97	509.23	504.980	101%
N	2.93	44.29	393.40	440.62	421.27	105%

Appendix E: Photographs of ISS Characterisation test

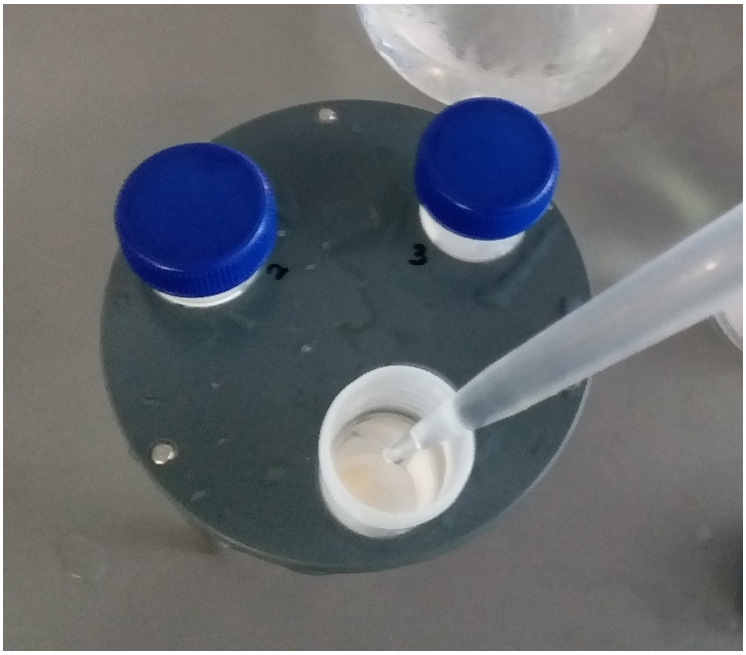

Figure 39E. Addition of cold PCA acid to sludge sample

Figure 40E. Extraction in refrigerated water bath at 0^0C

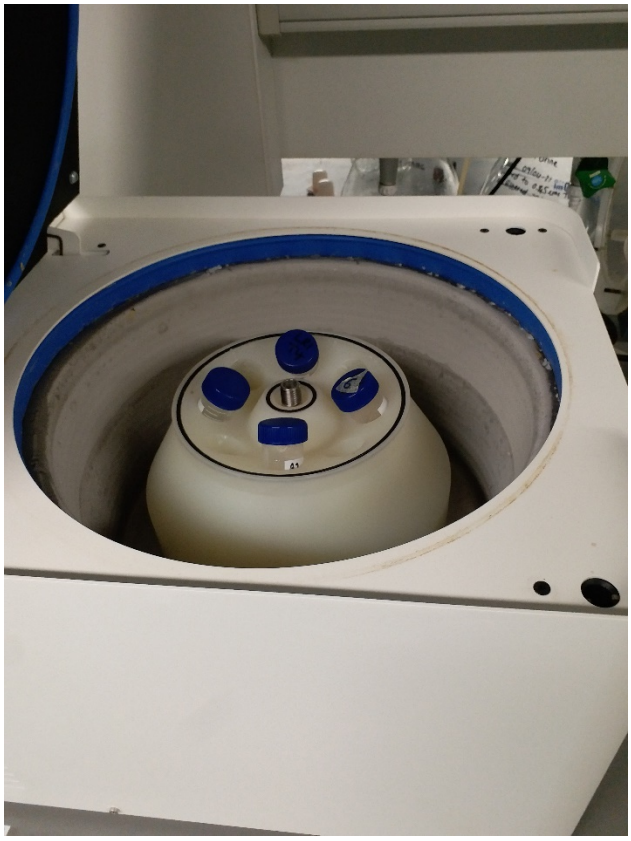

Figure 41E. Centrifugation at 0^0C in a refrigerated centrifuge

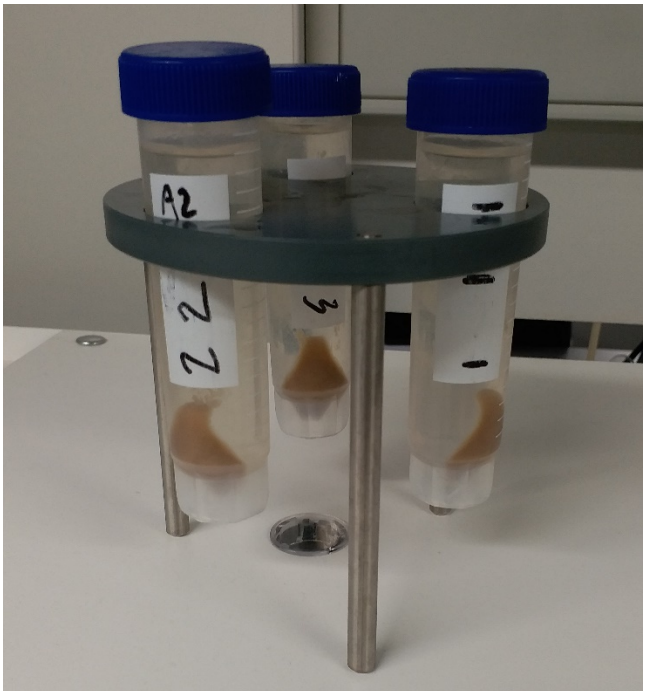

Figure 42E. Sample after centrifugation with cold perchloric acid

Appendix F: Multicriteria analysis for ICT

Table 42F. Scoring system for multi-criteria analysis

Score	DMP	Literature support	Simplicity of test	Expected Accuracy of test	Expected Reproducibility	Data processing	Equipment procurement	Expenditure
5	Simple	Extensive	Simple	Accurate	Reproducible	Low	Low	Cheap
4								
3								
2								
1	Complex	Scarce	Complex	Inaccurate	Irreproducible	High	High	Expensive

Table 43F. Multi-criteria analysis on potential characterisation tests

	Weight	Dilution	Elevated temperatures	Electric field	Anaerobic digestion	Cold PCA fractionation	Non PCA fractionation	Differential settling velocity	Microscopy with QIA	Staining with cytometer	NMR analysis
Section		2.6.1	2.6.2	2.6.3	2.6.4	2.6.5.1	2.6.5.2	2.6.6	2.6.7.2	2.6.7.3	2.6.8
Expenditure	15%	5	5	4	4	5	4	4	1	1	1
Literature support	15%	3	2	1.5	4	5	4	2	4	3	4
Complexity of test	15%	5	3	2	3	4	3	2	2	2	4
Expected Accuracy of test	20%	3	2	2	2	4	3	2	2	2	5
Expected Reproducibility	10%	2	2	2	2	4	3	2	2	2	5
Data processing	5%	5	4	4	4	5	4	3	1	1	4
Equipment procurement	5%	5	5	2	3	5	4	4	1	1	1
DMP	15%	5	5	4	4	5	3	3	2	2	4
Score	100%	**4**	**3.3**	**2.63**	**3.2**	**4.55**	**3.4**	**2.6**	**2.05**	**1.9**	**3.7**

Appendix G: Characteristics of NDEBPR WAS

Table 44G. Detailed UCT AS system overview

Influent and Effluent Results		Flow	COD	TKN	FSA	Nitrate	TP	OP	Total K	Filt K
	Units	(l/d)	(mgCOD/l)	(mgN/l)	(mgN/l)	(mgN/l)	(mgP/l)	(mgP/l)	(mg/l)	(mg/l)
	Influent	58	953.34	74.9	43	-	86.8	85.5	245.9	
	Effluent	54	57.8	1.4	0.1	8.9	59.3	59.3	193.3	193.3

System Performance Results	Sludge age	COD removal	TKN removal	TP removal	Aerobic TSS (measured)	Aerobic VSS (measured)	Aerobic ISS	Nitrogen nitrified	Nitrate denitrified
	(d)	(%)	(%)	(%)	mgTSS/l)	(mgVSS/l)	(mgISS/l)	(mgN/ l influent)	(mgN/ l influent)
	12.1	95	97	38	6799.82	4814.82	1985	35.3	17.3

Waste Activated Sludge Composition (Aerobic)	Component	Active OHO	Endogenous OHO	Active PAO	Endogenous PAO	UPO	PP	USO	Supernatant	Total
	Units	mg/l (conc.)	mg/l (conc.)	mg/l (conc.)	mg/l (conc.)	mg/L (conc.)	mg/l (conc.)	mg/l (conc.)	mg/l (conc.)	mg/l (conc.)
	VSS	577.66	335.56	2966.71	359.09	528.44	0	45.03		4812.46
	N	47.18	33.56	296.67	35.91	52.84	0	1.3	0.29	466.16
	P	14.44	8.39	74.17	8.98	13.211	310.1	0.1	57.7	487.091

Appendix H: Analysis calculations

The following section outlines the calculations carried out in the analysis of the results. Where relevant, reference to this section was made in the main body of this research.

A. Determining the elemental concentration from known mineral precipitate concentrations

In all test cases, a known amount of struvite and ACP was added to 50 ml of solution (distilled water or NDEBPR WAS). This section presents how the expected concentration of the ions in the PCA extract was calculated.

Struvite

The stoichiometric formula of struvite is typically $MgNH_4PO_4.6H_2O$. For this elemental composition the molar mass is 245 mg/mol. The struvite used in this study was obtained commercially from Merck and had half of the hydration typically found in struvite. The formula was $MgNH_4PO_4.3H_2O$ and thus had a molar mass of 191 mg/mol. Hence, the following equation applied to determine the expected concentration of ions in the PCA extract.

$$Mg\ (in\ mgMg/L)\ = \frac{Struvite\ concentration\ in\ solution}{191} \times\ 24 \qquad \text{(H1)}$$

$$N\ (in\ mgCa/L)\ = \frac{Struvite\ concentration\ in\ solution}{191} \times\ 14 \qquad \text{(H2)}$$

$$P\ (in\ mgP/L)\ = \frac{Struvite\ concentration\ in\ solution}{191} \times\ 31 \qquad \text{(H3)}$$

$Where,$

$$24 \quad = Molar\ mass\ of\ magnesium\ in\ g/mol$$

$$14 \quad = Molar\ mass\ of\ nitrogen\ in\ g/mol$$

$$31 \quad = Molar\ mass\ of\ phosphorus\ in\ g/mol$$

$$191 \quad = Molar\ mass\ of\ struvite\ in\ g/mol$$

ACP

The ACP used in this study was also commercially obtained and had the following stoichiometric formula: $Ca_3(PO_4)_2$. The molar mass of ACP was 310 mg/mol. The expected ionic concentrations in the PCA extract were therefore calculated as shown below. Where both ACP and struvite were present, the expected P concentrations was the sum of P from Equation H3 and Equation H5.

$$Ca\ (in\ mgMg/L)\ = \frac{ACP\ concentration\ in\ solution}{310} \times\ 40\ \times\ 3 \qquad \text{(H4)}$$

$$P\ (in\ mgP/L)\ = \frac{ACP\ concentration\ in\ solution}{310} \times\ 31\ \times\ 2 \qquad \text{(H5)}$$

$Where,$

$40\ = Molar\ mass\ of\ calcium\ in\ g/mol$

$31\ = Molar\ mass\ of\ phosphorus\ in\ g/mol$

$310\ = Molar\ mass\ of\ ACP\ in\ g/mol$

B. Determining of elemental recovery for mineral precipitate

$$\textbf{Percentage recovery}\ = \frac{\textbf{Actual ion concentration}}{\textbf{Expected ion concentration}} \times\ \textbf{100} \qquad \text{(H6)}$$

C. Determining of elemental recovery for sludge (with or without mineral precipitate)

$$\textbf{Percentage recovery} = \frac{\sum \textbf{Extracts elemental concentration}}{\textbf{MLSS elemental concentration}} \times\ \textbf{100} \qquad \text{(H7)}$$